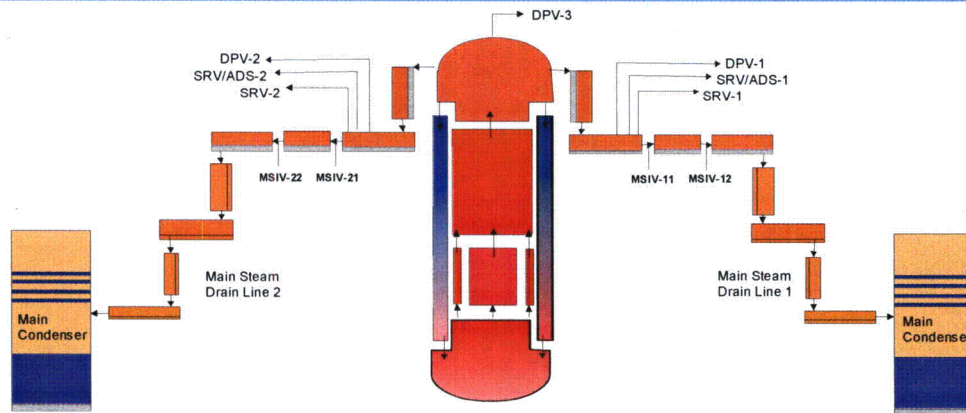


**Enclosure 2**

**MFN 07-466, Supplement 1**

**Estimation and Modeling of  
Effective Fission Product Decontamination Factor for  
ESBWR Containment – Part 3  
Research Report VTT-R-06771-07, Revision 2**

**Public Version**



## Estimation and Modeling of Effective Fission Product Decontamination Factor for ESBWR Containment – Part 3 revision 2

Authors:

Ilona Lindholm  
Karri Penttilä  
Anssu Ranta-Aho  
Jukka Rossi



Report's title Estimation and Modeling of Effective Fission Product Decontamination Factor for ESBWR Containment – Part 3 Revision 2		
Customer, contact person, address GE-Hitachi Energy Nuclear of Americas Wayne Marquino 3901 Castle Hayne Road, Wilmington, NC 28401, U.S.A.	Order reference  431007936	
Project name Extension of estimation and modeling of effective FP decontamination factor for ESBWR	Project number/Short name 18722/GE-jatko	
Author(s) Ilona Lindholm, Karri Penttilä, Anssu Ranta-Aho, Jukka Rossi	Pages 177	
Keywords ESBWR, Severe Accidents, Source Term	Report identification code VTT-R-06771-07 rev 2	
<p>Summary</p> <p>This report is the Third Part belonging to the Report VTT-R-04413-06 and complements the previously issued reports "Estimation and Modeling of effective Fission Product Decontamination Factor for ESBWR Containment" - Part 1 and Part 2. This is the second revision of the report VTT-R-0667-07 and replaces the previous version rev 0 (dated 08/10/2007 and rev 1 (dated 09/10/2007).</p> <p>The sensitivity of pH in the containment pools to the anticipated mass of CsOH was estimated with ChemSheet code and the fission product Source Term accounting for the Main Steam Line leak path was estimated with MELCOR 1.8.6YN code to support GE's response to selected questions of the Letter RAI No. 90. This report includes also the technical support for pH related questions of the Letter RAI No. 142.</p> <p>The CsOH mass was varied to be 100 %, 50 %, 25 %, 10 % and 0 % of the maximum amount of CsOH released to containment as predicted by MELCOR.</p> <p>The Wetwell pool remains basic in all three scenarios with 100 % and 50 % of CsOH mass. With less than 25 % CsOH the Suppression Pool becomes acidic in Scenarios 1 and 2. The Lower Drywell pool becomes acidic in all three accident scenarios. In the worst case, with 0 % CsOH in Scenario 3, the Lower Drywell Pool turns acid at 8.4 days from the beginning of the accident. Reactor Pressurized Vessel (RPV) becomes acidic in scenarios 1 and 2 but not in scenario 3. AS-2 shows the earliest change of GDCS pool to acidic, with 100 % CsOH at about 11.6 hr into the accident and with values less than or equal to 25 % CsOH the GDCS pool is always acidic.</p> <p>In the analyses of CsI retention to MSL leak path, the average total removal fraction to the MSL leak path section between MSIV-1 and the Main Condenser inlet was in 63.7 % in AS-1, 89.4 % in AS-2, 91.0 % in AS-3 and 53.3 % in MSL Guillotine Break (AS-4). The average retention fractions in the Main Condenser at 24 hr into the accident were 99.3 %, 96.9 %, 99.6 % and 97.9 % in AS-1, AS-2, AS-3 and AS-4, respectively.</p>		
GEH Report		
Espoo 06.03.2008		
Signatures	Signatures	Signatures
Kari Larjava Vice President, Professor	Eija Karita Puska Senior Research Scientist	Ilona Lindholm Senior Research Scientist
VTT's contact address VTT Technical Research Centre of Finland, P.O.Box 1000, FI-02044 VTT, Finland		
Distribution (customer and VTT) GEH 2 copies, VTT 1 copy		
<p><i>The use of the name of the VTT Technical Research Centre of Finland (VTT) in advertising or publication in part of this report is only permissible with written authorisation from the VTT Technical Research Centre of Finland.</i></p>		

## **Preface**

This report is a report of General Electric Nuclear Energy under the GEH Purchase Order No. 4431007936. The contact persons at GEH were Mr. Wayne Marquino, Mr. Chris Pratt for technical scope and Mr. Mark Harvey and Mr. Stephan Mindel for Quality Assurance issues.

Espoo 5.3.2008

I. Lindholm  
K. Penttilä  
A. Ranta-Aho  
J. Rossi

## Contents

Preface .....	2
1 Executive Summary.....	5
2 Introduction.....	9
3 Goal.....	9
4 Estimation of Dose rates .....	10
4.1 Dose Rates in the Atmosphere .....	10
4.2 Dose rates in the water pools.....	10
5 Formation of HCl and HNO <sub>3</sub> .....	14
5.1 Formation of HCl.....	14
5.2 Formation of HNO <sub>3</sub> .....	15
6 pH Sensitivity Studies.....	15
7 pH Sensitivity Studies for AS-1.....	17
7.1 pH in RPV .....	24
7.2 pH in LDW .....	25
7.3 pH in GDCS .....	26
7.4 pH in WW.....	27
8 pH Sensitivity Studies for AS-2.....	27
8.1 pH in RPV .....	34
8.2 pH in LDW .....	35
8.3 pH in GDCS .....	36
8.4 pH in WW.....	37
9 pH Sensitivity Studies for AS-3.....	38
9.1 pH in RPV .....	45
9.2 pH in LDW .....	46
9.3 pH in GDCS .....	47
9.4 pH in WW.....	48
10 Sensitivity study of the effect of radiation source from the Lower Head melt pool to the pH of the RPV pool.....	48
11 Analyses of Source Term Along Main Steam Line Leak Path .....	50
12 MELCOR Model of Main Steam Lines, Main Steam Drain Lines and the Main Condenser.....	50
13 AS-1: Bottom Drain Line break with ADS and with MSIV leak.....	56
14 AS-2: Bottom Drain Line break without ADS/DPV and with/without MSIV leak ....	65
15 AS-3: Loss of Preferred Power without ADS/DPV and with/without MSIV leak ....	74

16 AS-4: Main Steam Line Break inside the Containment with MSIV Leak .....	82
17 Comparison of AS-1, AS-2 and AS-3 Cases with and without MSIV leak .....	91
17.1 Comparison of AS-1 with and without MSIV leak .....	91
17.2 Comparison of AS-2 with and without MSIV leak .....	95
17.3 Comparison of AS-3 with and without MSIV leak .....	99
18 Summary And Conclusions .....	103
19 References .....	104
20 APPENDIX A: Dose rates due to three accident sequences (AS-1, AS-2, AS-3) in four water pools (WW, GDCS, DW, RPV). .....	105
21 APPENDIX B: Sensitivity Analysis for LDW mixing .....	106
22 APPENDIX C: Sensitivity Analysis of pH with Including Radiation from the Core Melt Pool in the Lower Head .....	109
23 APPENDIX D: Concentration Tables for Sensitivity Calculations .....	113
24 APPENDIX E: Validation of Thermodynamic System .....	129
25 APPENDIX F: Comparison of results : AS-1 without MSIV leak of FR Part 2 and FR Part 3 .....	133
26 APPENDIX G: Comparison of results: AS-2 without MSIV leak of FR Part 2 and FR Part 3 .....	148
27 APPENDIX H: Comparison of results : AS-3 without MSIV leak of FR Part 2 and FR Part 3 .....	164

## 1 Executive Summary

The purpose of this work is to investigate further the sensitivity of the quantity of CsOH in the containment water pools to the pool pH and to study the fission product source term via potential leak path through the Main Steam Line (MSL) and Main Steam Drain Line (MSDL) to the Main Condenser. This report is the Third Part belonging to the Report VTT-R-04413-06 and complements the previously issued reports "Estimation and Modeling of effective Fission Product Decontamination Factor for ESBWR Containment" Part 1 and Part 2.

The pH calculations were performed with ChemSheet code. The first task was to elaborate in tabular form the pressures, temperatures and concentrations of different chemical compounds in the pools from the pH analyses reported in [1] and [2]. Further the pH calculations were extended to 30 days. This effort contributes to GE's response to Letter RAI No. 90 items 15.4-28 and 15.4-13.

The second task was to evaluate the sensitivity of the obtained pH results to the amount of CsOH in the pools. The needed sensitivity runs were run with total CsOH masses equal to 50 %, 25 %, 10 % and 0 % of the total CsOH mass in the base case results. This work supports GE in responding the Letter RAI No. 90, item 15.4-22.

The Source Term analyses were performed with an updated MELCOR input to include a more detailed description of MSL, MSDL and Main Condenser. Also the alignment of SRVs and DPVs in the MSL was updated.

The studied accident scenarios, denoted AS-1, AS-2 and AS-3, were the same LOCA and Loss of Preferred Power sequences as in FR Part 2 [2] but with or without a failure of Main Steam Line Isolation Valve (MSIV) inside the containment and closure with a small leak in the MSIV outside the containment in one of the four MSLs. The fourth accident scenario was a MSL break, which was used to investigate the CsI leakage first to the containment atmosphere and then from containment to the MSL and to the Main Condenser.

The pH in the containment water pools is important in Source Term estimations, because in acidic water pool iodine dissolved in water forms easily iodine gas that escapes from the water pools to the containment atmosphere. In caustic or neutral pools elemental iodine is not formed.

ChemSheet analyses of pool pH were extended to 30 days. The formation rate of hydrochloric acid (HCl) as a result from radiolysis in the containment atmosphere was assessed as proposed in NUREG-5090 as presented in [1] and [2] except that HCl formation rates are scaled by 1.25 to account for the effect of more conservative estimate of the dose rate in the atmosphere. The nitric acid formation in the water pools and in the steam atmosphere is calculated according to the method and formula presented in NUREG-5090. The dose rates were determined using the masses of dissolved fission products as calculated by MELCOR. Also the initial pH in GDCS and WW was corrected to 5.7 (instead of 5.3 in FR Part 2 [2]).

Five sensitivity calculations were done with varying CsOH formation rates (100 %, 50 %, 25 %, 10 % and 0 %). In 100% calculation CsOH formation rates in pools were taken from MELCOR simulation and in others the formations rates were scaled with respective values

(0.5, 0.25 and 0.1). Table I and II gather the key pH results of the performed studies with times in hours and days, respectively.

The Wetwell (WW) remains basic in all scenarios with 100 % and 50 % of the maximum available CsOH mass but with values less than or equal to 25 % of maximum CsOH WW becomes acidic in scenarios 1 and 2. The Lower Drywell (LDW) becomes acidic in all scenarios at the phase of the simulation. In the worst case, with 0 % CsOH of the maximum value in scenario 3, the LDW turns acid at 8.4 days from the beginning of the accident. Reactor Pressurized Vessel (RPV) becomes acidic in scenarios 1 and 2 but not in scenario 3.

The GDCS pool becomes acidic at an earlier time. AS-2 shows the earliest change to acidic, with 100 % CsOH at about 11.6 hr into the accident and with values less than or equal to 25 % of maximum CsOH the GDCS pool is always acidic.

The key factor to keep pH of the pools alkaline is the distribution of sodium borate buffer between the pools. In scenario 3 less buffer solution goes to the LDW than in scenario 1 and 2 and therefore LDW pH turns acidic earlier in scenario 3. Also in scenario 3 enough buffer solution goes to the WW to keep it alkaline all the time.

MELCOR 1.8.6YN results of CsI removal in the MSL, MSDL and Main Condenser are shown in Table III. Cases both with and without MSIV leak path were calculated.

**Table I.** Time when pool pH becomes permanently less than 7. Times in hours.

CsOH fraction	Scenario	Time when a containment pool becomes acidic (pH < 7) permanently [hr]			
		RPV	LDW	GDCS	WW
100 %	AS-1	-	661.50	12.96	-
	AS-2	712.17	623.50	11.57	-
	AS-3	-	219.50	12.52	-
50 %	AS-1	704.17	603.50	11.69	-
	AS-2	670.17	582.17	10.42	-
	AS-3	-	210.83	8.58	-
25 %	AS-1	675.50	573.50	10.49	260.83
	AS-2	649.50	560.84	9.18	717.50
	AS-3	-	206.83	0.00	-
10 %	AS-1	658.83	556.17	7.96	24.83
	AS-2	636.84	548.84	6.68	242.84
	AS-3	-	204.17	0.00	-
0 %	AS-1	647.50	544.17	0.00	0.00
	AS-2	628.17	540.17	0.00	40.17
	AS-3	-	202.17	-	-

**Table II.** Time when pool pH becomes permanently less than 7. Times in days.

<sup>1</sup> CsOH fraction	Scenario	Time when a containment pool becomes acidic (pH < 7) permanently [days]			
		RPV	LDW	GDCS	WW
100 %	AS-1		27.56	0.54	
	AS-2	29.67	25.98	0.48	
	AS-3		9.15	0.52	
50 %	AS-1	29.34	25.15	0.49	
	AS-2	27.92	24.26	0.43	
	AS-3		8.78	0.36	
25 %	AS-1	28.15	23.90	0.44	10.87
	AS-2	27.06	23.37	0.38	29.90
	AS-3		8.62	0.00	
10 %	AS-1	27.45	23.17	0.33	1.03
	AS-2	26.53	22.87	0.28	10.12
	AS-3		8.51	0.00	
0 %	AS-1	26.98	22.67	0.00	0.00
	AS-2	26.17	22.51	0.00	1.67
	AS-3		8.42		

<sup>1</sup> percent of the CsOH mass in the base case MELCOR results. In the base case all CsOH in excess to that needed for formation of CsI is assumed to form CsOH.

The MSL in the MELCOR input are modeled as two equivalent flow paths, single MSL and triple MSL with volume, flow junction area and heat structure surface area of the three MSLs lumped together. The single MSL is leaking, the MSIVs in the other MSLs are assumed to close completely. The MSL and MSDL pipe are insulated with calcium silica insulation. The pipe steel structure and the insulation are modeled as same heat structure with different material properties in different mesh intervals. The Main Condenser is modeled as single volume with condenser tubes being horizontal pipes with inner surface at constant temperature, which is the average temperature of the coolant along the tube. The Hotwell pool is defined to the bottom of the Main Condenser volume. All three Condenser units are lumped into one Control Volume.

The retention is highest in the Main Condenser, at least 96.9 % of the incoming CsI has been removed from the airspace at 24 hr into the accident. The retention to MSL between the MSIV-1 and MSIV-2 is 18.6 - 48 %, with the lowest retention in AS-2. The retention in the MSDL is low, only a few per cent of the CsI flowing into the MSDL. There is practically no condensation along the MSDL because of relatively thick insulation and small pipe diameter. The total removal fraction in the MSL downstream of the MSIV-1 inside containment down to the inlet of Main Condenser is lowest (53.3 %) in AS-4 with Main Steam Line Break inside the containment. Scenario AS-1 resulted in total average retention fraction between MSIV-1 and the Main Condenser of 63.7 %. In AS-2 and AS-3 the MSL removal fractions are 89.4 % and 91 %, respectively.

**Table II.** Key figures-of-merit of calculated accident scenarios.

CsI item	AS-1 with MSIV leak [%]	AS-2 with MSIV leak [%]	AS-3 with MSIV leak [%]	AS-4 with MSIV leak [%]	AS-1 no MSIV leak [%]	AS-2 no MSIV leak [%]	AS-3 no MSIV leak [%]
<sup>1</sup> Release fraction from core	73.5	71.9	87.9	82.7	71.6	65.5	69.2
<sup>2</sup> Release fraction from RPV	84.0	77.8	89.2	97.6	87.6	76.6	89.7
<sup>2</sup> Release fraction from RPV to leaking MSL	21.6	10.3	26.2	99.9	N/A	N/A	N/A
Average retention fraction : MSIV1 ↔ MSIV-2	48.0	18.6	0	45.7	N/A	N/A	N/A
Average retention in MSL from MSIV-2 to MSDL	23.3	86.3	90.4	13.1	N/A	N/A	N/A
Average retention to MSDL	1.3	4.5	6.6	1.1	N/A	N/A	N/A
Average retention to Main Condenser	99.3	96.9	99.6	97.9	N/A	N/A	N/A
Total average retention: MSIV-1 ↔ Main Condenser inlet	63.7	89.4	91.0	53.3	N/A	N/A	N/A
<sup>3</sup> Release fraction via containment nominal leakage path	$1.49 \cdot 10^{-3}$	$1.08 \cdot 10^{-3}$	$3.60 \cdot 10^{-4}$	$1.38 \cdot 10^{-3}$	$1.47 \cdot 10^{-3}$	$1.27 \cdot 10^{-3}$	$7.99 \cdot 10^{-4}$
<sup>3</sup> Fraction released through SRVs	0	14.3	98.75	0	0	18.8	95.0
<sup>3</sup> Fraction released through SRV/ADS	3.8	16.0	0.94	0.2	5.4	14.4	1.22
<sup>3</sup> Fraction released through DPVs in MSLs	69.3	8.3	0.29	0.05	68.9	6.20	3.73
<sup>3</sup> Fraction released through DPVs in RPV Upper Plenum <sup>3</sup>	26.9	0.38	0.011	0.006	25.7	0.70	0.023
Max airborne CsI mass in containment as fraction of total released from RPV	38.1	37.2	12.9	18.5	38.6	45.2	34.5
Average PCCS DF for CsI	9.70	18.49	3.41	8.505	7.03	8.70	5.25
Average containment DF for CsI	992049	4089310	217703	457428	11484	1812193	14099

<sup>1</sup> fraction from initial core inventory

<sup>2</sup> fraction from mass released from core

<sup>3</sup> fraction from mass released from RPV



## 2 Introduction

The studied ESBWR plant has a rated power of 4590 MWt and the Reactor Coolant System (RCS) and Containment design is according to ESBWR Design Control Document Tier 1 and 2 rev 1. As to the containment passive safety systems, four double-module units of Isolation Condensers are capable of providing coolant injection to the RCS at high pressure and a total of six double-module Passive Containment Coolant System Condensers (PCCS) provide long term pressure control of the containment. In addition to that an attractive feature of the PCCS is the potential for fission product retention to the heat exchanger tubes and to condensate flow.

This report is the Third Part of the Report "Estimation and Modeling of effective Fission Product Decontamination Factor for ESBWR Containment" and complements the previously issued reports "Estimation and Modeling of effective Fission Product Decontamination Factor for ESBWR Containment" Part 1 [1] and Part 2 [2].

## 3 Goal

The purpose of this work is to investigate further the sensitivity of the quantity of CsOH in the containment water pools to the pool pH and to study the fission product source term via potential leak path through the Main Steam Line (MSL) and Main Steam Drain Line (MSDL) to the Main Condenser.

The pH calculations are performed with ChemSheet code. The first task is to elaborate in tabular form the pressures, temperatures and concentrations of different chemical compounds in the pools from the pH analyses reported in [1] and [2]. Further the pH calculations should be extended to 30 days. This effort contributes to GE's response to Letter RAI No. 90 items 15.4-28 and 15.4-13.

The second task is to evaluate the sensitivity of the obtained pH results to the amount of CsOH in the pools. The needed sensitivity runs are with total CsOH mass equal to 50 %, 25 % and 10 % of the total CsOH mass in the base case results. This work supports GE in responding the Letter RAI No. 90, item 15.4-22.

The first Source Term Task is the updating of the existing MELCOR input with Main Steam Line (MSL), Main Steam Drain Line (MSDL) and the Main Condenser input. This model is used in the second source term task to investigate the CsI releases through the Main Steam Line leak path.

The studied accident scenarios in source term tasks 2 and 3, denoted AS-1, AS-2 and AS-3, are the same as in FR Part 2 [2] but with or without a failure of Main Steam Line Isolation Valve (MSIV) inside the containment and closure with a small leak in the MSIV outside the containment in one of the four MSLs.

The fourth accident scenario is a MSL break, which is used to investigate the CsI leakage first to the containment atmosphere and then from containment to the MSL and to the Main Condenser (source term task 4).

## 4 Estimation of Dose rates

Estimates for the radiation dose rates in the containment is needed for calculation of the formation of HCl and HNO<sub>3</sub> acids in the containment. HCl is formed in the atmosphere from the chlorine released by radiolysis from the cables and most of HNO<sub>3</sub> is formed under radiation conditions in the water pools containing nitrogen or air. In the performed studies additional conservatism is brought in to these analyses by assuming that the HNO<sub>3</sub> is also formed in the steam in the atmosphere containing N<sub>2</sub>.

For estimation of acid formation, the dose rates in the atmosphere and in each water pool need to be determined first.

### 4.1 Dose Rates in the Atmosphere

The applied dose rates in the containment atmosphere are based on the previous dose rates calculated by GE with RADTRAD taking into account the most important radionuclides in AS-1 [1].

The dose estimates calculated with RADTRAD at the specified time steps are shown in Table 1. The dose rates were obtained using natural deposition coefficients for containment derived from MELCOR results of [1] for total airborne radionuclide masses. The decrease of the activities between time steps was approximated to be linear. The total dose is taken as a sum of atmospheric  $\beta$ - and  $\gamma$ -doses. The dose rates of Table 1 were applied to the total amount of cables in the containment, which implies that the dose rates were assumed to be the same both in the Upper Drywell and in the Lower Drywell.

**Table 1.** *Assumed radiation doses in the containment atmosphere.*

$t_1$ , h	$t_2$ , h	$(t_1-t_2)$ , s	$(\gamma+\beta)$ Mrad TID	TID, Mrad $(t_1-t_2)$
0.44	0.83	988	0.932	0.932
0.83	1.23	1440	3.11	2.178
1.23	1.83	2160	10.07	6.96
1.83	2.33	1800	18.32	8.25
2.33	3	2412	28.46	10.14
3	6	10800	65.6	37.14
6	8.33	8388	85.3	19.7
8.33	12	13212	110.5	25.2
12	24.33	44388	176.1	65.6

For the current pH calculation of this report the estimated dose rates of Table 1 were multiplied by a factor of 1.25 to conservatively account for the effect of the rest of the “less effective” fission product nuclides that were omitted in the RADTRAD calculation.

### 4.2 Dose rates in the water pools

The dose rates in the water pools affect the major formation of HNO<sub>3</sub> in the pools. The dose rates generated by dissolved fission products were determined separately for each of the pools: Suppression Pool, Lower Drywell pool, GDCS pool and the RPV water inventory. The base idea for estimation of the dose rate in each pool is to use the fission product mass (Cs, I, Te) calculated with MELCOR that is dissolved in each pool in each accident scenario AS-1,

AS-2 and AS-3. The fission product class mass calculated by MELCOR is further split into nuclides according to the elemental masses and the distribution of each element into masses of different nuclides by applying the verified ORIGEN data for time zero provided by GE.

In the case of the RPV pool, the core melt in the Lower Head provides another source of radiation in addition to that of the released and dissolved fission products. The effect of dose rate to the overlying water pool was estimated with MCNP5 code [3]. The effect of melt pool itself to the dose rate and formation of  $\text{HNO}_3$  is limited due to the fact that heavy oxides are self-absorbing effectively radiation and water itself has a strong dumping effect for penetration length of radiation. The effect of melt pool was estimated conservatively by using the whole core inventory as basis (by not reducing the released, volatile fission products from the inventory). Furthermore, no credit was taken from a layer of metallic melt atop the oxide pool which would further absorb photons and reduce the dose rate to the overlying water. Physicochemical studies suggest that metal and oxide phases of core melt would separate in the RPV lower head, with lighter metallic phase on top [4].

The base case calculations were performed by assuming only the dose rates from the dissolved fission products in the RPV pool for  $\text{HNO}_3$  generation. Sensitivity studies were performed with the dose rates from both dissolved fission products and from the Lower Head melt pool to investigate the effect to pool pH. The calculated estimates for the melt pool dose rates are based on excessively conservative estimates for simplification of the calculation effort (e.g. the melt pool gamma source is based on whole core source at 1 hr after the shutdown).

#### Dose rate from the dissolved fission products

The element masses as a function of time in the pools of WW, LDW, GDCS and RPV are pulled out from the MELCOR results. On the other hand reactor core radioactive inventory is known via the ORIGEN results provided by GE. File contains inventories for the time points of 0, 1 hour, 1 day and 30 days. Radioactive decay calculations with the RASCAL code and lognormal interpolation are used to solve inventory at other time points [5].

In the case of dose rate in water, the most important elements here are Cs, I, Rb, Te, Se, Ba and Sr. From the MELCOR results each element specific mass fraction is first obtained by dividing the MELCOR mass at the time point with the ORIGEN mass at time point 0. Because MELCOR does not consider the effect of radioactive decay, comparison with the shutdown values prevents negative mass fractions in long-term estimates. Multiplying by this mass fraction value the isotope specific inventory value of ORIGEN, the corresponding MELCOR activity value is obtained. Finally the dose rate is determined by multiplying the isotope specific dose factor and dividing by the water volume. Besides, conversions due to actual power and other scaling factors and units shall be taken account. The results of dose rates in water pools are presented in Appendix A.

The calculation principles of activities and the dose rate in the pool are presented with Eqs. 1 and 2. Dose rates were determined assuming infinite water pool. A simplistic approach was adopted and the FRG-12 Table III.2 [6] effective dose factors were used. This is justified due to small differences in the photon mass energy-absorption coefficients between water and human tissues. For example, the preceding coefficient for the 1 MeV photon is 0.031 in water and 0.0308 in muscle.

$$A(t)_{isotope}^{MELCOR} = A(t)_{isotope}^{ORIGEN} \cdot \frac{m(t)_{class}^{MELCOR}}{m(0)_{class}^{MELCOR}} \quad (1)$$

where  $A(t)_{isotope}^{MELCOR}$  is the activity of the isotope in MELCOR [Bq],

$A(t)_{isotope}^{ORIGEN}$  is the activity of the isotope in ORIGEN [Bq],

$m(t)_{class}^{MELCOR}$  is the mass of the class in MELCOR [kg],

$m(t)_{class}^{ORIGEN}$  is the mass of the class in ORIGEN [kg].

The dose rate in pool is calculated as

$$D(t)_{isotope} = A(t)_{isotope}^{MELCOR} \cdot DF_{isotope} \cdot V^{-1} \quad (2)$$

where  $D(t)_{isotope}$  is the dose rate of the isotope [Gy/h],

$DF_{isotope}$  is the dose factor for water immersion [Gy/Bqm<sup>-3</sup>h] [6],

$V$  is the liquid volume in the pool [m<sup>3</sup>].

#### Dose rate from the Lower Head melt pool

The dose rate in the RPV pool was estimated from the amount of dissolved fission products (Cs, I, Te) in the total amount of water in all RPV control volumes. The effective dose rate from the core melt pool in the lower head was estimated with MCNP5 code [3] and with the standard MCNP4C data library [[


]]

## 5 Formation of HCl and HNO<sub>3</sub>

### 5.1 Formation of HCl

The calculation of HCL production from cable insulators was performed in the way introduced in the report NUREG/CR-5950 [8]. According to the report, the amount of HCl produced from Hypalon used as the isolation material in electrical cables in the containment is estimated as  $4.6 \times 10^{-4}$  mol per lb of insulation per Mrad. This estimate is based on the model description of electrical cable and a radiation G value of 2.1. The extent of HCl production would depend on the total dose. The applied mass of Hypalon insulation was 7480 lbs. This insulation mass was provided by GE and has been used in previous calculations for ABWR.

MELCOR results indicate, that the fission product release to the containment starts at about 2000 s and HCl production from cables as well as HNO<sub>3</sub> production in the steam atmosphere is assumed to start immediately after that.

All HCl formation and HNO<sub>3</sub> formation in the containment atmosphere are based on dose rates of Table 1 multiplied by a factor of 1.25 for conservatism. For HCl formation it is further assumed that 92 % of the cables reside in the Lower Drywell and 8 % of the cables are in the Upper Drywell.

Further conservative assumption is the formation of HNO<sub>3</sub> in the water vapour in the atmosphere in addition to nitric acid formation in the water pools.

The formation of HCl in the containment atmosphere is calculated with the Eq. (4):

$$R = K \times M \times \frac{\Delta D}{\Delta t}, \quad (4)$$

where

$$K = 4.6 \cdot 10^{-4} \text{ (mol}_{\text{HCl}} \text{ Mrad}/(\text{hr} \cdot \text{lb}))$$

$M$  = mass of insulation material (lb)

$$\frac{\Delta D}{\Delta t} = \text{radiation dose rate (Mrad/hr)}$$

The formation of  $\text{HNO}_3$  in the water vapour of the control volume atmosphere is calculated using the same formula (5) as for the water pools, presented in Chapter 5.2, but by applying the steam mass instead of pool mass.

## 5.2 Formation of $\text{HNO}_3$

The formation of  $\text{HNO}_3$  in water pools was not included in the pH calculations of FR Part 1 and Part 2. This error has been corrected in the results of this report and  $\text{HNO}_3$  formation rate in the RPV, LDW, GDCS and WW is calculated from the radiation dose rate of fission products in the water.  $\text{HNO}_3$  formation rate is calculated for both atmosphere and pools using the formula presented in NUREG/CR-5950 [8]:

$$\text{HNO}_3 [\text{mol}] = \text{Radiation} [\text{Mrad}] * 7.3 * 10^{-6} \left[ \frac{\text{mol}}{\text{kg} * \text{Mrad}} \right] * \text{water mass} [\text{kg}] \quad (5)$$

For atmospheric formation of  $\text{HNO}_3$  the water mass in (4) is the steam mass of a control volume from the MELCOR calculations. For  $\text{HNO}_3$  formation in the pools the water mass is the pool mass calculated by MELCOR. It is assumed that 1 kg of water equals to 1 standard liter in these studies.

Estimated radiation rates at selected time points are tabulated in Appendix A. In ChemSheet pH model the radiation rates at given time step (from MELCOR simulation) are linearly interpolated from the tabulated values and multiplied with the length of the time step to obtain the radiation dose. These dose values are then used in equation 5 to get the formed nitric acid amounts in the pools during the time step.

## 6 pH Sensitivity Studies

The sensitivity studies were done for the base cases ("pH case A" in FR Part 1 [1]) for AS-1, AS-2 and AS-3 scenarios. In the sensitivity calculations the amounts of cesium hydroxide in the pools (RPV, LDW, GDCS and WW) were scaled with 100% (base case  $\text{CsOH}$ ), 50 %, 25 %, 10 % and 0 % to study the effect of uncertainty in cesium forming other, less caustic compounds than  $\text{CsOH}$  to the pH of the pools.

The base case values for  $\text{CsOH}$  and  $\text{CsI}$  masses in the RPV, LDW, GDCS and WW water pools were taken from MELCOR calculations. In the ChemSheet model they need to be given as source terms (formation as kg/s) because of the mixing between the pools and possible chemical reactions affecting the concentration of  $\text{Cs}^+$ ,  $\text{I}^+$  and  $\text{OH}^-$  ions. The  $\text{CsOH}$  and  $\text{CsI}$

masses were converted to formation rates. If at time step  $t_1$  mass is  $m_1$  and at time step  $t_2$  mass is  $m_2$ , then formation is  $(m_2 - m_1)/(t_2 - t_1)$  [kg/s]. These formation rates were calculated for selected time periods in such a way that CsOH and CsI masses calculated with ChemSheet pH model were equal to those calculated with MELCOR (the main difficulty is the effect of mixing of CsOH and CsI between GDCS, RPV and LDW that needs to be taken into account).

Initially each scenario was calculated with MELCOR to 86400 seconds (24 hours). To confirm the flow rate values (mainly water flow from RPV to LDW and to UDW) after the first day MELCOR calculations were continued to 48 hours. The time averaged flow rates were calculated from the extended MELCOR runs between 36 and 48 hours and used in ChemSheet pH model as constant flow rates between 24 and 720 hours (1 to 30 days).

Additional sensitivity analysis to investigate the effect of mixing of RPV and LDW water pools through the BDL failure were performed. In the base calculations the mixing between the RPV and LDW pools were taken into account by extrapolating the flow rates from the MELCOR results from 24 hrs to 30 days. In the sensitivity calculations presented in Appendix B, the mixing flow rate between RPV and LDW beyond 24 hrs was assumed to be zero. The mixing sensitivity run is labeled as "NM" (No Mixing) in pH charts. Other assumptions than setting the RPV-LDW flow rates to zero are the same as in the base with 100 % CsOH.

Another additional sensitivity case for each scenario was calculated to estimate the effect of additional radiation dose rate from the Lower Head melt pool to the overlying water. The results are presented in Appendix C. Other assumptions than scaling the radiation rate in the RPV are the same as in the base calculation with 100 % CsOH.

In all sensitivity calculations HCl formation rates in UDW and LDW were scaled by 125 % from the values used in FR Part1 and Part 2 reports [1] and [2] to account for additional conservatism in the calculated atmospheric dose rates. A total of 92 % of HCl is formed in LDW and 8% in UDW due to location of cable masses in the containment.

All  $\text{HNO}_3$  (with up-scaling by 125 % to account the conservatism in airborne dose rates) formed in the atmospheric steam is added in the  $\text{HNO}_3$  balance of UDW (this has been changed from FR Part1 and Part2 report calculations where  $\text{HNO}_3$  was formed in GDCS). Most of HCl and  $\text{HNO}_3$  in UDW flow through PCCS to GDCS and from there to RPV and LDW.

Initial pH in GDCS and WW is set to 5.7 by adding small initial amount of HCl to them (total of 11.9 moles).

The sodium pentaborate solution was released from SLCS into the RPV in each calculated scenario. In AS-1 the sodium pentaborate injection starts at 6080 s, in AS-2 at 5140 s and in AS-3 at 13800 s, respectively. The mass fraction of sodium pentaborate in SLCS injection is 12.5 %. The volume of solution in SLCS tanks was given as 15600  $\text{m}^3$ . The density of soluble sodium pentaborate was estimated to be 1  $\text{kg}/\text{dm}^3$ . The amount of water in SLCS was set to 13650 kg and the mass of sodium pentaborate to 1950 kg. The release rate was 36.8  $\text{kg}/\text{s}$  ( $2 \cdot 18.4 \text{ kg}/\text{s}$ ).

Concentration tables for RPV, LDW, GDCS and WW water pools from each CsOH sensitivity calculation are presented in Appendix D. These tables contain temperature,



pressure, amount of water, concentration of species affecting the pH and pH values at 16 selected time points. They also contain pH values that were calculated using the species in the tables to verify pH values calculated with the ChemSheet model tables (but still using same Gibbs energy method to calculate equilibrium composition and pH from that).

## 7 pH Sensitivity Studies for AS-1

Figure 1 shows the pools masses and flow rates that were used from 24 hours to 720 hours. There is a slow mixing between the RPV and the LDW. Direction of mixing is changed at each time step. There is an average net flow of 0.14 kg/s from the LDW to the RPV. This is balanced by net steam flow of 0.14 kg/s from the UDW to the LDW (ANNULUS and MDW). The positive and negative flow rates are the average rates taken from the MELCOR flow rates between 36 and 48 hours. During the first day there is also some overflow of water from the RPV to the UDW and further down to the mid-drywell (MDW) and eventually to the LDW. Also some water flows to the WW (and that is why there is some sodium pentaborate also in the WW). The LDW becomes full during first day and after that water flows to the MDW and the ANNULUS compartment (LDW and MDW are inter-connected by flow junctions and MDW and ANNULUS are inter-connected by a flow junction). In the ChemSheet pH calculations the LDW, the MDW and the ANNULUS are considered as one volume (their water and gas masses are combined).

The RPV water pool mass is the sum of water in the core, bypass, lower plenum, downcomer and chimney compartments. In the calculations of FR Part 2 [2] the water in the downcomer and chimney were not included.

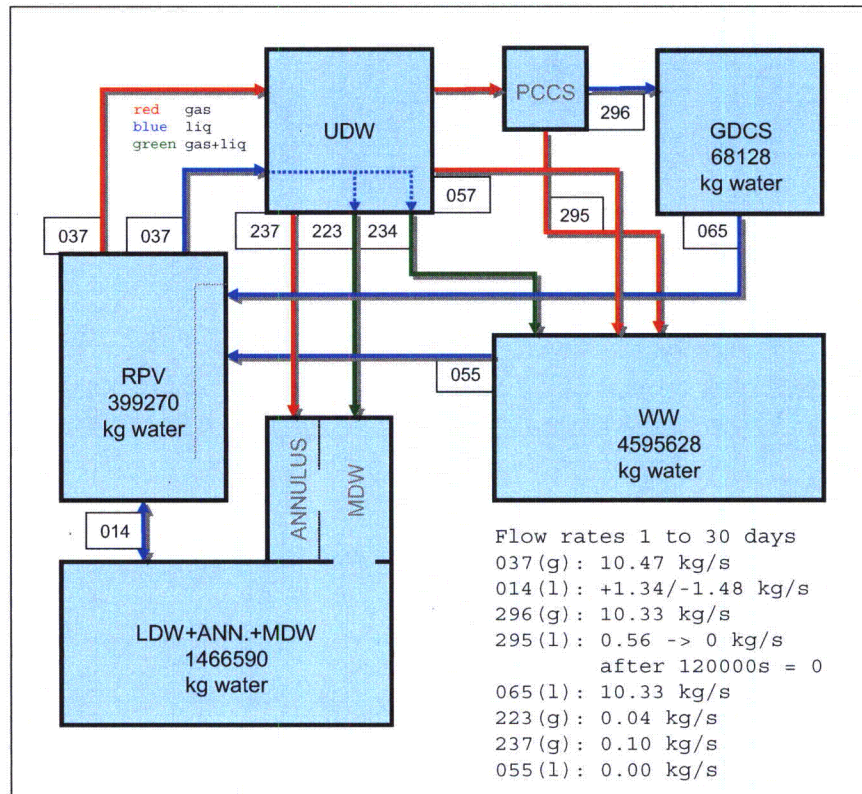


**Figure 1.** Pool masses and flow rates in scenario AS-1 from 24 to 720 hour.

Figure 2a shows MELCOR results of RPV water flow rates in AS-1 from 0 to 24 hours and figure 2b shows MELCOR result for 14 flow rate in AS-1 from 24 to 48 hours.

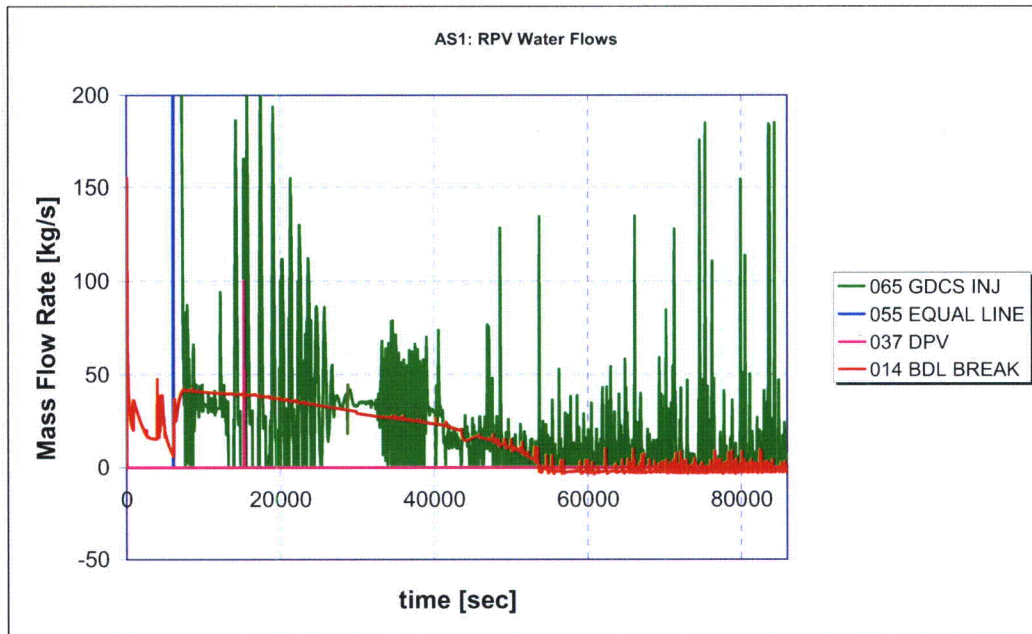


**Figure 2a.** MELCOR result for RPV water flow rates in AS-1 between 0 and 24 hours.

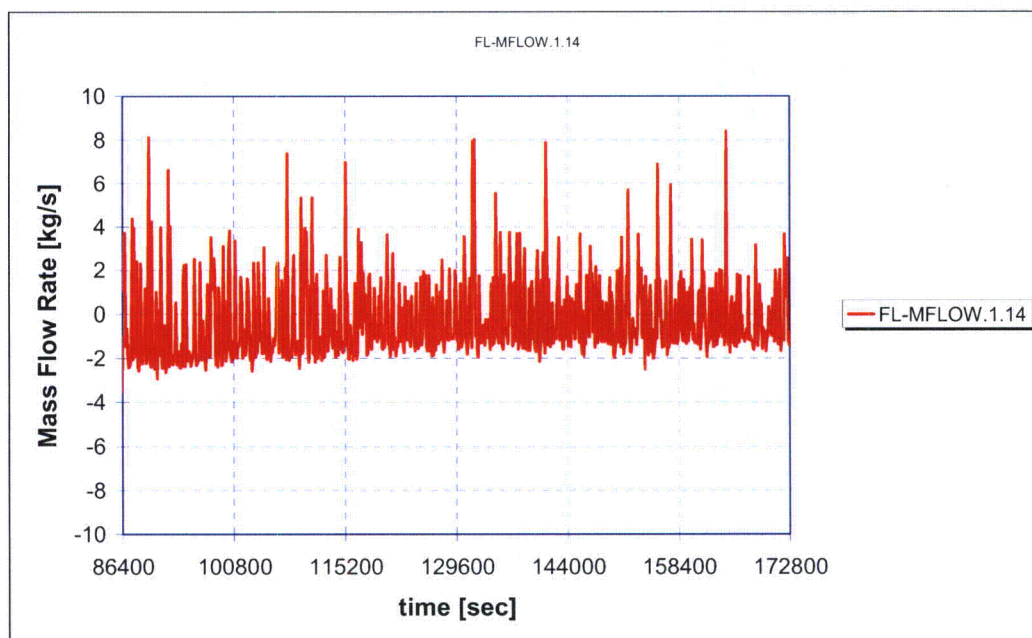


**Figure 2b.** MELCOR result for 14 flow rate in AS-1 between 24 and 48 hours. Average positive flow rate between 36 and 48 hours is 1.34 kg/s and average negative flow rate is 1.48 kg/s.



Figure 3 shows the distribution of boron concentration. The buffer is slowly accumulating into the LDW pool through the BDL break flow. The water volume in the RPV is larger than in the calculations of FR Part 3 rev 1 [9], because also the water mass in the chimney and in the downcomer are accounted for in the ChemSheet model. Further, the buffer is mixed into a larger water volume, which takes a longer time to flow out from the RPV through the BDL break than in FR Part 3 rev 1 calculations and thus RPV pool has buffering for a longer period of time.

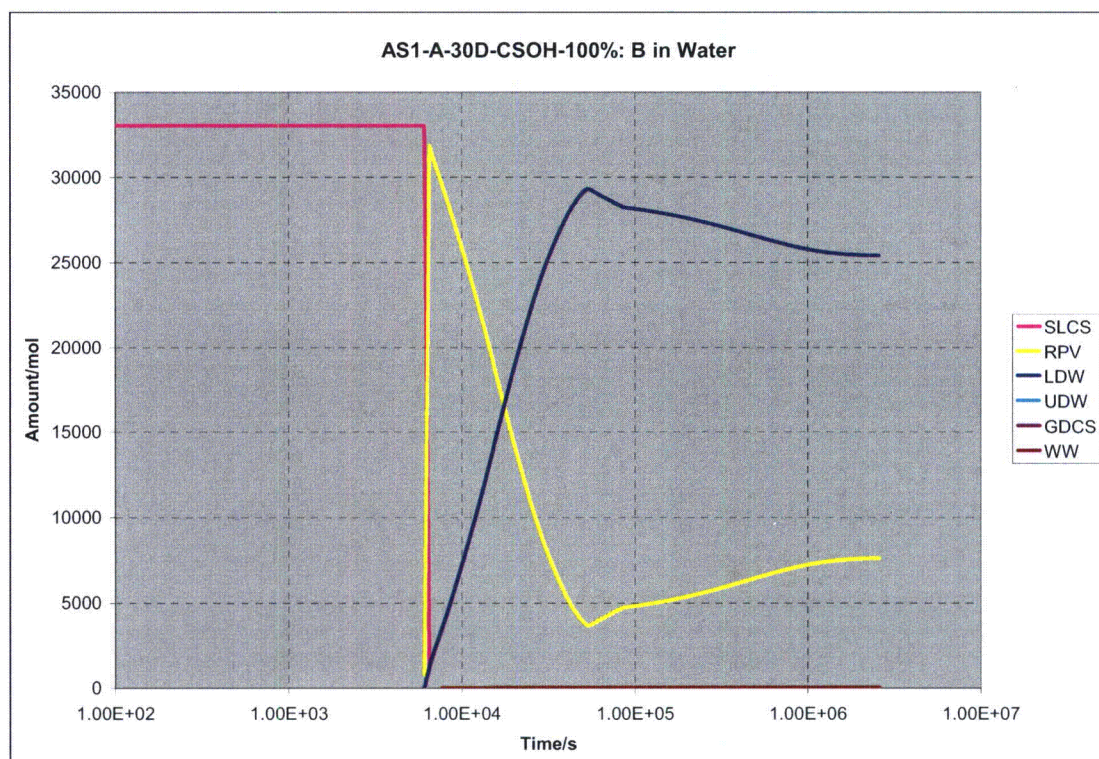


**Figure 3.** The distribution of elementary boron in AS-1 scenario. Boron is as boric acid ( $B(OH)_3$ ,  $B(OH)_4(-a)$ ).

Table 4 shows HCl and  $HNO_3$  formation rates in atmosphere in scenario AS-1 (all  $HNO_3$  is formed in UDW and 8 % of HCl in UDW and 92 % in LDW). The dose rates have been scaled up by 125 % from the original dose rates calculated by RADTRAD by GE.

**Table 4.** Scaled formation rates of HCl and HNO<sub>3</sub> in atmosphere in scenario AS-1.

t1	t2	HCl	HNO <sub>3</sub>	HCl	HNO <sub>3</sub>
s	s	mol/s	mol/s	mol	mol
2000	2988	4.000E-03	2.588E-05	3.952	0.026
2988	4428	6.500E-03	4.250E-05	9.360	0.061
4428	6588	1.388E-02	6.950E-05	29.970	0.150
6588	8388	1.975E-02	1.463E-04	35.550	0.263
8388	10800	1.813E-02	1.713E-04	43.718	0.413
10800	21600	1.475E-02	1.155E-04	159.300	1.247
21600	29988	1.013E-02	1.235E-04	84.929	1.036
29988	43200	8.250E-03	1.525E-04	108.999	2.015
43200	86400	6.375E-03	1.350E-04	275.400	5.832
86400	172800	5.741E-03	1.216E-04	496.044	10.508
172800	259200	4.750E-03	1.006E-04	410.400	8.694
259200	345600	4.156E-03	8.800E-05	359.100	7.603
345600	432000	3.730E-03	7.900E-05	322.272	6.826
432000	518400	3.404E-03	7.213E-05	294.084	6.232
518400	604800	3.149E-03	6.675E-05	272.052	5.767
604800	691200	2.939E-03	6.225E-05	253.908	5.378
691200	777600	2.766E-03	5.863E-05	239.004	5.065
777600	864000	2.620E-03	5.550E-05	226.368	4.795
864000	950400	2.499E-03	5.288E-05	215.892	4.568
950400	1036800	2.391E-03	5.063E-05	206.604	4.374
1036800	1123200	2.295E-03	4.863E-05	198.288	4.201
1123200	1209600	2.213E-03	4.688E-05	191.160	4.050
1209600	1814400	1.983E-03	4.200E-05	1199.016	25.402
1814400	2419200	1.670E-03	3.538E-05	1010.016	21.395
2419200	2592000	1.670E-03	3.538E-05	288.576	6.113
		Total/mol		6933.96	142.01

HNO<sub>3</sub> formations in water pools are calculated from the applied radiation dose rates of fission products in pools according to equation 5 (total HNO<sub>3</sub> formation in all pools is 518 mol). Table 5 shows the used radiation rates and resulting HNO<sub>3</sub> amounts.

**Table 5.** Radiation rates [rad/hr] and resulting amounts of HNO<sub>3</sub> in the water pools in scenario AS-1 (total formation is 518 mol).

t/s	WW/rad/h	GDCS/rad/h	LDW/rad/h	RPV/rad/h
2500	8792.778	19345.897	664.842	12.953
3600	8244.851	19330.110	5953.060	1419.877
6052	42739.062	89201.669	101257.117	16234.911
7200	55588.801	92355.191	157177.574	43872.145
10800	157255.024	79928.162	155248.618	68964.962
14400	62925.317	80285.301	112480.745	64371.239
21600	59187.464	75934.976	92060.895	65058.132
28800	52810.349	63328.915	80371.043	61161.804
43200	54112.019	38684.201	96637.994	54432.634
86400	43439.055	867.692	85100.293	66819.227
172800	21035.805	422.702	42011.257	32978.898
259200	16191.747	326.392	32662.979	25638.410
345600	13929.777	281.379	28282.751	22199.794
432000	12608.805	255.075	25718.675	20187.151
720000	10527.804	213.596	21666.044	17006.401
1080000	9479.919	192.680	19615.483	15397.128
1440000	8940.643	181.903	18555.860	14565.569
1800000	8605.577	175.200	17895.353	14047.232
2160000	8373.962	170.563	17437.554	13687.974
2520000	8202.484	167.127	17097.851	13421.391
2592000	7132.740	145.624	14956.447	11740.859
HNO <sub>3</sub> /mol in 30 d	292.686	3.939	181.745	40.060

The total HNO<sub>3</sub> formation is the sum of HNO<sub>3</sub> formation in the UDW atmosphere and in water pools and is 660 moles during 30 days.

Tables 6 and 7 show the formation rates of CsOH and CsI that were calculated from MELCOR results.

**Table 6.** CsOH formation rates [kg/s] in pools in scenario AS-1 (total formation is 226.1 kg).

t/s	WW/kg/s	GDCS/kg/s	LDW/kg/s	RPV/kg/s
0	0	0	0	0
757.0069	0.0566	0.025692	0.002374	2.68E-06
982.0218	0.001674	0.003254	0.001708	0
1530.026	0.000207	0.000779	0.000361	8.78E-06
2700.094	0.000225	0.003166	0.000257	8.6E-05
3700.13	0.106385	0.051447	0.001672	0.000236
4100.052	0.034881	0.049688	0.004691	7.32E-05
4290.013	0.043305	0.04605	0.00695	0
4960.031	0.009817	0.010352	0.044927	0
5230.12	0.003864	0.004247	0	0
6100.051	0.009811	0.000381	0	0
7410.969	0.001563	0.00235	0	0
8900.201	9.9E-05	9.34E-05	0	0.000177
30318.18	0	0	0	1.78E-05
86400	0	0	0	0
87000	0	0	0	0
Total/kg	115.63	85.00	20.50	5.00

**Table 7.** CsI formation rates [kg/s] in pools in scenario AS-1 (total formation is 32.7 kg).

t/s	WW/kg/s	GDCS/kg/s	LDW/kg/s	RPV/kg/s
0	0	0	0	0
757.0069	0.007075	0.003242	0.0003	3.09E-07
982.0218	0.000213	0.000411	0.000216	0
1530.026	3.14E-05	0.000112	4.58E-05	1.32E-06
2700.094	3.36E-05	0.000473	3.7E-05	1.29E-05
3700.13	0.01553	0.007695	0.000249	3.45E-05
4100.052	0.005143	0.007351	0.0007	1.08E-05
4290.013	0.006525	0.006956	0.001037	0
4960.031	0.0013	0.001271	0.001651	0
5230.12	0.000506	0.000452	0.001588	0.000138
6100.051	0.001534	6.87E-05	0.000209	0
7410.969	0.000249	2.01E-05	6.71E-05	0
8900.201	1.48E-05	6.54E-06	0	2.8E-05
30318.18	0	0	0	0
86400	0	0	0	0
87000	0	0	0	0
Total/kg	16.83	11.69	3.40	0.75



Figures 4 and 5 show the calculated CsOH and CsI masses in pools (including the formation rates and the mixing effect). Results for the LDW include also CsOH and CsI in the annulus and in the middle drywell.

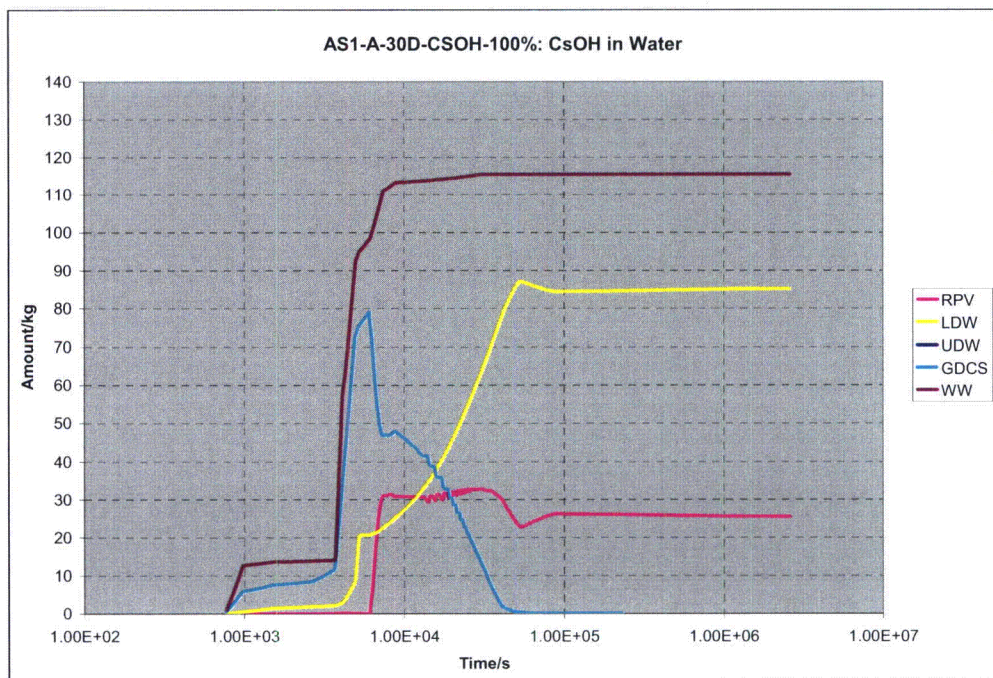


**Figure 4.** Calculated CsOH amounts in pools in scenario AS-1 as a function of time.

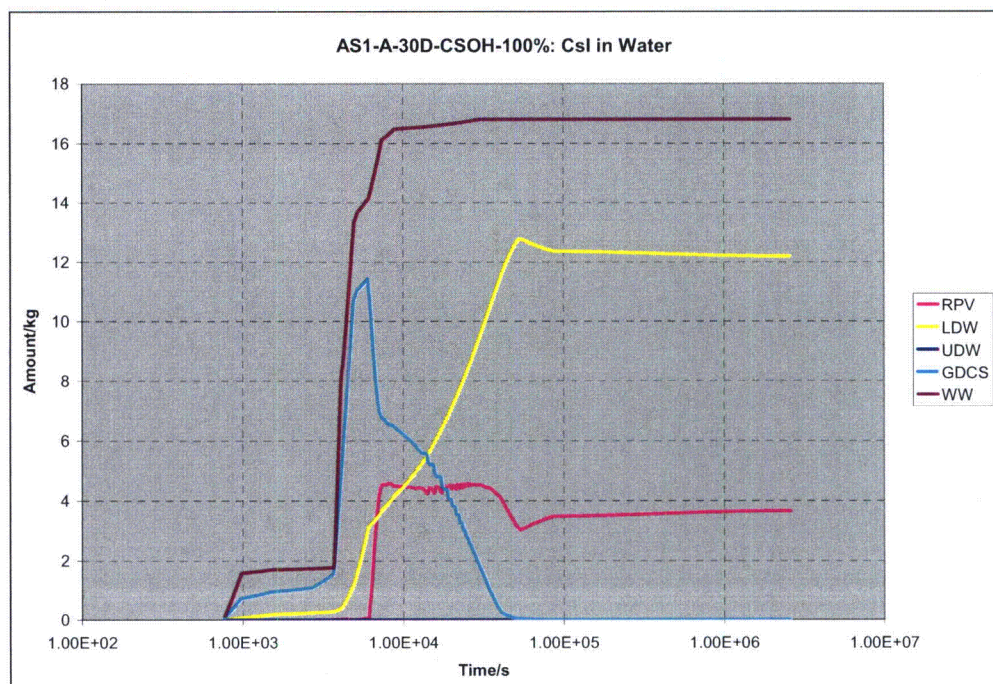


**Figure 5.** Calculated CsI(a) amounts in pools in scenario AS-1 as a function of time.



Figures 6 and 7 show the calculated HCl and HNO<sub>3</sub> molar amounts in pools (including the formation rates and the mixing effect).

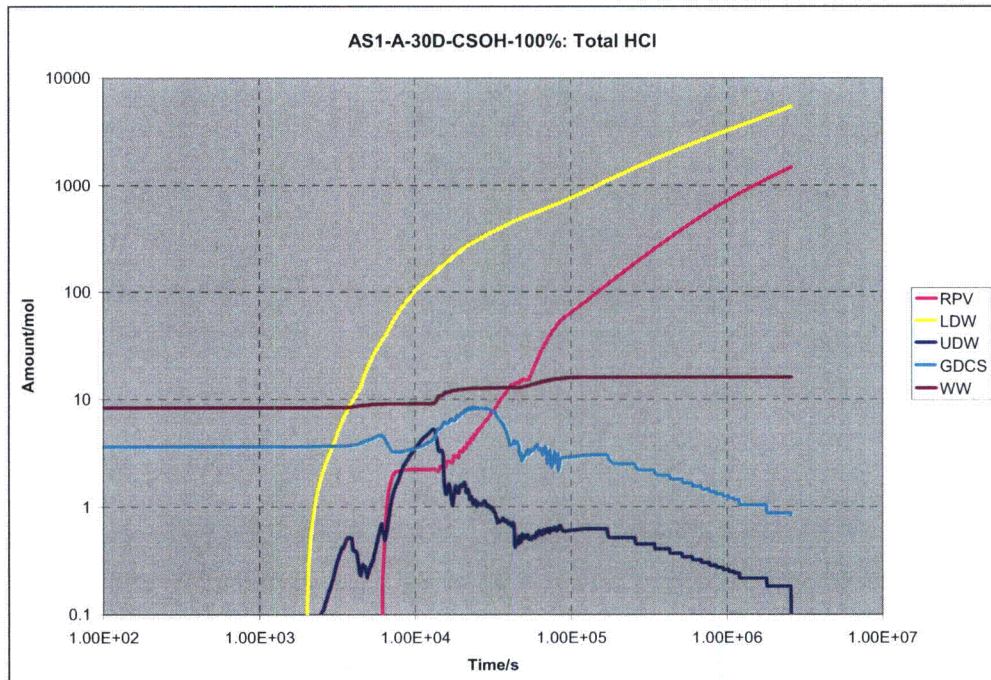


**Figure 6.** Calculated gaseous (in UDW) and aqueous HCl (other pools) amounts in scenario AS-1 as a function of time.

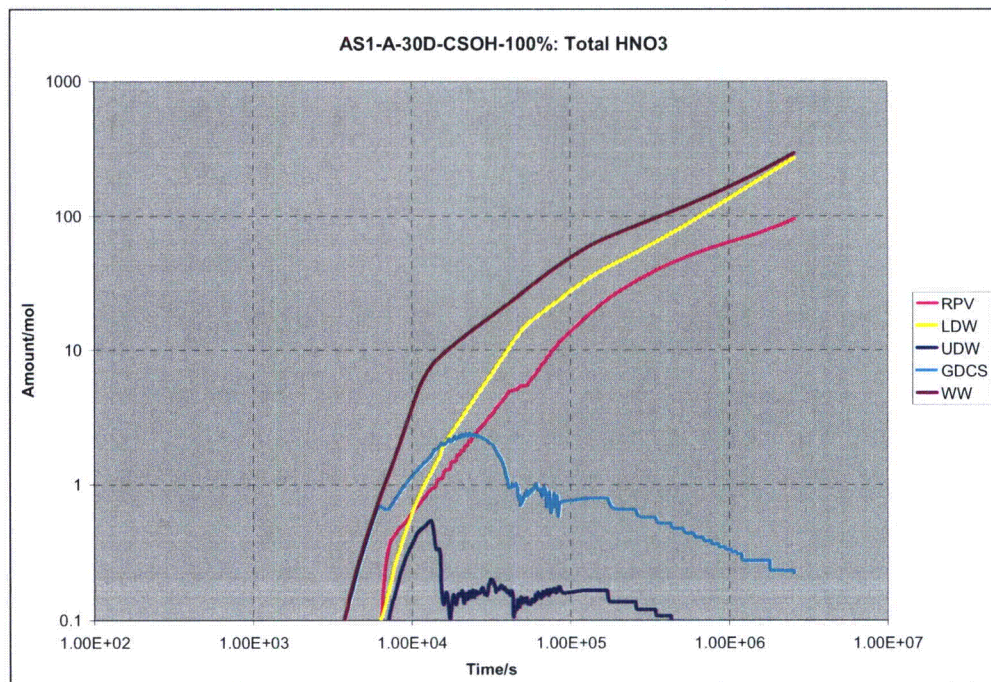


**Figure 7.** Calculated gaseous (in UDW) and aqueous HNO<sub>3</sub> (other pools) amounts in scenario AS-1 as a function of time.

## 7.1 pH in RPV

Figure 8 shows the calculated pH in RPV in scenario AS-1. The pH in RPV becomes permanently less than seven at 704.17 hrs (50 % of CsOH), 675.50 hrs (25 % of CsOH), 658.83 hrs (10 % of CsOH) and 647.50 hrs (0 % of CsOH). With 100 % of CsOH the pH remains over seven.

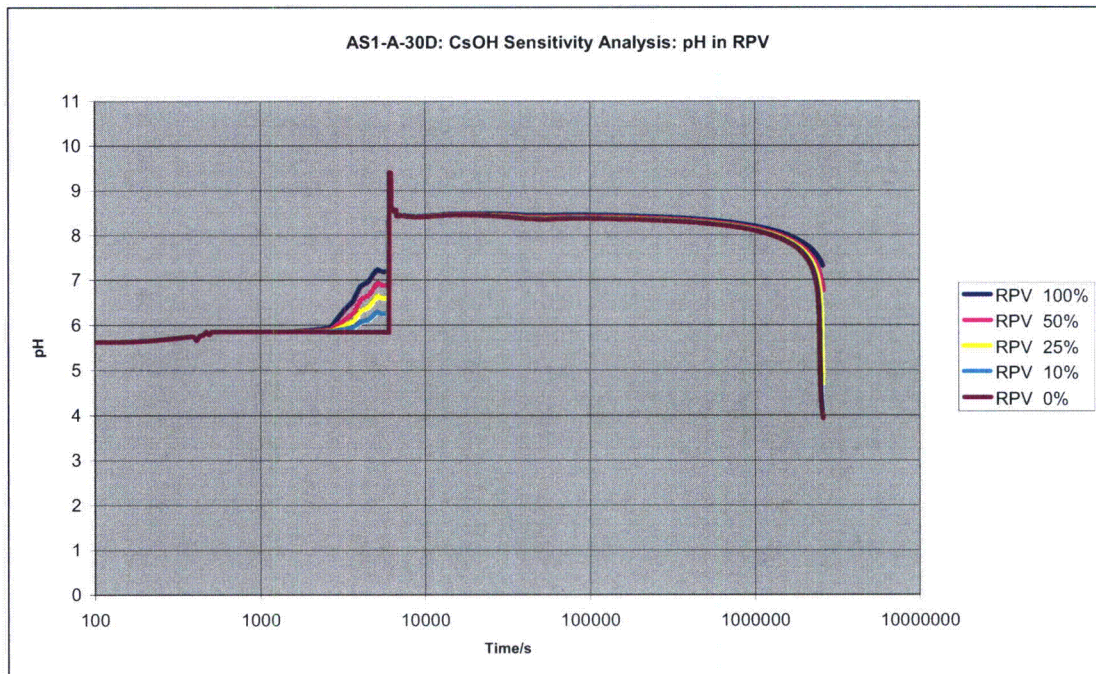


**Figure 8.** *pH in RPV in AS-1 with scaled amounts of CsOH.*



## 7.2 pH in LDW

Figure 9 shows the calculated pH in LDW in scenario AS-1. The pH in LDW becomes permanently less than seven at 661.50 hrs (100 % of CsOH), 603.50 hrs (50 % of CsOH), 573.50 hrs (25 % of CsOH), 556.17 hrs (10 % of CsOH) and 544.17 hrs (0 % of CsOH).

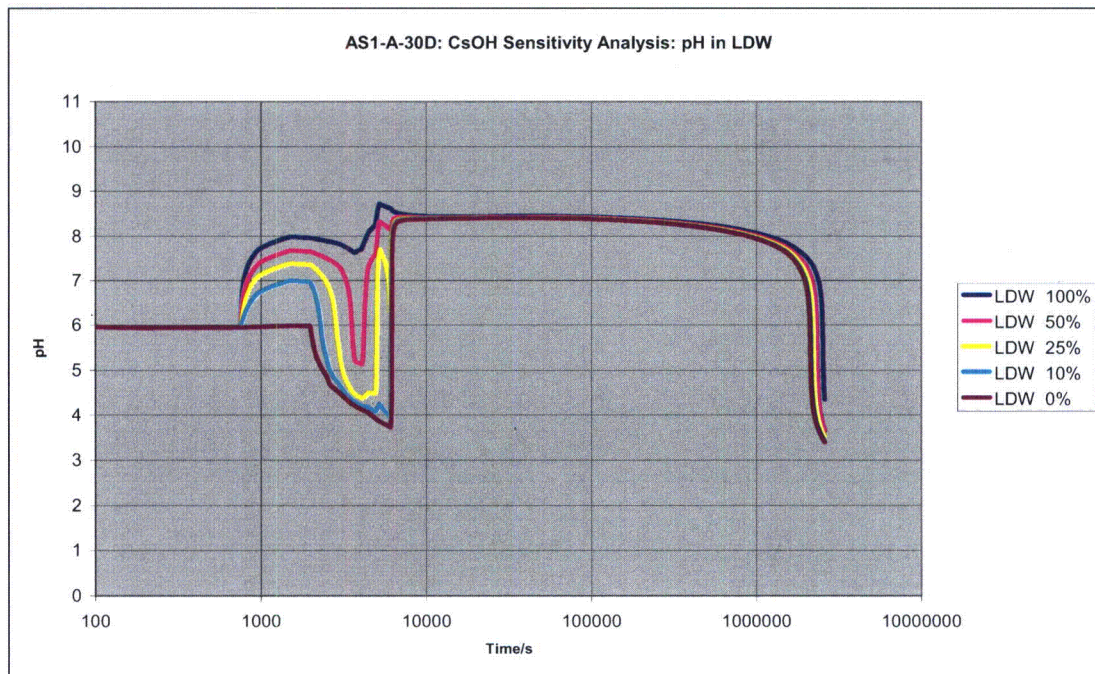


**Figure 9.** pH in LDW in AS-1 with scaled CsOH amounts.

### 7.3 pH in GDCS

Figure 10 shows the calculated pH in GDCS in scenario AS-1. The pH in GDCS becomes permanently less than seven at 12.96 hrs (100 % of CsOH), 11.69 hrs (50 % of CsOH), 10.49 hrs (25 % of CsOH), 7.96 hrs (10 % of CsOH) and 0.0 hrs (0 % of CsOH).

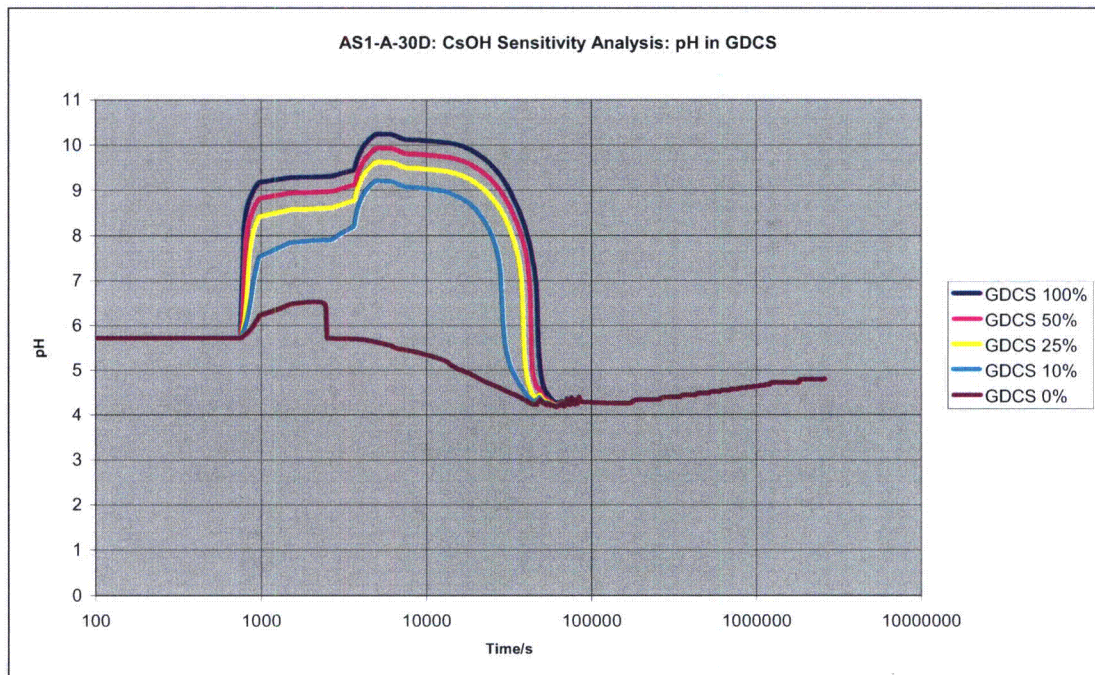
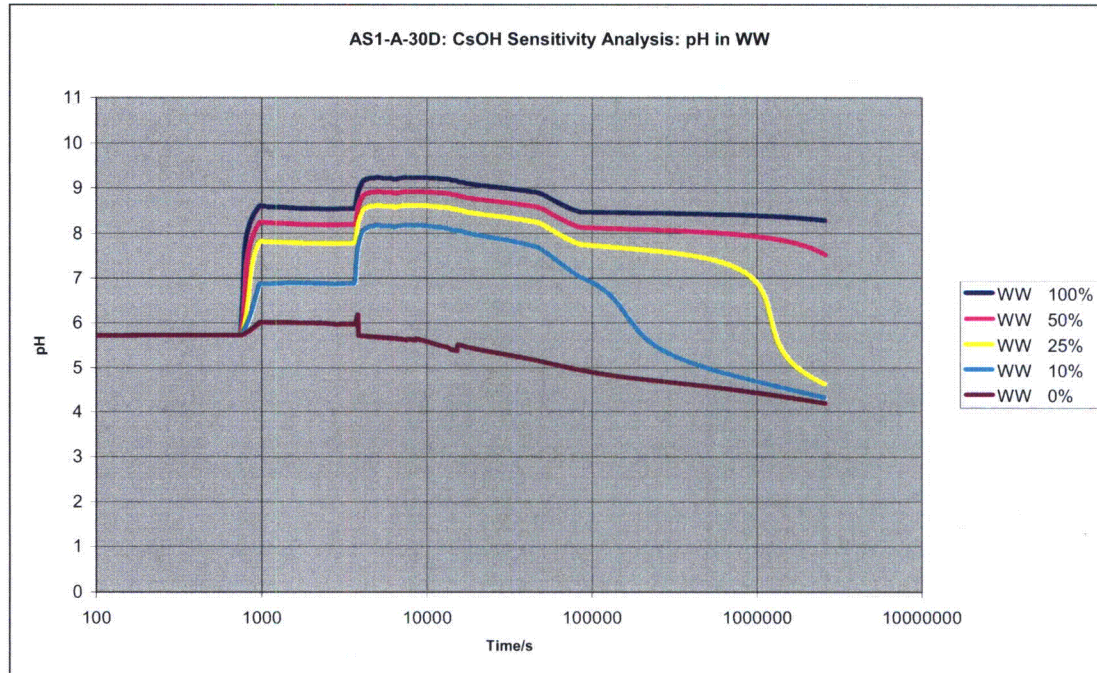


**Figure 10.** *pH in GDCS in AS-1 with scaled amounts of CsOH.*



## 7.4 pH in WW

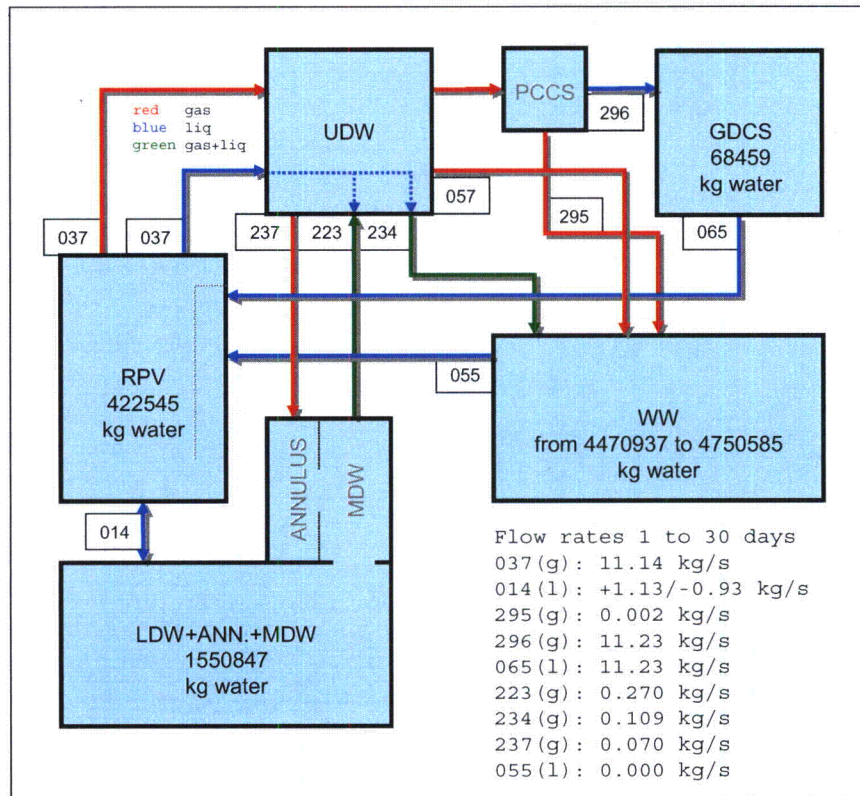
Figure 11 shows the calculated pH in WW in scenario AS-1. The pH in WW becomes permanently less than seven at 260.83 hrs (25 % of CsOH), 24.83 hrs (10 % of CsOH) and 0.0 hrs (0 % of CsOH). With 100 % and 50 % of CsOH the pH remains above seven.



**Figure 11.** *pH in WW in AS-1 with scaled amounts of CsOH.*

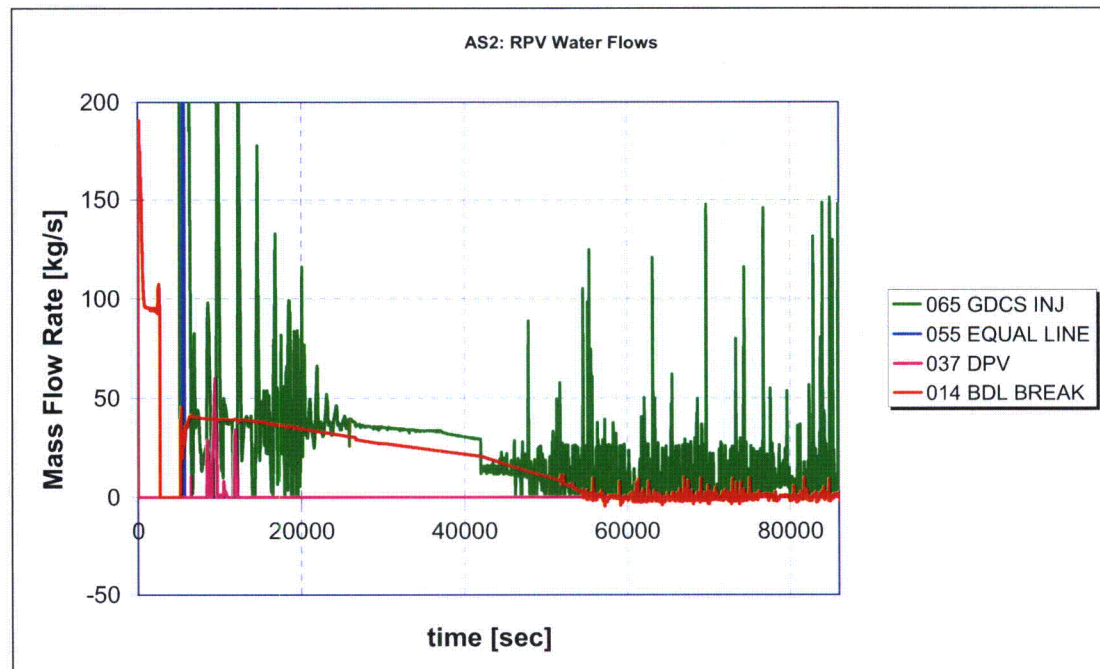
## 8 pH Sensitivity Studies for AS-2

Figure 12 shows the pool masses and flow rates that were used from 24 hours to 720 hours. There is a slow mixing between the RPV and the LDW. Direction of mixing is changed at each time step. There is average net flow of 0.20 kg/s from RPV to LDW. This is balanced by net steam flow of 0.20 kg/s from the LDW (ANNULUS and MDW) to the UDW. The positive and negative flow rates are the average rates taken from the MELCOR flow rates between 36 and 48 hours. During the first day there is also some overflow of water from the RPV to the UDW from where it flows down to the mid-drywell (MDW) and the LDW. Also some water flows to the WW (much less than in AS-1). The LDW becomes full during first day and after that the water flows from the LDW to the MDW and to the ANNULUS (LDW and MDW are connected by flow junction and further MDW and ANNULUS are connected by flow junction). In the ChemSheet pH calculations LDW, MDW and ANNULUS are considered as one volume (their water and gas masses are combined).



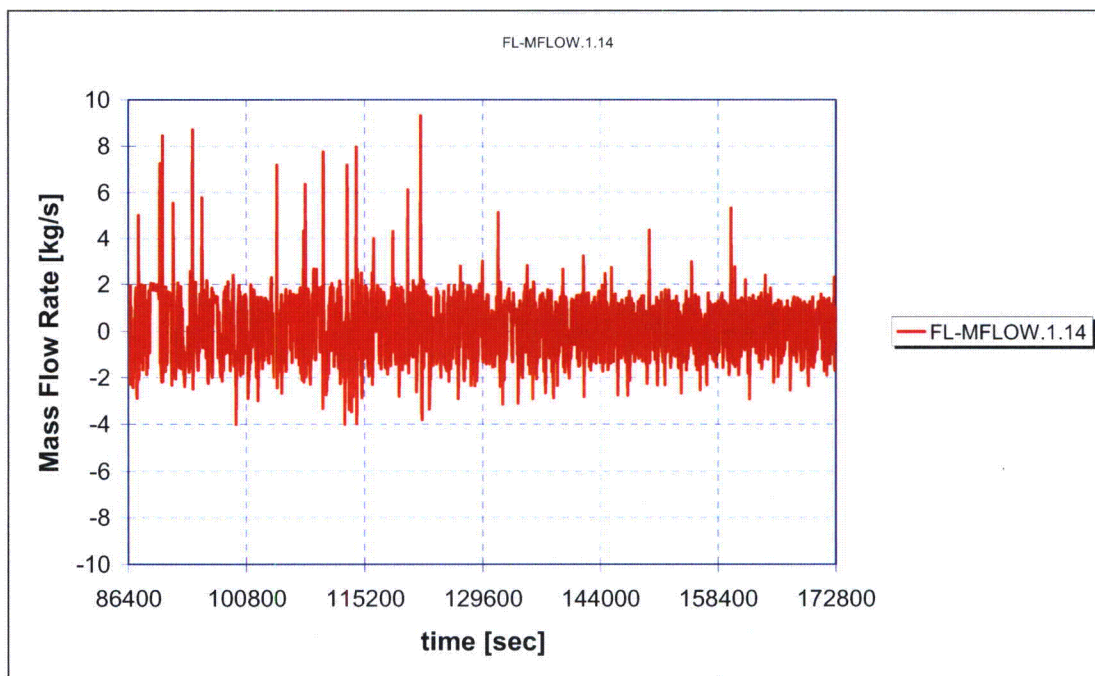
**Figure 12.** Mass flow rates in scenario AS-2 from 1 d to 30 d.

Figure 13a shows MELCOR results of RPV water flow rates in AS-2 from 0 to 24 hours and figure 13b shows MELCOR result for 14 flow rate in AS-2 from 24 to 48 hours. The boron distribution in the RPV and the LDW pools is illustrated in Fig 14.



**Figure 13a.** MELCOR result for RPV water flow rates in AS-2 between 0 and 24 hours.





**Figure 13b.** MELCOR result of BDL break flow rate in AS-2 between 24 and 48 hours. Average positive flow rate between 36 and 48 hours is 1.13 kg/s and average negative flow rate is 0.93 kg/s.

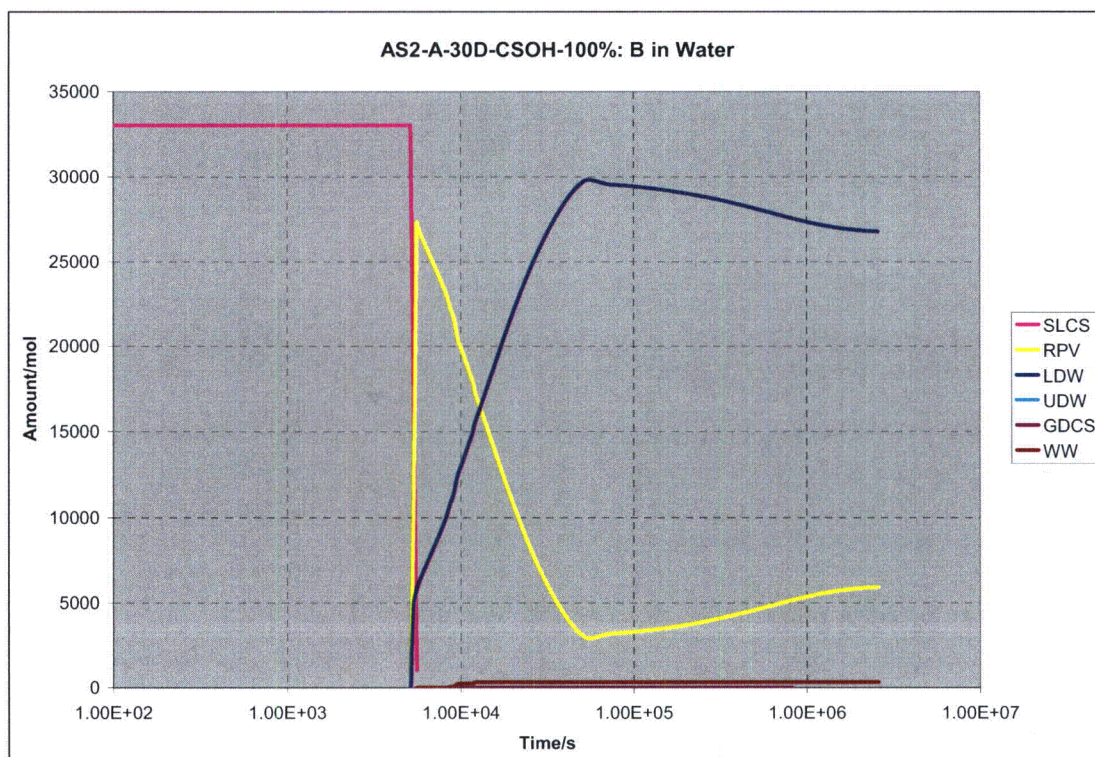


**Figure 14.** The distribution of elementary boron in AS-2. Boron is as boric acid ( $B(OH)_3$ ,  $B(OH)_4(-a)$ ).

Table 8 shows HCl and HNO<sub>3</sub> formation rates in atmosphere in scenario AS-2 (all HNO<sub>3</sub> is formed in UDW and 8 % of HCl in UDW and 92 % in LDW). The dose rates have been scaled up by 125 % from the original dose rates calculated by RADTRAD by GE.

**Table 8.** Scaled formation rates of HCl and HNO<sub>3</sub> in atmosphere in scenario AS-2.

t1	t2	HCl	HNO3	HCl	HNO3
s	s	mol/s	mol/s	mol	mol
1500	2488	4.000E-03	2.588E-05	3.952	0.026
2488	3928	6.500E-03	4.250E-05	9.360	0.061
3928	6088	1.388E-02	6.950E-05	29.970	0.150
6088	7888	1.975E-02	1.463E-04	35.550	0.263
7888	10300	1.813E-02	1.713E-04	43.718	0.413
10300	21100	1.475E-02	1.155E-04	159.300	1.247
21100	29488	1.013E-02	1.235E-04	84.929	1.036
29488	42700	8.250E-03	1.525E-04	108.999	2.015
42700	86400	6.375E-03	1.350E-04	278.588	5.900
86400	172800	5.741E-03	1.216E-04	496.044	10.508
172800	259200	4.750E-03	1.006E-04	410.400	8.694
259200	345600	4.156E-03	8.800E-05	359.100	7.603
345600	432000	3.730E-03	7.900E-05	322.272	6.826
432000	518400	3.404E-03	7.213E-05	294.084	6.232
518400	604800	3.149E-03	6.675E-05	272.052	5.767
604800	691200	2.939E-03	6.225E-05	253.908	5.378
691200	777600	2.766E-03	5.863E-05	239.004	5.065
777600	864000	2.620E-03	5.550E-05	226.368	4.795
864000	950400	2.499E-03	5.288E-05	215.892	4.568
950400	1036800	2.391E-03	5.063E-05	206.604	4.374
1036800	1123200	2.295E-03	4.863E-05	198.288	4.201
1123200	1209600	2.213E-03	4.688E-05	191.160	4.050
1209600	1814400	1.983E-03	4.200E-05	1199.016	25.402
1814400	2419200	1.670E-03	3.538E-05	1010.016	21.395
2419200	2592000	1.670E-03	3.538E-05	288.576	6.113
Total/mol				6937.15	142.08

HNO<sub>3</sub> formations in water pools are calculated from radiation rates of fission products in pools according to equation 5 (total HNO<sub>3</sub> formation in all pools is 479 moles). Table 9 shows the used radiation dose rates and resulting amounts of HNO<sub>3</sub>.

**Table 9.** Radiation rates [rad/hr] and resulting amounts of HNO<sub>3</sub> in pools in scenario AS-2 (total formation in all pools is 479 mol).

t/s	WW/rad/h	GD/CS/rad/h	LDW/rad/h	RPV/rad/h
2500	10152.596	29.296	9262.117	0.000
3600	10695.882	5497.976	9011.970	0.000
6052	50792.005	49271.200	459180.005	30448.720
7200	52959.608	53564.279	376335.681	26920.940
10800	49906.697	56948.841	232555.932	28737.254
14400	47663.403	57696.744	175778.402	33063.158
21600	46316.068	53458.928	152675.216	38645.072
28800	44371.310	48076.146	138083.026	42338.562
43200	41058.529	20185.190	134070.362	60777.424
86400	31290.827	1972.230	106315.953	117600.639
172800	14599.804	919.828	50365.044	55203.772
259200	11004.011	693.054	38283.694	41749.833
345600	9325.745	587.136	32633.010	35465.756
432000	8347.188	525.356	29333.164	31799.581
720000	6811.330	428.365	24142.426	26040.573
1080000	6043.429	379.862	21538.272	23157.347
1440000	5650.989	355.073	20203.400	21682.113
1800000	5408.586	339.761	19376.872	20770.010
2160000	5241.870	329.231	18807.256	20142.191
2520000	5118.987	321.469	18386.665	19679.111
2592000	4369.273	274.132	15798.971	16844.253
HNO3/mol in 30 d	192.452	2.554	221.408	62.372

Sum of HNO<sub>3</sub> formation in UDW atmosphere and in water pools during 30 days is 621 moles.

Tables 10 and 11 show the formation rates of CsOH and CsI that were calculated from MELCOR results.

**Table 10.** *CsOH formation rates [kg/s] in pools in scenario AS-2 (total formation is 173.5 kg).*

t/s	WW/kg/s	GDCS/kg/s	LDW/kg/s	RPV/kg/s
0	0	0	0	0
1484.075	0.003734	1.9E-07	0	0.01687
2390.61	0.001212	1.93E-05	0	0
2646.199	0.007295	0.009421	0.000527	0
2830.06	0.011461	0.012629	0.000269	0
4470.172	0.024597	0.001792	0.005392	0
4635.07	0.022193	0.002458	0.019233	0
5145.074	0.09684	0.023747	0.013753	0
5325.033	0.015554	0.011156	0.003892	0.000204
6340.306	0.015978	0	0.002053	0.000658
7100.181	0.002178	0	0.001101	0.000185
9810.098	0.000485	0	0	0.000182
12555.05	0	0	0	0.000202
26775.1	0	0	0	0
86415.41	0	0	0	0
87000	0	0	0	0
Total/kg	91.80	39.60	22.21	19.87

**Table 11.** *CsI formation rates [kg/s] in pools in scenario AS-2 (total formation is 26.5 kg).*

t/s	WW/kg/s	GDCS/kg/s	LDW/kg/s	RPV/kg/s
0	0	0	0	0
1484.075	0.000557	2.83E-08	0	0.001819
2390.61	0.000182	2.89E-06	0	0
2646.199	0.001104	0.001428	7.58E-05	0
2830.06	0.001737	0.001968	4.22E-05	0
4470.172	0.003696	0.000291	0.000841	0
4635.07	0.003335	0.000256	0.002999	0
5145.074	0.015627	0.003257	0.002146	0
5325.033	0.002468	0.001671	0.000348	0.000148
6340.306	0.002477	0	0.000323	0.000132
7100.181	0.00034	0	0.00025	3.69E-05
9810.098	9.05E-05	0	0	3.64E-05
12555.05	0	0	0	4.92E-05
26775.1	0	0	0	0
86415.41	0	0	0	0
87000	0	0	0	0
Total/kg	14.29	5.95	3.41	2.80



Figures 15 and 16 show the calculated CsOH and CsI masses in pools (including the formation rates and the mixing effect). Results for LDW include also CsOH and CsI in annulus and Middle Drywell.

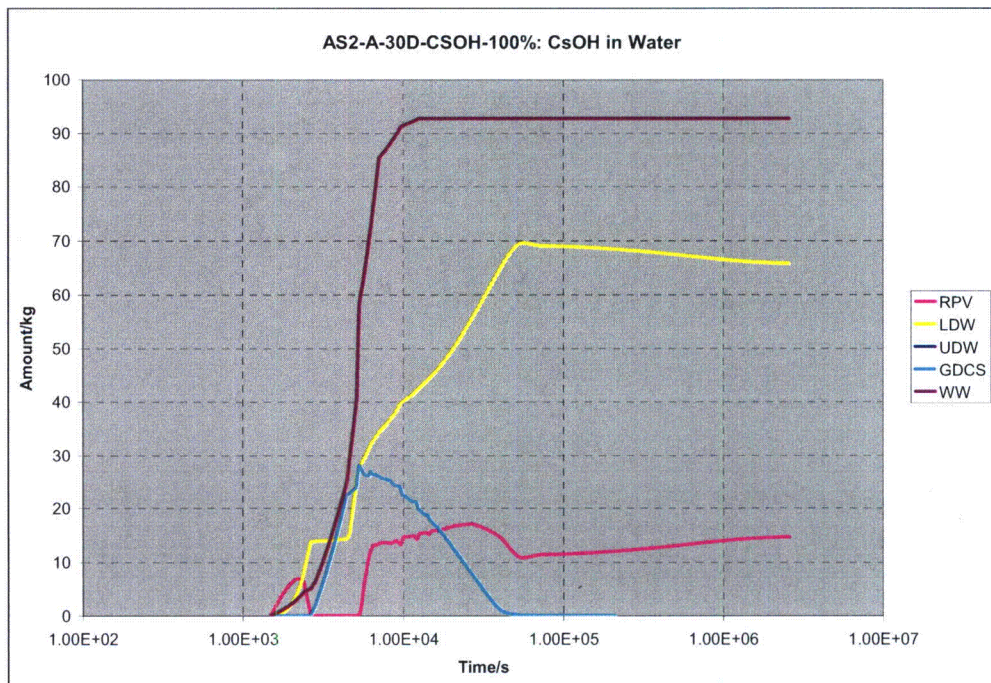


**Figure 15.** Calculated CsOH(a) amounts in pools in scenario AS-2 as a function of time.

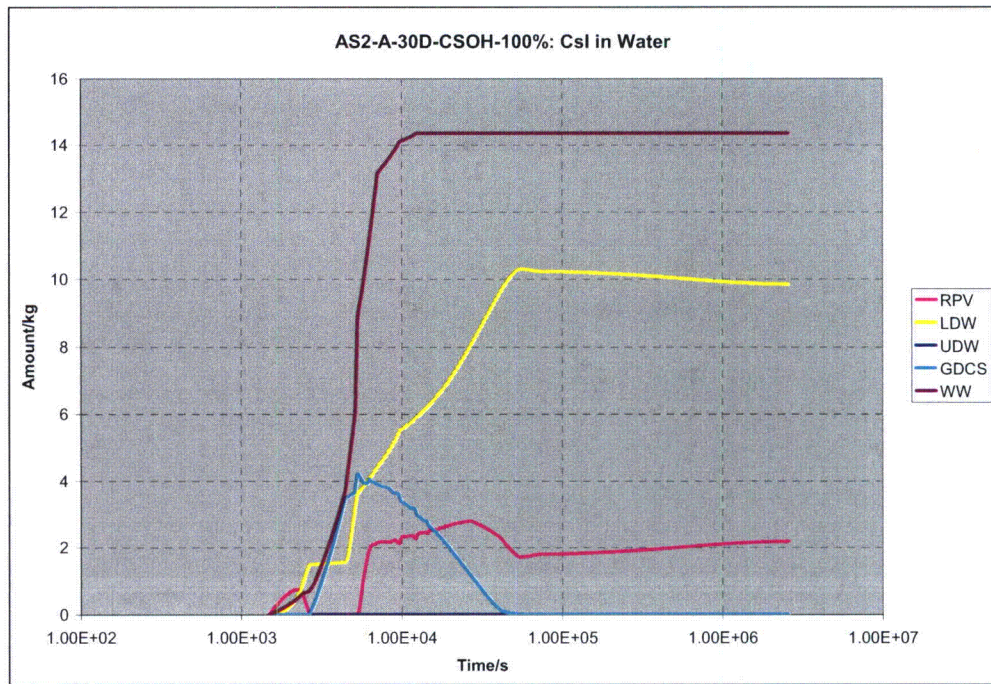


**Figure 16.** Calculated CsI(a) amounts in pools in scenario AS-2 as a function of time.



Figures 17 and 18 show the calculated molar amounts of HCl and HNO<sub>3</sub> in the pools (including the formation rates and the mixing effect).

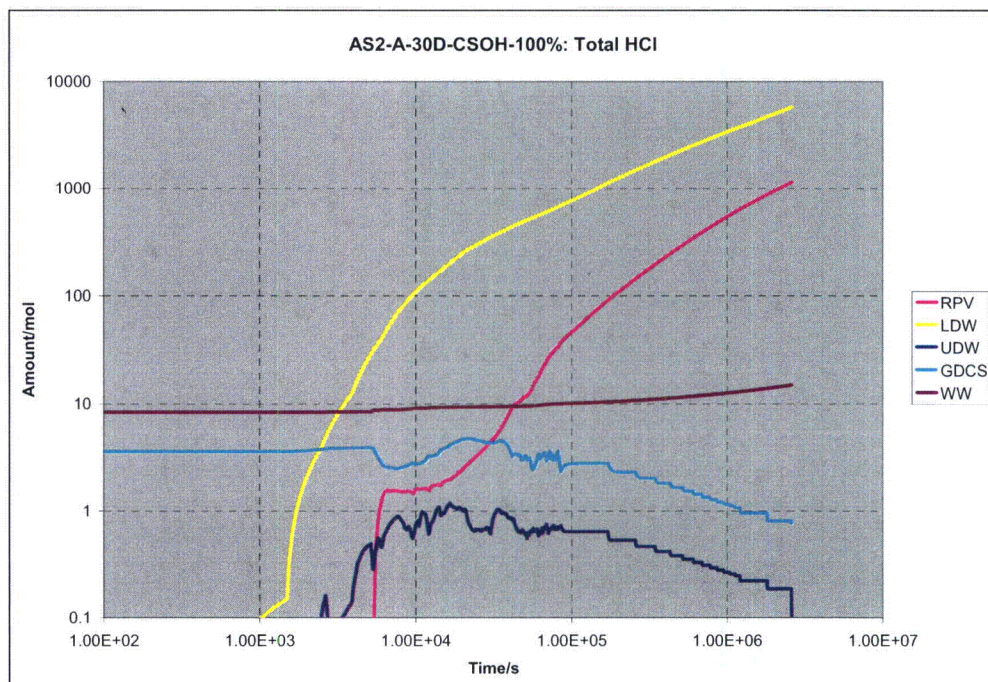


**Figure 17.** Calculated gaseous (in UDW) and aqueous HCl (others) amounts in scenario AS-2 as a function of time.

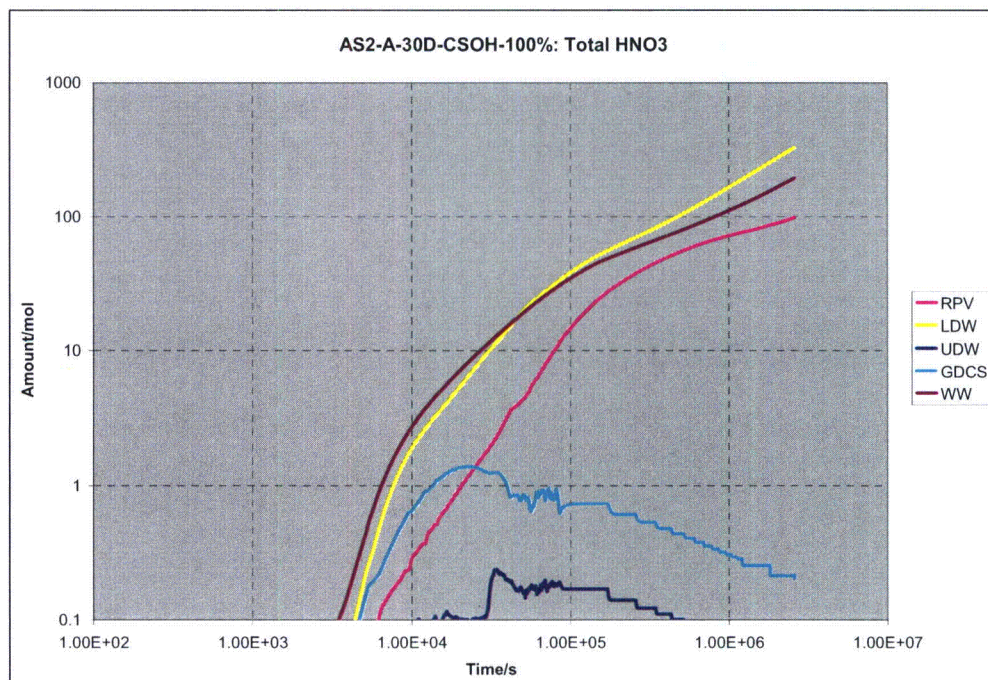


**Figure 18.** Calculated gaseous (in UDW) and aqueous HNO<sub>3</sub> (others) amounts in scenario AS-2 as a function of time.

## 8.1 pH in RPV

Figure 19 shows the calculated pH in RPV in scenario AS-2. In AS-2 scenario the RPV Lower Head becomes empty of coolant prior to reflooding due to higher pressure difference between the RPV and the containment. RPV is dry from 2436 s to 5145 s, during which period pH can not be estimated in the RPV. This can be seen as cut-off in the pH curve in Fig. 19. In AS-1 the Lower Head does not dry out prior to reflooding due to lower driving pressure difference than in AS-2. The pH in RPV becomes permanently less than seven at 712.17 hrs (100 % of CsOH), 670.17 hrs (50 % of CsOH), 649.50 hrs (25 % of CsOH), 636.84 hrs (10 % of CsOH) and 628.17 hrs (0 % of CsOH).

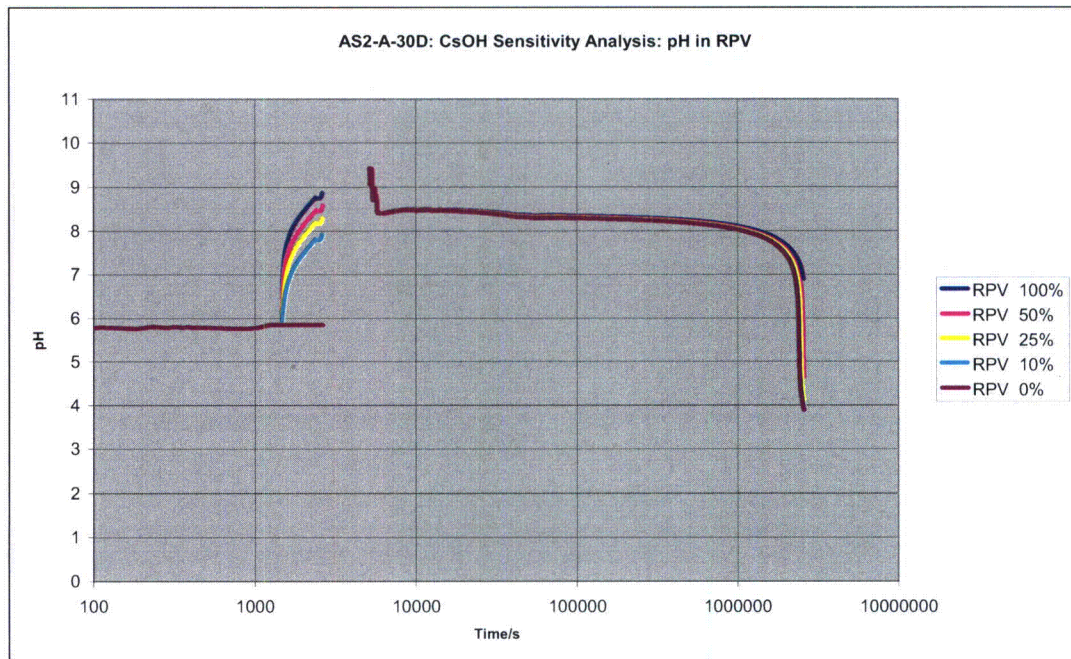


**Figure 19.** *pH in RPV in AS-2 with scaled amounts of CsOH.*



## 8.2 pH in LDW

Figure 20 shows the calculated pH in LDW in scenario AS-2. The pH in LDW becomes permanently less than seven at 623.50 hrs (100 % of CsOH), 582.17 hrs (50 % of CsOH), 560.84 hrs (25 % of CsOH), 548.84 hrs (10 % of CsOH) and 540.17 hrs (0 % of CsOH).

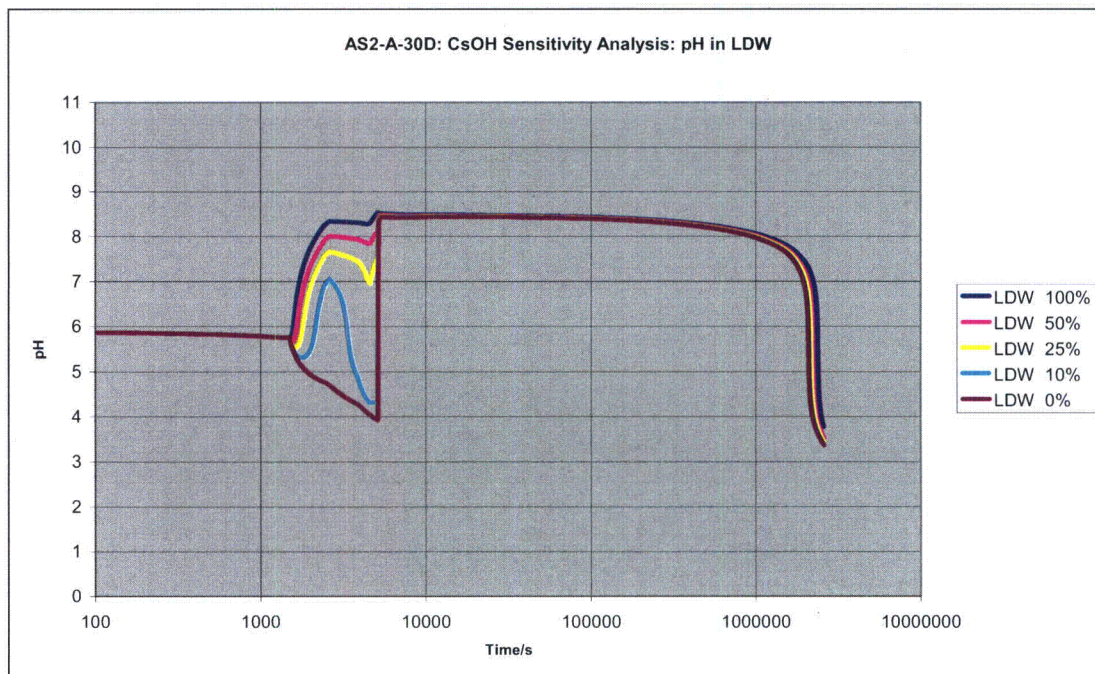


**Figure 20.** *pH in LDW in AS-2 with scaled amounts of CsOH.*

### 8.3 pH in GDCS

Figure 21 shows the calculated pH in GDCS in scenario AS-2. The pH in GDCS becomes permanently less than seven at 11.57 hrs (100 % of CsOH), 10.42 hrs (50 % of CsOH), 9.18 hrs (25 % of CsOH), 6.68 hrs (10 % of CsOH) and 0.0 hrs (0 % of CsOH).

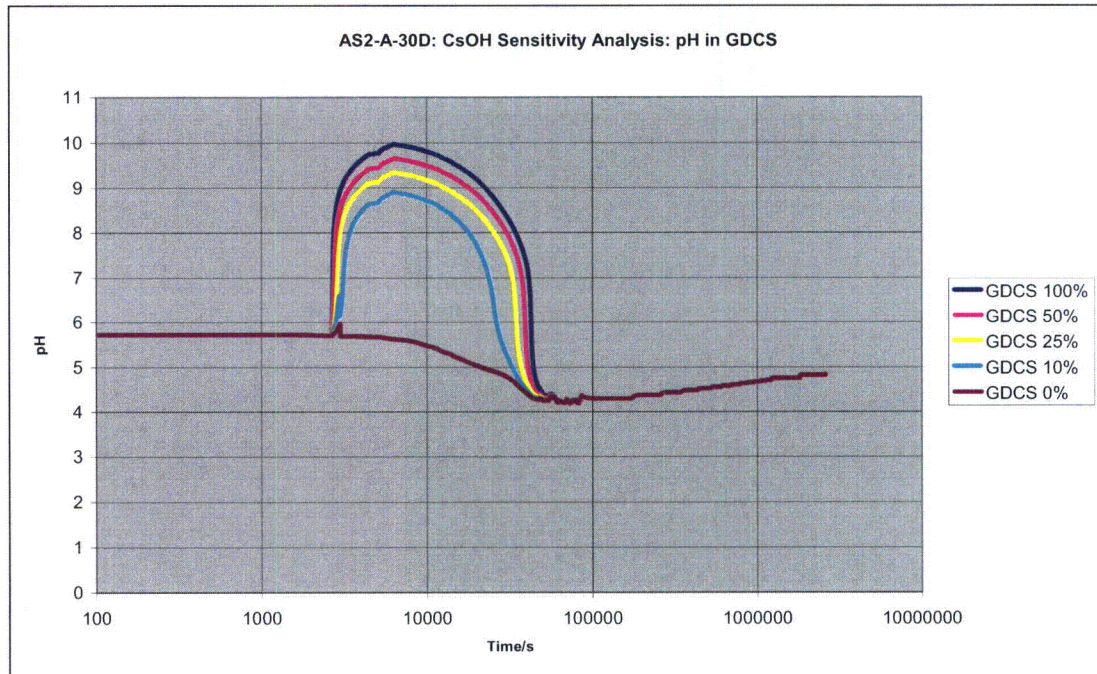


**Figure 21.** *pH in GDCS in AS-2 with scaled amounts of CsOH.*

## 8.4 pH in WW

Figure 22 shows the calculated pH in WW in scenario AS-2. The pH in WW becomes permanently less than seven at 717.50 hrs (25 % of CsOH), 242.84 hrs (10 % of CsOH) and 40.17 hrs (0 % of CsOH). With 100 % and 50 % of CsOH the pH remains over seven.

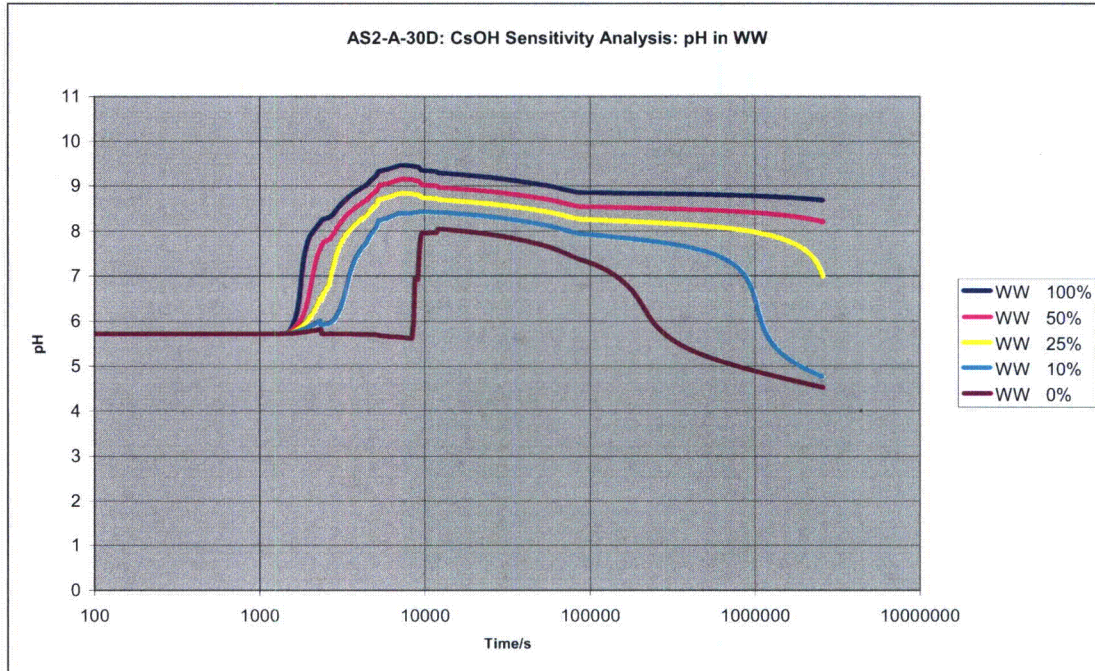
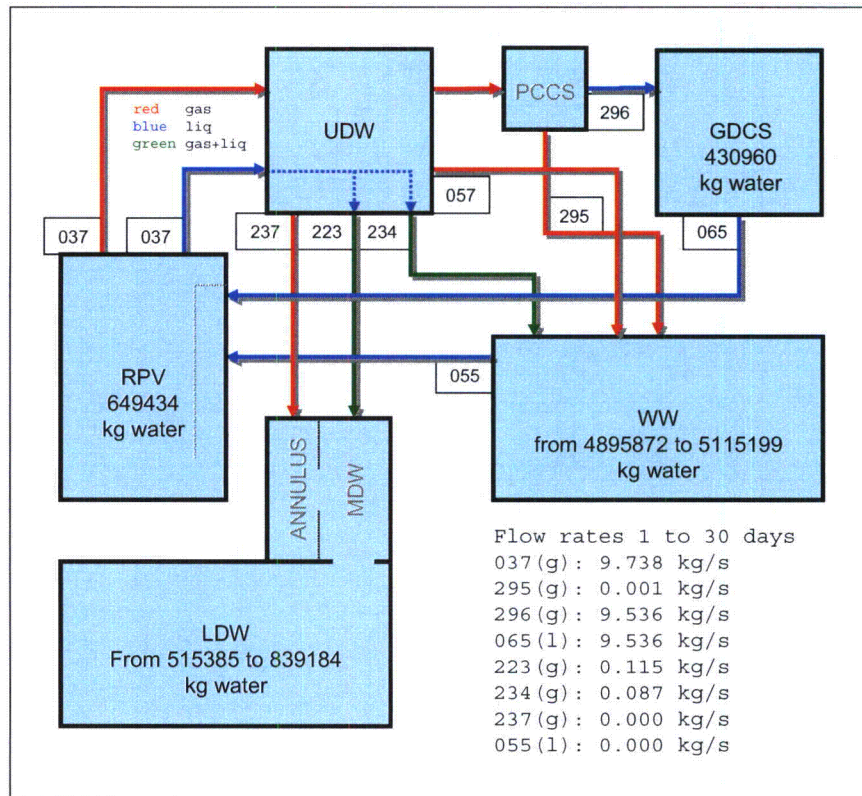


**Figure 22.** pH in the WW in AS-2 with scaled amounts of CsOH.



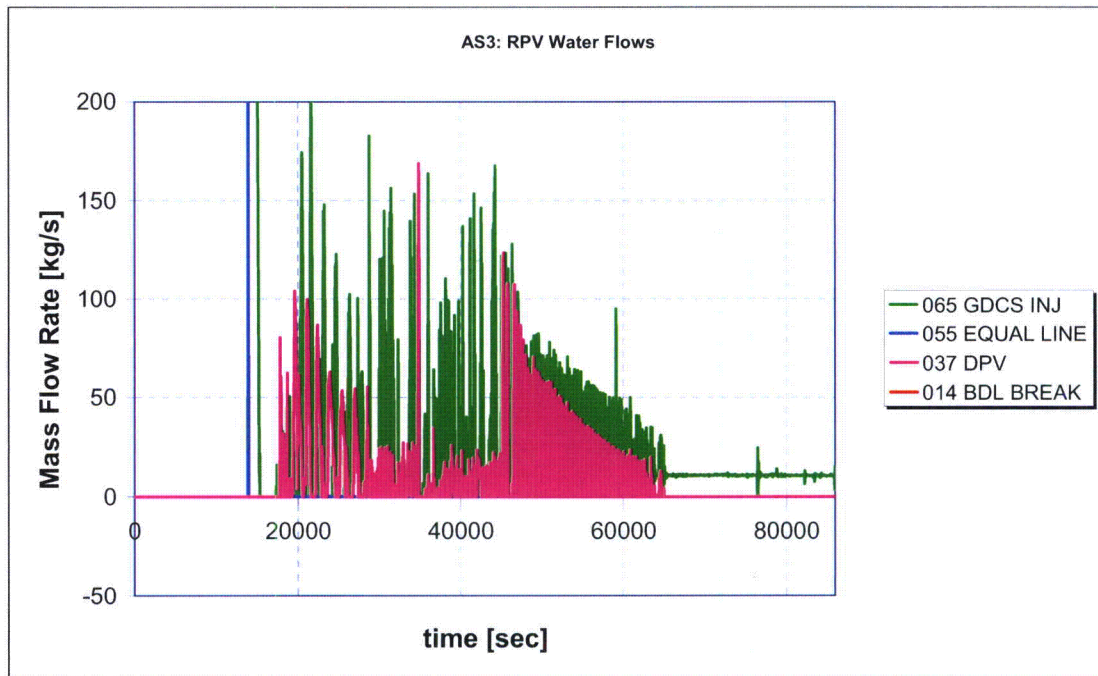
## 9 pH Sensitivity Studies for AS-3

Figure 23 shows the pools masses and the flow rates that were used from 24 hours to 720 hours. There is no break at the bottom of RPV but there is water flow from the RPV to the UDW (through the DPVs (flow path 037 in Fig 23) from where the water flows to the LDW (223) and WW (234). The water flow from RPV ends after 1st day and after that there is only gas (steam) flow from the RPV to the UDW and from the UDW to the LDW and the WW (between 126000 and 138000 seconds there is short period of water flow – from the extended MELCOR simulation between 1<sup>st</sup> day and 2<sup>nd</sup> day). Because of the average steam flow of 0.115 kg/s from the UDW to the LDW (where it condenses) the water mass of the LDW is increased by 323937 kg during 29 days (this includes the water flow between 126000-138000s).



**Figure 23.** Flow values in scenario AS-3 from 1 d to 30 d.

Figure 24a shows MELCOR results of RPV water flow rates in AS-3 from 0 to 24 hours and figure 24b shows MELCOR result for 037, 223 and 234 integrated water flows from 0 to 48 hours.



**Figure 24a.** MELCOR result for RPV water flow rates in AS-3 between 0 and 24 hours.

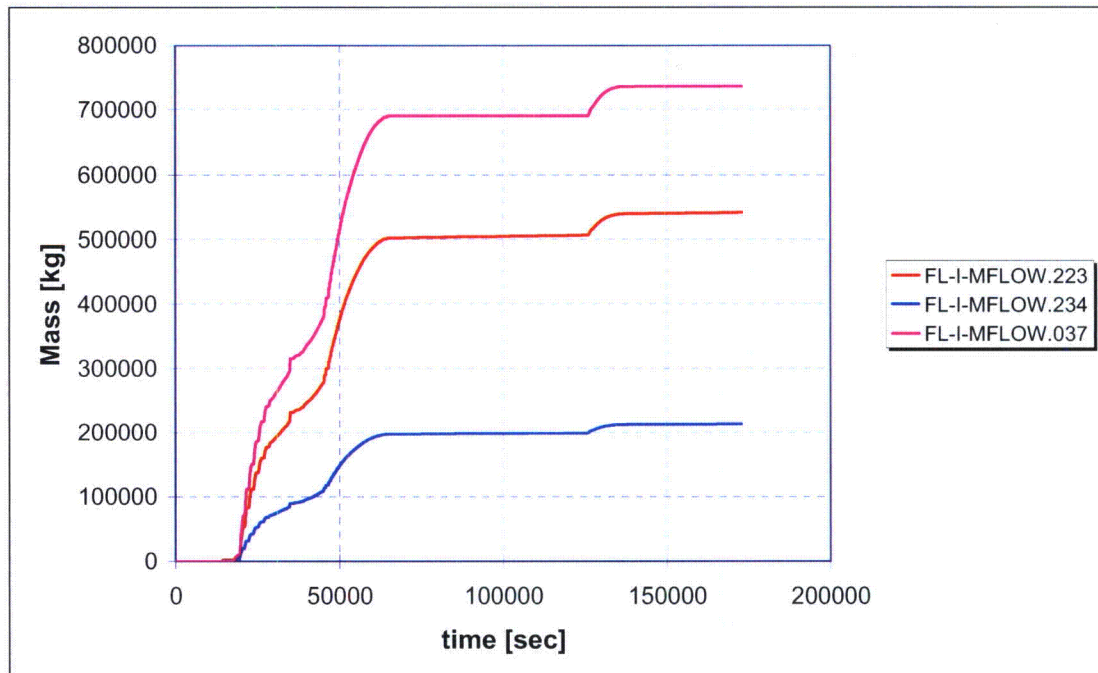


**Figure 24b.** MELCOR result for 037, 223 and 234 integrated water flows in scenario AS-3 between 0 and 48 hours. This figure shows that water flow from RPV to UDW (037 flow) is divided between LDW (223 flow between UDW and LDW) and WW (234 flow between UDW and LDW)) in 0.72/0.28 ratio (at 65000 s) and that integrated mass of combined 223 and 234 flow is 1.4 % more than integrated mass of 037 flow. This difference is explained by condensation of steam in UDW that contributes to the 223 and 234 water flows. After 65000 s there is water flow from RPV to UDW only between 126000 and 138000 s (which has also been included to ChemSheet pH model).



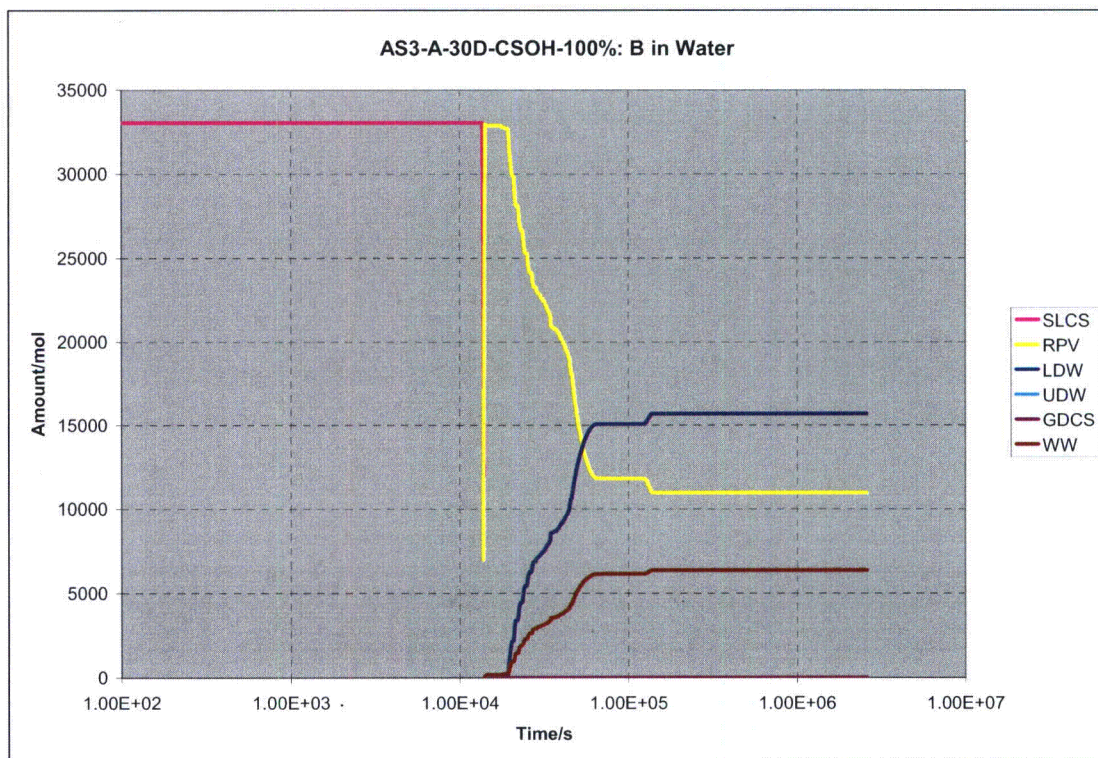


**Figure 25.** The distribution of elementary boron in AS-3. Boron is as boric acid ( $B(OH)_3$ ,  $B(OH)_4(-a)$ ).

Table 12 shows HCl and  $HNO_3$  formation rates in atmosphere in scenario AS-3 (all  $HNO_3$  is formed in UDW and 8 % of HCl in UDW and 92 % in LDW). The dose rates have been scaled up by 125 % from the original dose rates calculated by RADTRAD by GE.



**Table 12.** Scaled formation rates of HCl and HNO<sub>3</sub> in atmosphere in scenario AS-3.

t1	t2	HCl	HNO <sub>3</sub>	HCl	HNO <sub>3</sub>
s	s	mol/s	mol/s	mol	mol
6600	7588	4.000E-03	2.588E-05	3.952	0.026
7588	9028	6.500E-03	4.250E-05	9.360	0.061
9028	11188	1.388E-02	6.950E-05	29.970	0.150
11188	12988	1.975E-02	1.463E-04	35.550	0.263
12988	15400	1.813E-02	1.713E-04	43.718	0.413
15400	26200	1.475E-02	1.155E-04	159.300	1.247
26200	34588	1.013E-02	1.235E-04	84.929	1.036
34588	47800	8.250E-03	1.525E-04	108.999	2.015
47800	86400	6.375E-03	1.350E-04	246.075	5.211
86400	172800	5.741E-03	1.216E-04	496.044	10.508
172800	259200	4.750E-03	1.006E-04	410.400	8.694
259200	345600	4.156E-03	8.800E-05	359.100	7.603
345600	432000	3.730E-03	7.900E-05	322.272	6.826
432000	518400	3.404E-03	7.213E-05	294.084	6.232
518400	604800	3.149E-03	6.675E-05	272.052	5.767
604800	691200	2.939E-03	6.225E-05	253.908	5.378
691200	777600	2.766E-03	5.863E-05	239.004	5.065
777600	864000	2.620E-03	5.550E-05	226.368	4.795
864000	950400	2.499E-03	5.288E-05	215.892	4.568
950400	1036800	2.391E-03	5.063E-05	206.604	4.374
1036800	1123200	2.295E-03	4.863E-05	198.288	4.201
1123200	1209600	2.213E-03	4.688E-05	191.160	4.050
1209600	1814400	1.983E-03	4.200E-05	1199.016	25.402
1814400	2419200	1.670E-03	3.538E-05	1010.016	21.395
2419200	2592000	1.670E-03	3.538E-05	288.576	6.113
Total/mol				6904.64	141.39

HNO<sub>3</sub> formations in water pools are calculated from radiation rates of fission products in pools according to equation 5 (total HNO<sub>3</sub> formation in all pools is 516 moles). Table 13 shows the used radiation dose rates and resulting HNO<sub>3</sub> formations.

**Table 13.** Radiation dose rates [rad/hr] and resulting amounts of HNO<sub>3</sub> in the pools in scenario AS-3 (total in all pools 516 mol).

t/s	WW/rad/h	GDGS/rad/h	LDW/rad/h	RPV/rad/h
2500	0.000	0.000	0.000	0.000
3600	0.000	0.000	0.000	0.000
6052	6127.318	0.001	0.000	22162.451
7200	7549.154	5.008	0.000	62148.650
10800	88341.805	346.975	0.000	279288.724
14400	91820.717	1605.105	8846034.69	52016.944
21600	87677.290	10995.218	436165.760	25757.697
28800	84098.507	12665.150	217644.595	22014.211
43200	79277.379	10039.986	151253.517	20620.199
86400	63375.371	3600.313	73589.889	14625.210
172800	30087.097	1699.401	35100.751	6996.650
259200	22903.036	1290.303	26794.590	5351.084
345600	19547.732	1099.989	22919.529	4584.365
432000	17589.481	989.138	20658.750	4137.260
720000	14510.099	815.149	17103.630	3434.288
1080000	12965.128	728.016	15319.018	3081.298
1440000	12172.936	683.385	14403.267	2900.066
1800000	11682.252	655.759	13835.651	2787.672
2160000	11343.971	636.723	13444.085	2710.098
2520000	11094.110	622.667	13154.699	2652.742
2592000	9553.741	536.085	11364.943	2297.082
HNO <sub>3</sub> /mol in 30 d	433.577	2.699	66.368	13.753

Sum of HNO<sub>3</sub> formation in UDW atmosphere and in water pools during 30 days is 657 moles.

Tables 14 and 15 show the formation rates of CsOH and CsI that were calculated from MELCOR results.

**Table 14.** *CsOH formation rates [kg/s] in pools in scenario AS-3 (total formation is 202.9 kg).*

t/s	WW/kg/s	GDCS/kg/s	LDW/kg/s	RPV/kg/s
0	0	0	0	0
5185.235	0.00286	0	0	0.001574
5255.131	0.011101	0	0	0.000529
6200.095	0	0	0	0.000672
6600.375	0.00288	2.6E-06	0	0.002519
7045.381	0.030553	4.85E-05	0	0.002244
8696.114	0.035215	8.12E-05	0	8.81E-05
11340.28	0.001763	8.26E-05	0	0.000292
13815.03	0.012062	0.000809	0	0.000376
13950.65	0.009514	0.001068	0.039016	0
14220.03	0.000656	0.000299	0.000522	8.43E-05
18360.58	0.000469	0.000545	0.000681	0
25200.16	5.69E-05	0	2.55E-05	0
56625.29	0	0	0	0
86400.38	0	0	0	0
87000	0	0	0	0
Total/kg	171.80	5.86	18.13	7.06

**Table 15.** *CsI formation rates [kg/s] in pools in scenario AS-3 (total formation is 32.0 kg).*

t/s	WW/kg/s	GDCS/kg/s	LDW/kg/s	RPV/kg/s
0	0	0	0	0
5185.235	0.000362	0	0	0.001054
5255.131	0.001412	0	0	9.13E-05
6200.095	0	0	0	5.04E-05
6600.375	0.000437	3.89E-07	0	0.000368
7045.381	0.004579	7.26E-06	0	0.000348
8696.114	0.005729	1.22E-05	0	3.88E-06
11340.28	0.000295	1.31E-05	0	1.74E-08
13815.03	0.001526	0.000135	0	0.000514
13950.65	0.001484	0.000167	0.005125	0
14220.03	0.000102	5.21E-05	0.000135	6.09E-05
18360.58	7.32E-05	0.000102	0.000119	0
25200.16	1.23E-05	0	0	0
56625.29	0	0	0	0
86400.38	0	0	0	0
87000	0	0	0	0
Total/kg	26.91	1.06	2.75	1.25

Figures 26 and 27 show the calculated CsOH and CsI masses in pools (including the formation rates and the mixing effect).

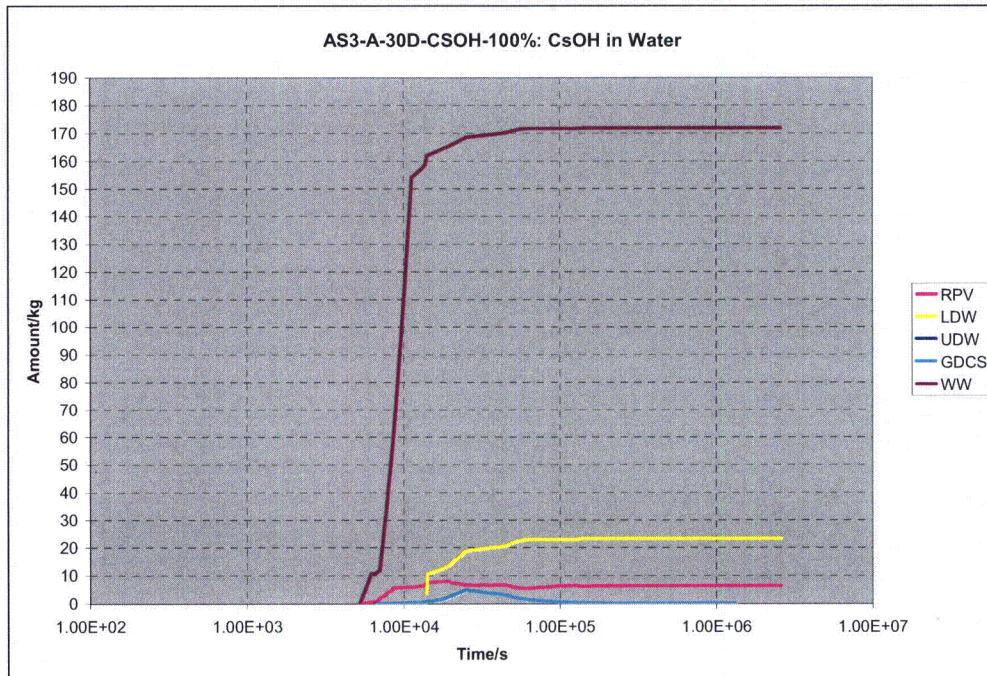


**Figure 26.** Calculated amounts of CsOH(a) in pools in scenario AS-3 as a function of time.

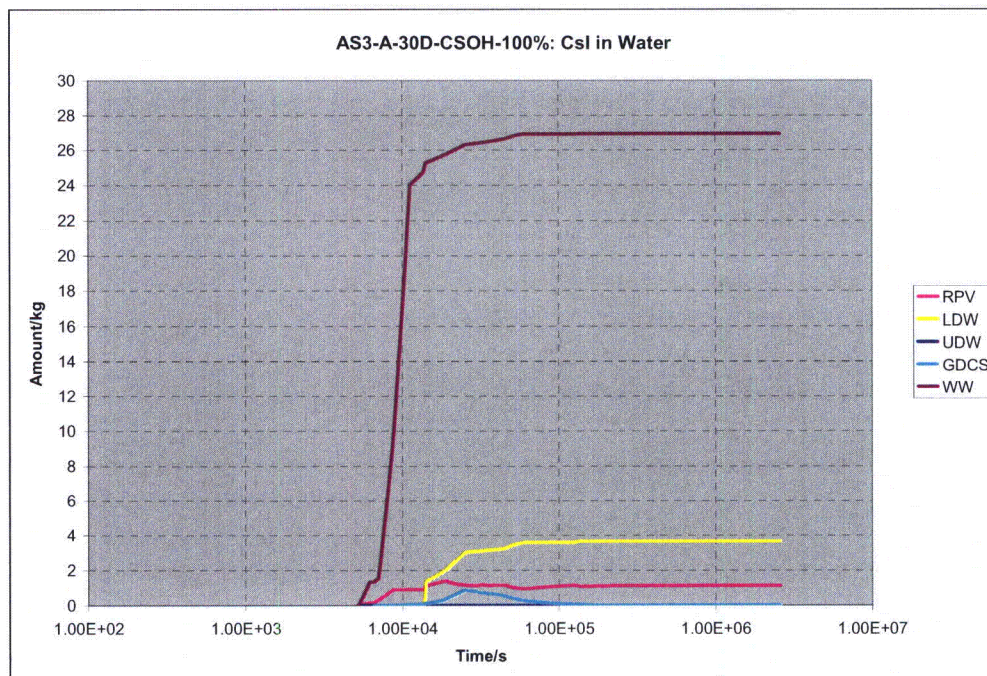


**Figure 27.** Calculated amounts of CsI(a) in pools in scenario AS-3 as a function of time.



Figures 28 and 29 show the calculated molar amounts of HCl and HNO<sub>3</sub> in the pools (including the formation rates and the mixing effect).

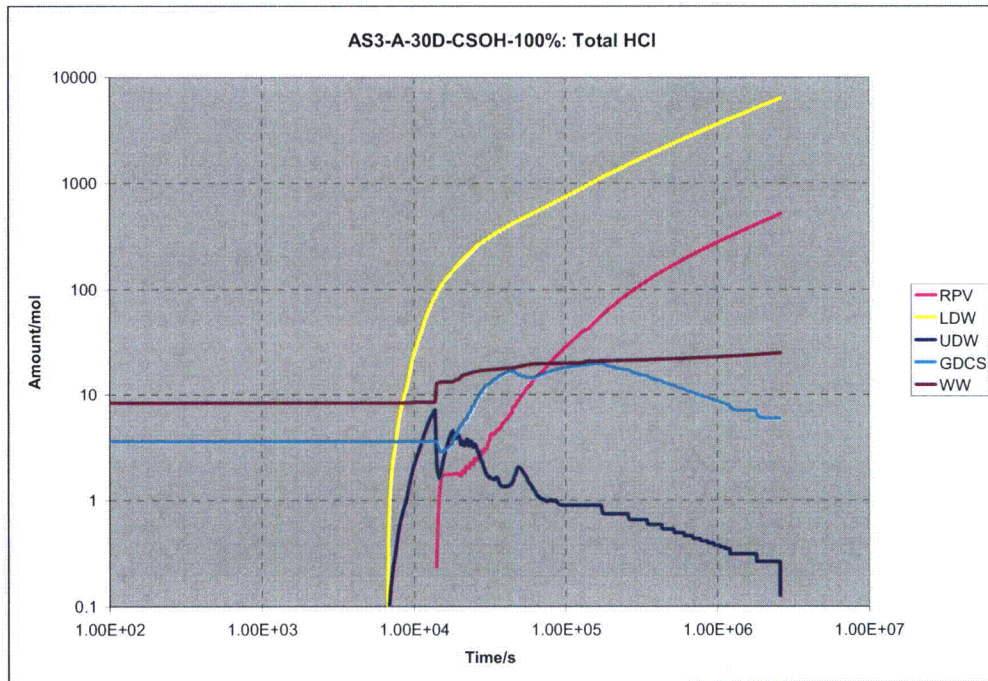


**Figure 28.** Calculated gaseous (in UDW) and aqueous HCl (others) amounts in scenario AS-3 as a function of time.

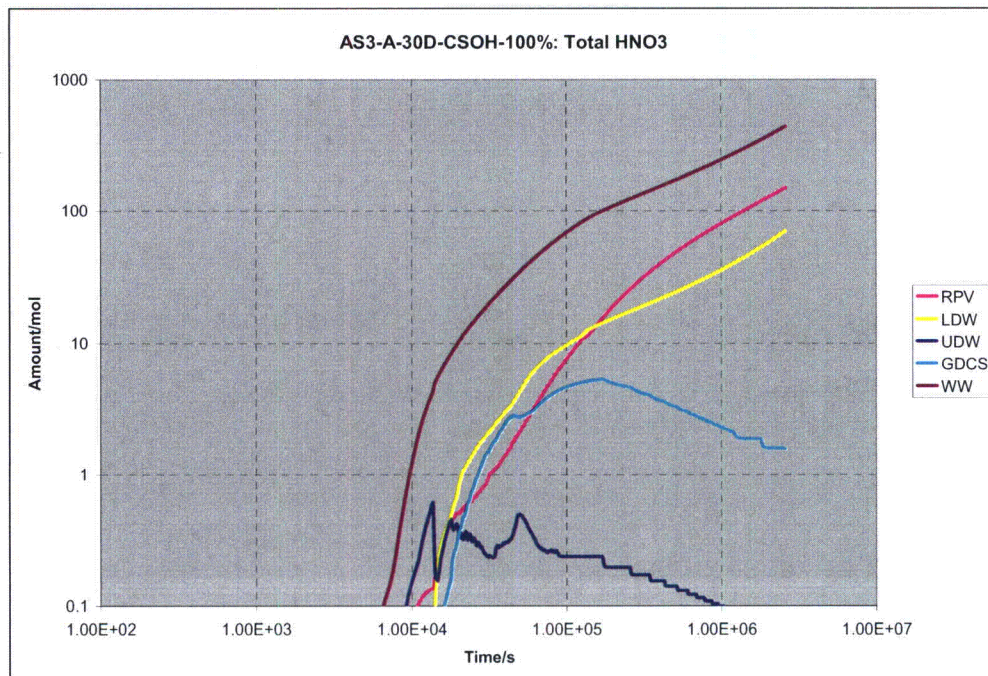


**Figure 29.** Calculated gaseous (in UDW) and aqueous HNO<sub>3</sub> (others) amounts in scenario AS-3 as a function of time.

## 9.1 pH in RPV

Figure 30 shows the calculated pH in RPV in scenario AS-3. The pH in RPV stays over seven to 720 hrs (because of sodium pentaborate from SLCS after 13800 s).

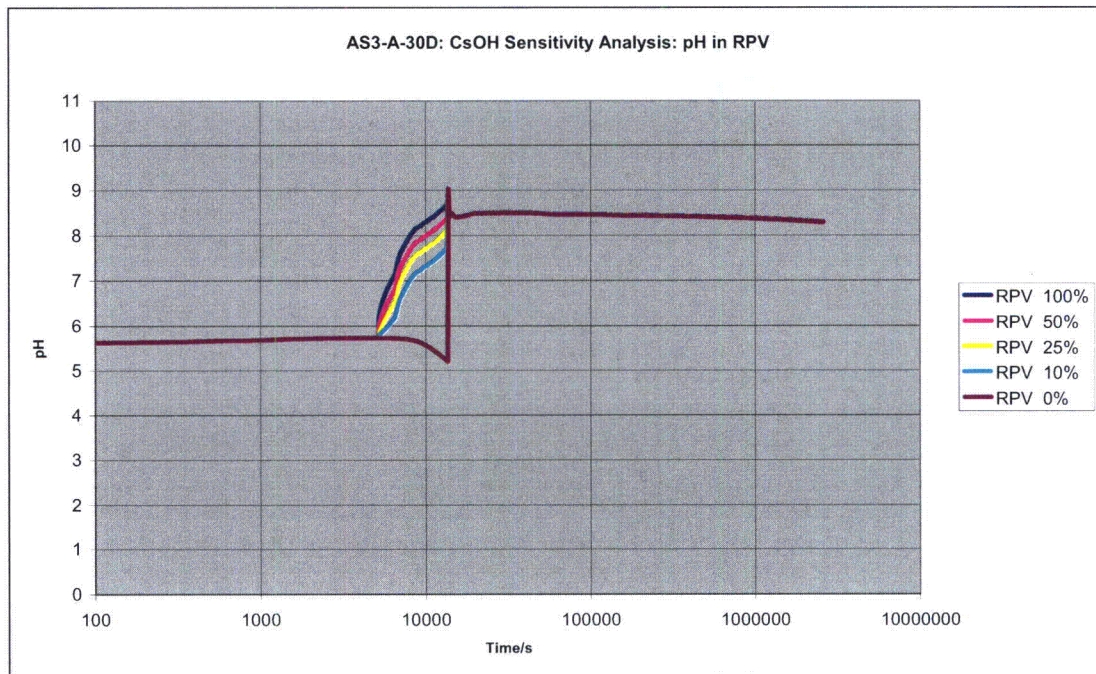


**Figure 30.** *pH in RPV in AS-3 with scaled amounts of CsOH.*



## 9.2 pH in LDW

Figure 31 shows the calculated pH in the RPV in scenario AS-3. LDW is dry until 13800s. The pH in LDW becomes permanently less than seven at 219.50 hrs (100 % of CsOH), 210.83 hrs (50 % of CsOH), 206.83 hrs (25 % of CsOH), 204.17 hrs (10 % of CsOH) and 202.17 hrs (0 % of CsOH). In AS-3 scenario there is less sodium pentaborate in the LDW than in AS-1 and AS-2 scenarios which make AS-3 more sensitive to HCl and HNO<sub>3</sub> formation.

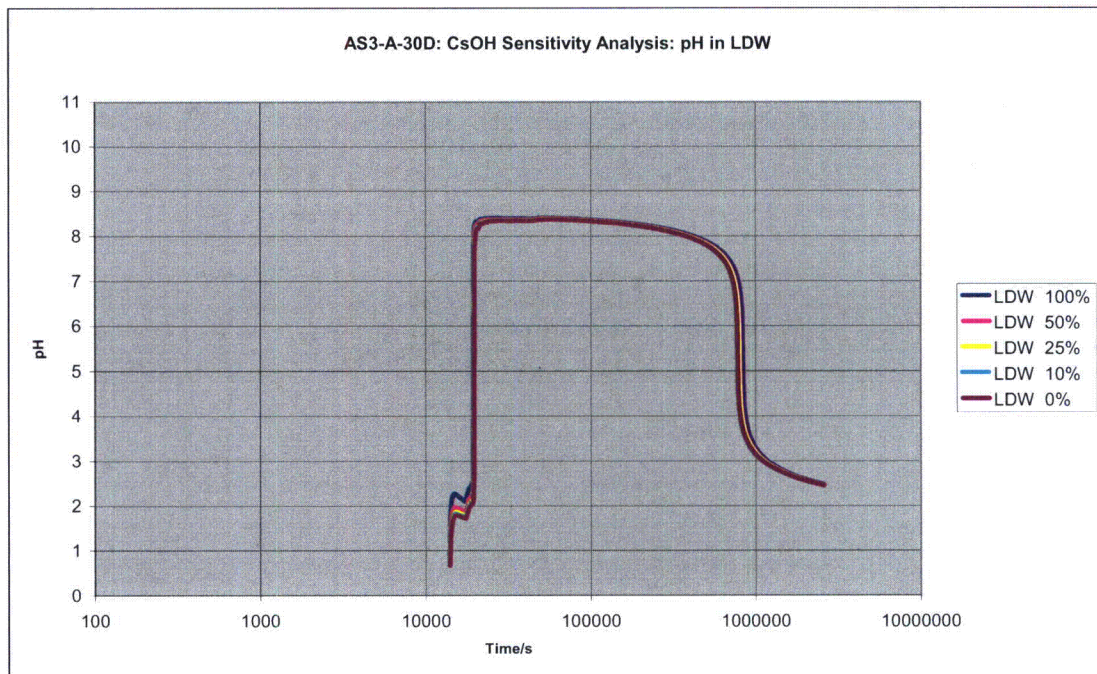


**Figure 31.** pH in LDW in AS-3 with scaled amounts of CsOH.

### 9.3 pH in GDCS

Figure 32 shows the calculated pH in GDCS in scenario AS-3. The pH in GDCS becomes permanently less than seven at 12.52 hrs (100 % of CsOH), 8.58 hrs (50 % of CsOH) and 0.0 hrs (25 %, 10 % and 0 % of CsOH).

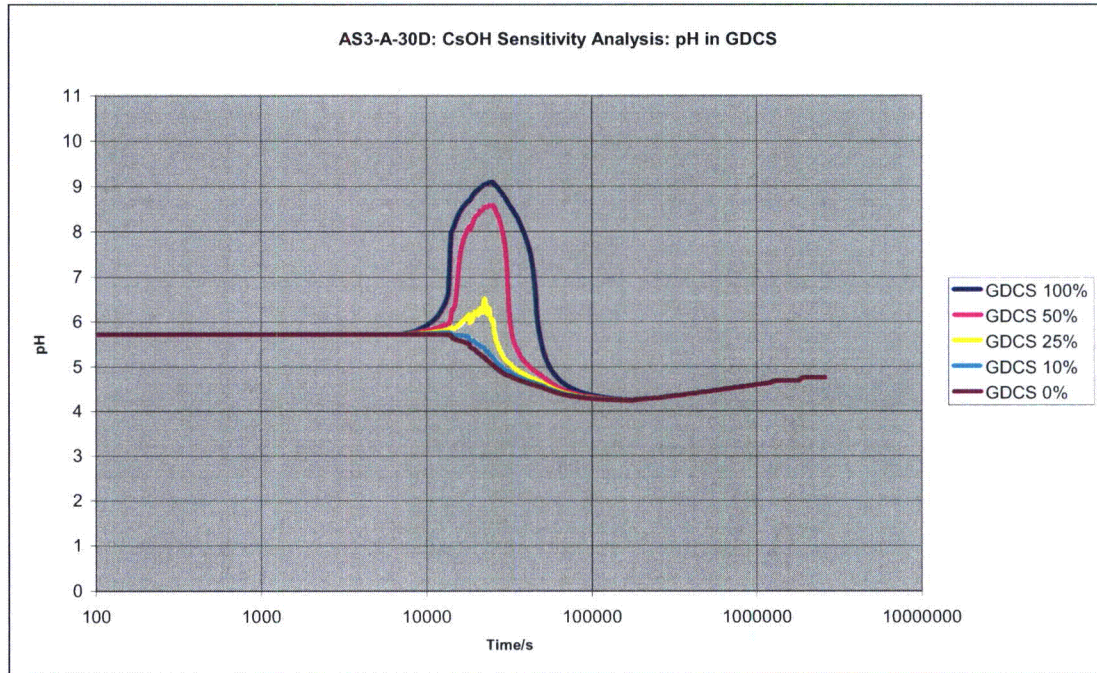


**Figure 32.** *pH in GDCS in AS-3 with scaled amounts of CsOH.*



## 9.4 pH in WW

Figure 33 shows the calculated pH in WW in scenario AS-3. The pH in WW stays over seven to 720 hrs (because of sodium pentaborate from RPV after 13800 s).

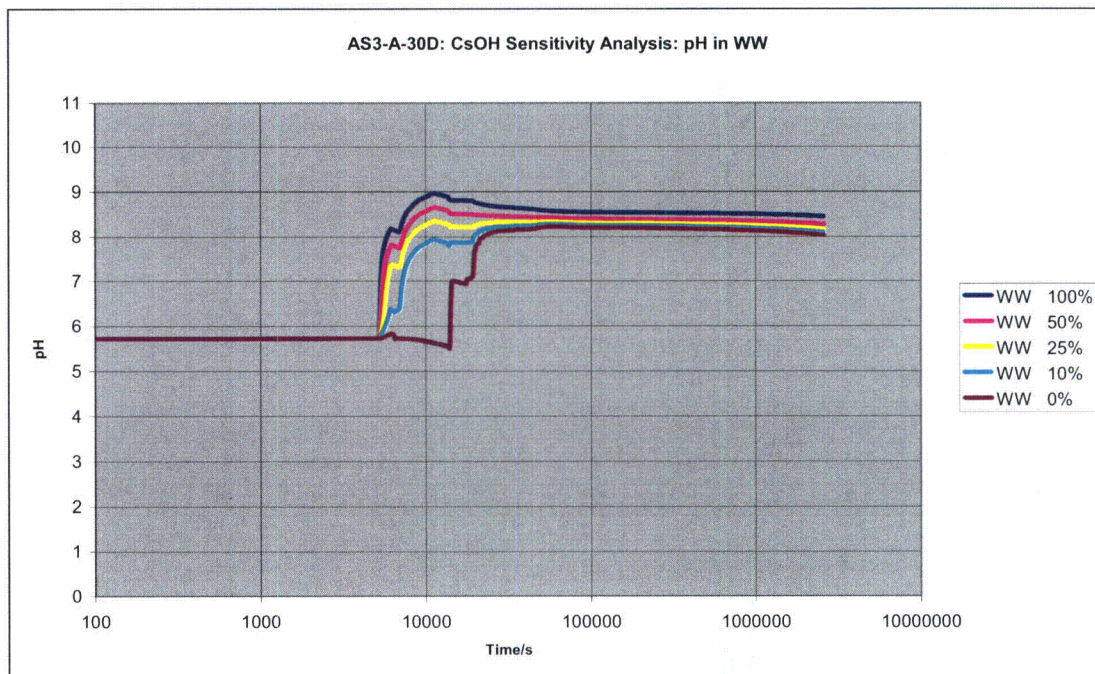


Figure 33. pH in WW in AS-3 with scaled amounts of CsOH.

## 10 Sensitivity study of the effect of radiation source from the Lower Head melt pool to the pH of the RPV pool

An additional sensitivity analysis was made to estimate how much effect on pH the extra  $\text{HNO}_3$  formation due to the radiation source of the RPV Lower Head melt pool would have. The additional  $\text{HNO}_3$  formation was conservatively approximated to be 80 moles during the 30 days. This is about 10 % more than 71.5 mol based on MCNP5 dose rates introducing additional conservatism to the dose rate estimation.

Results of the sensitivity analysis are shown in Appendix C. Table 16 shows the time when pool pH becomes permanently less than 7 in the base case and in case where RPV radiation is scaled to produce extra 80 mol of  $\text{HNO}_3$ .



**Table 16.** *Time when pool pH becomes permanently less than 7 in base case and in case where RPV radiation is scaled to produce extra 80 mol of HNO<sub>3</sub>. Times in hours.*

Scenario	Base case	Scaled HNO <sub>3</sub>	Base case	Scaled HNO <sub>3</sub>
	RPV/hr		LDW/hr	
AS-1			661.5	651.5
AS-2	712.17	689.5	623.5	614.83
AS-3			219.5	218.83

The largest difference in time when pH changes permanently, 22.67 hr earlier, is with RPV pH in AS-2 scenario. It can be seen that differences in times are relatively small and do not change the situation with pH values in any scenario significantly.

[[



RESEARCH REPORT VTT-R-06771-07 rev 2

51 (177)





















































|









































## 17 Comparison of AS-1, AS-2 and AS-3 Cases with and without MSIV leak

Accident scenarios AS-1, AS-2 and AS-3 were also calculated without MSIV leak, i.e. all MSIVs are assumed to fully close in all MSLs. This allows a full assessment of the effects of MSIV leak to the source term. The calculated AS-1, AS-2 and AS-3 without MSIV leak are the same scenarios reported in FR Part 2 [6], but now calculated with the updated MELCOR input with more accurate modeling of MSLs, SRVs and DPVs. Also a later MELCOR version 1.8.6YN was applied in the new runs instead of the application of previous version MELCOR 1.8.6YK-VTT fix applied for FR Part 2 calculations. A comparison of the results of the FR Part 2 and the new runs with updated MSL model is shown in Appendices F, G and H. The comparable cases are the scenarios AS-1, AS-2 and AS-3 without MSIV leak.

### 17.1 Comparison of AS-1 with and without MSIV leak

The total airborne CsI masses in the containment are very similar in both cases with and without MSIV leak till about 25000 s. After that the case with no MSIV leak results in higher airborne mass (Fig. 85).

The CsI release from the containment is illustrated in Fig. 86. Both cases result in practically similar releases. The peak value of airborne mass in the Main Condenser is more than an order of magnitude higher than the cumulative release via containment nominal leakage, but the Main Condenser pressure remains below 0.01 MPa.

The average decontamination factors of CsI in the PCCS are practically the same in case AS-1 with and without MSIV leak (Fig. 87).

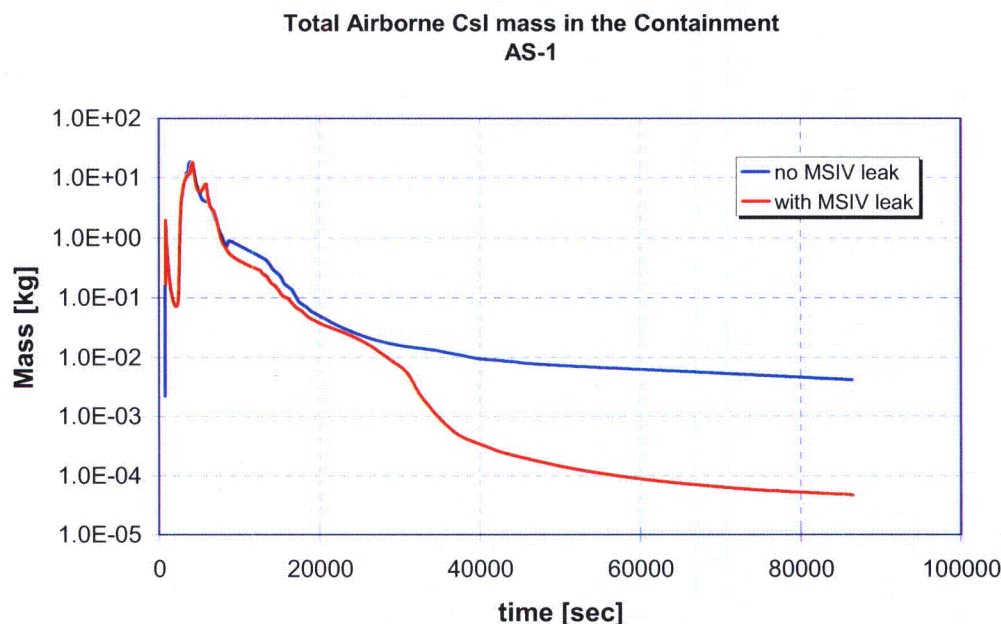


**Figure 85.** Comparison of total airborne CsI mass in the containment in AS-1 with and without MSIV failure and leak.

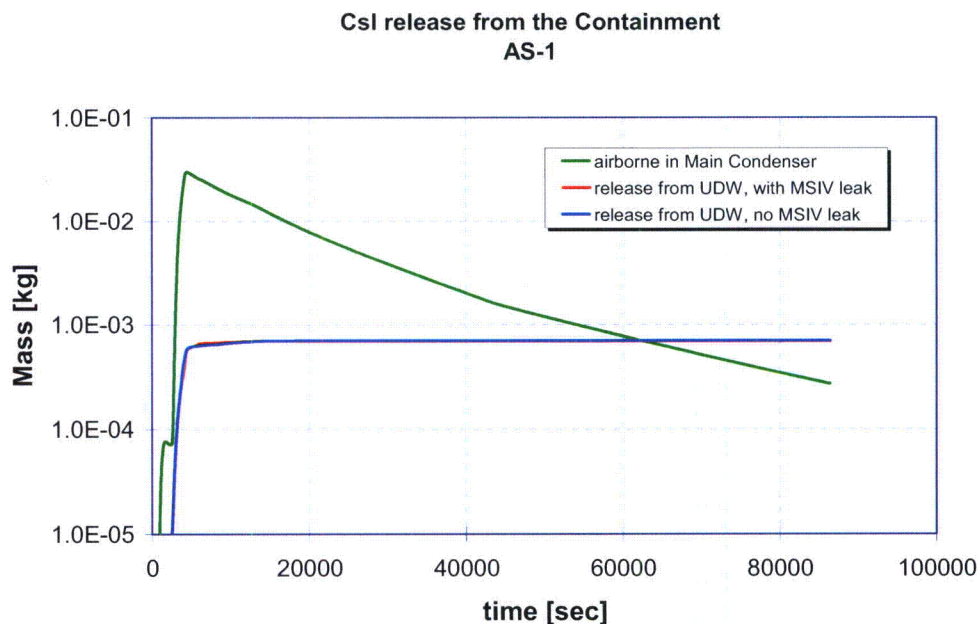


**Figure 86.** CsI release from the containment. AS-1-with and without MSIV failure and leak.

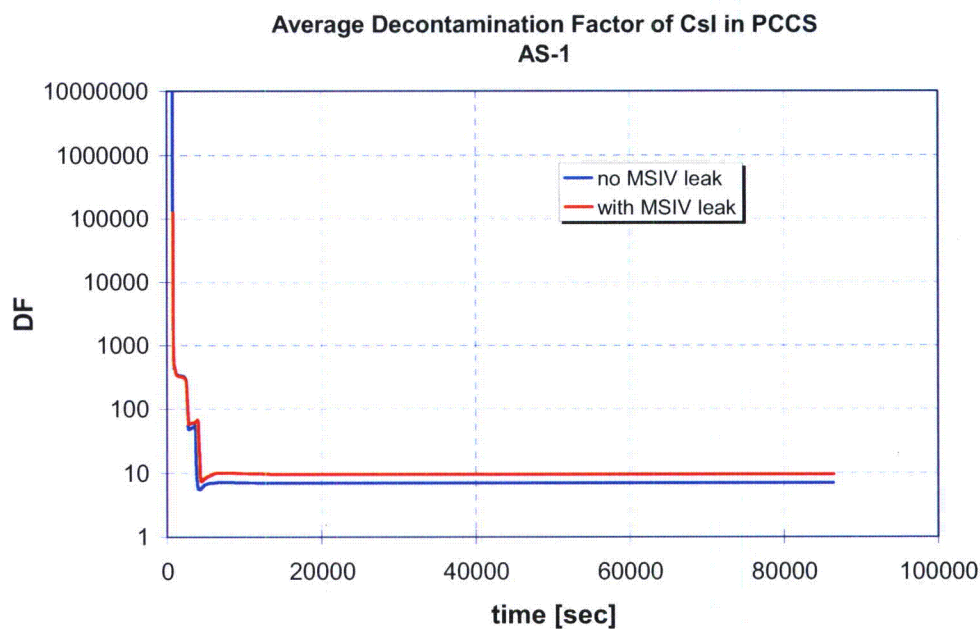


**Figure 87.** Average CsI decontamination factor in the PCCS. DF is calculated as cumulative mass of CsI entering the PCCS (flow junction 233) divided by the sum of cumulative masses of CsI exiting the PCCS through the Vent Line (flow junction 295) and the Drain Line (flow junction 296). AS-1-with and without MSIV failure and leak.

The average containment decontamination factor for CsI is clearly higher in case with MSIV leak after about 25000 s (Fig. 88). This is due to the fact that the release from the RPV is slightly higher in case with leaking MSL and the airborne CsI on the containment is lower with leaking MSL. The decontamination factor is determined as total release of CsI from the RPV divided by total airborne mass of CsI in containment.

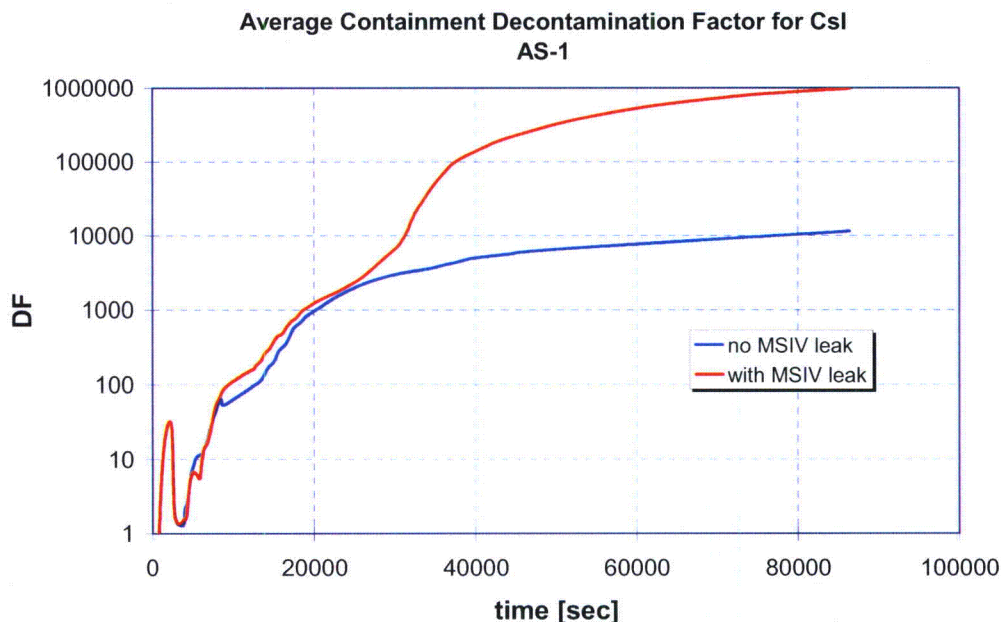


**Figure 88.** Average decontamination factor of CsI in the containment. DF is calculated as cumulative CsI mass released from the RPV into the containment divided by the total airborne CsI mass in the containment. AS-1-with and without MSIV failure and leak.

About half of the Cs and CsI is transported to the Suppression Pool through SRV/ADS valves, horizontal top vent and PCCS vent. Cs is assumed to form CsOH in the MELCOR calculations. The instantaneous pool scrubbing decontamination factor for AS-1 (without MSIV leak) during the main Cs release phase from the core (2500 – 4600 s) varies between 3 and 200 and during the phase (3800 – 8000 s) when the bulk of the CsOH is formed and accumulated in the Suppression Pool, the aerosol pool scrubbing DF in the Suppression pool is between 3 – 10000 (Fig. 89). Another important component to the CsOH mass in the Wetwell is that the Vertical Vents are included in the Wetwell pool inventory. The condensate flow from the Upper Drywell walls containing CsOH is drained into the Vertical Vent compartment. The condensate flow may contribute by 50 % to the total Wetwell CsOH mass. Figure 90 illustrates the CsOH mass distribution in different volume categories.



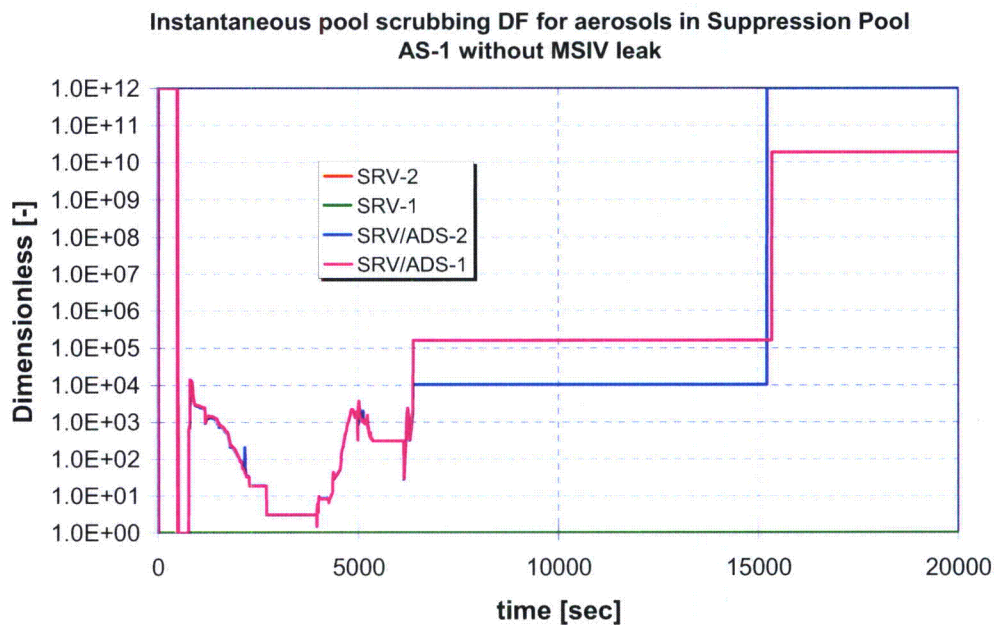


**Figure 89.** Instantaneous decontamination factor of CsI aerosol in the Suppression Pool. AS-1 without MSIV failure and leak.

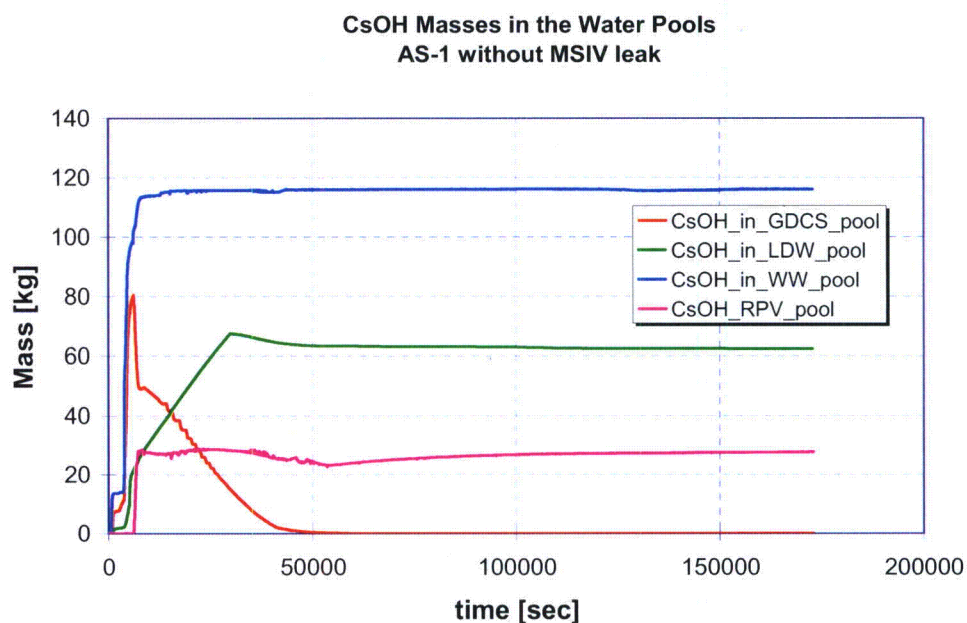


**Figure 90.** CsOH masses in different water pools. Calculation was extended to two days for stable situation. AS-1 without MSIV leak.

## 17.2 Comparison of AS-2 with and without MSIV leak

As in AS-1 also in case of AS-2 the scenario with no MSIV leak results in average a higher airborne CsI mass than the case with MSIV leak (Fig. 91). The airborne mass stays close to the maximum a little longer in case with MSIV leak.

The CsI leakages from the containment through nominal leakage are similar. The airborne CsI mass in the Main Condenser is higher than the cumulative mass of nominal leakage throughout the calculation (Fig. 92). This is different from AS-1.

The PCCS removed more efficiently CsI aerosols in case with MSIV leak than without (Fig. 93). The stabilized average PCCS decontamination factor in AS-2 is 18.49 vs. 8.70 in cases with and without MSIV leak, respectively. Also the average decontamination factor of CsI in the containment is more than twice as high in case with MSIV leak (4089310) than in case without MSIV leak (1812193) at the end of the simulation (Fig. 94).

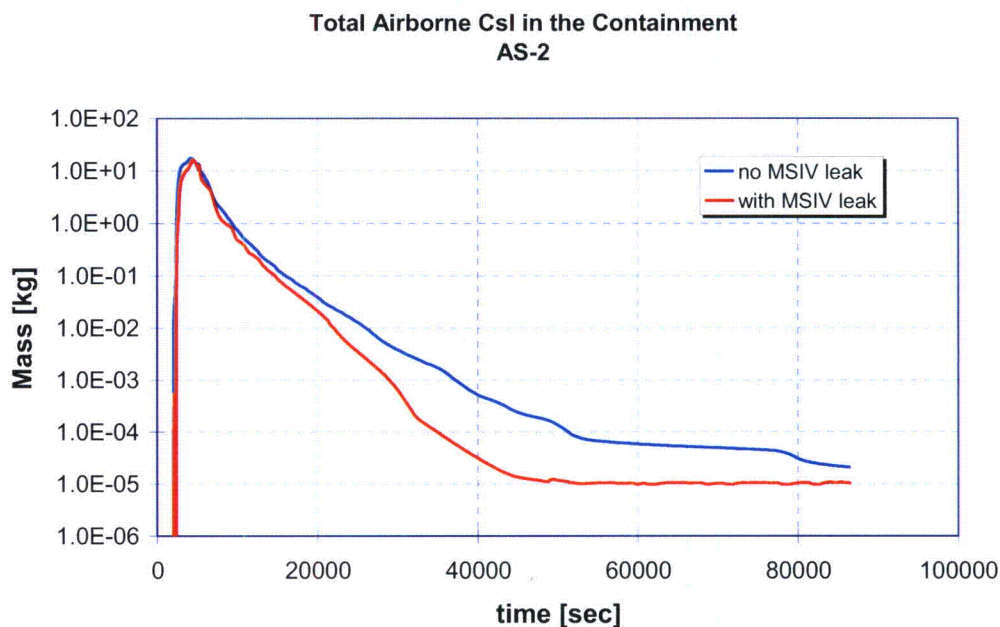


**Figure 91.** Comparison of total airborne CsI mass in the containment in AS-2 with and without MSIV failure and leak.

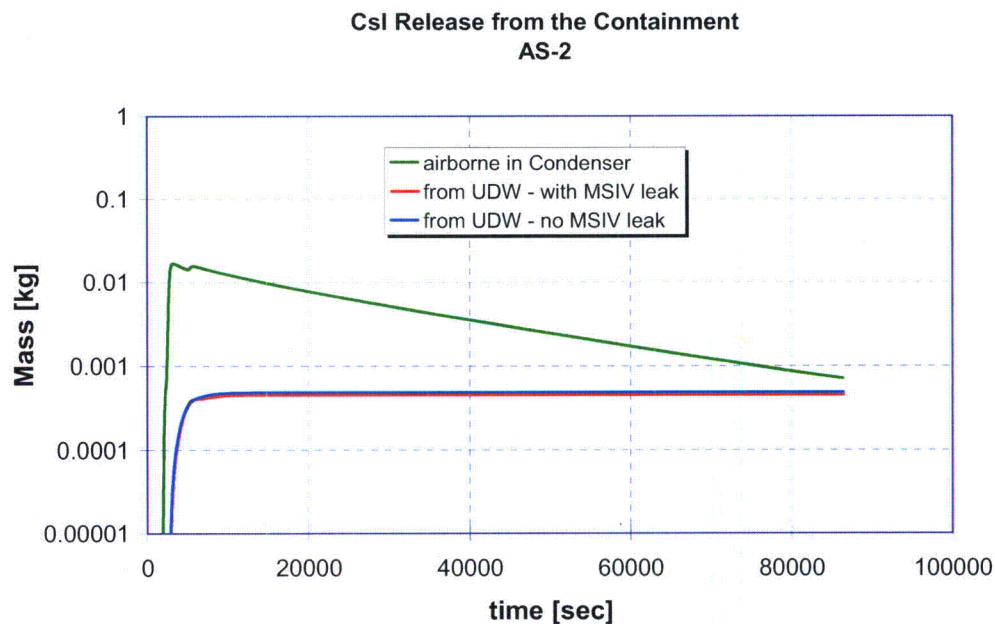


**Figure 92.** CsI release from the containment. AS-2 with and without MSIV failure and leak.

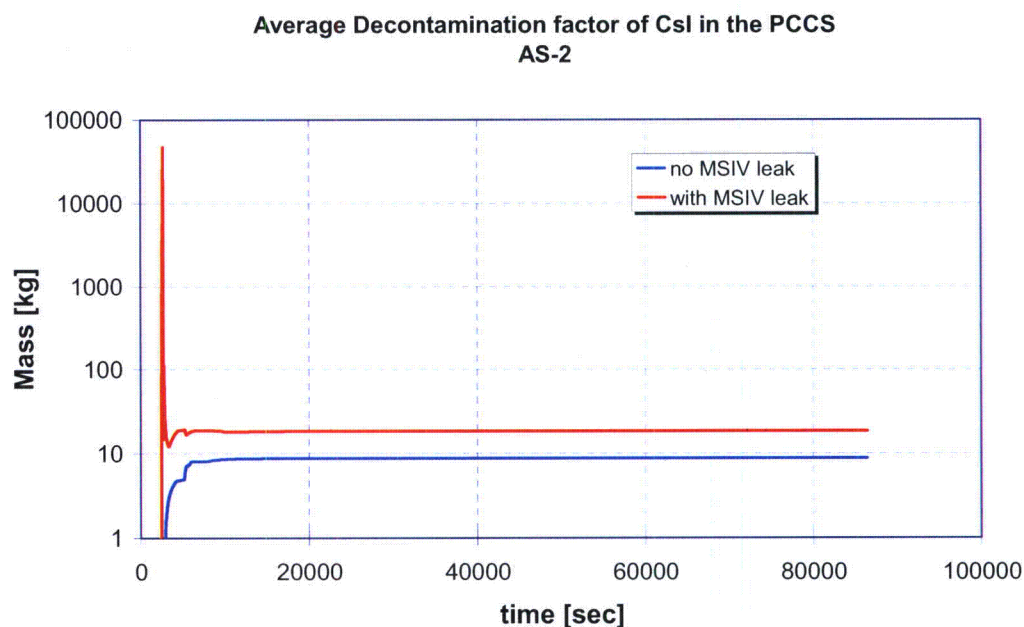


**Figure 93.** Average CsI decontamination factor in the PCCS. DF is calculated as cumulative mass of CsI entering the PCCS (flow junction 233) divided by the sum of cumulative masses of CsI exiting the PCCS through the Vent Line (flow junction 295) and the Drain Line (flow junction 296). AS-2 with and without MSIV failure and leak.

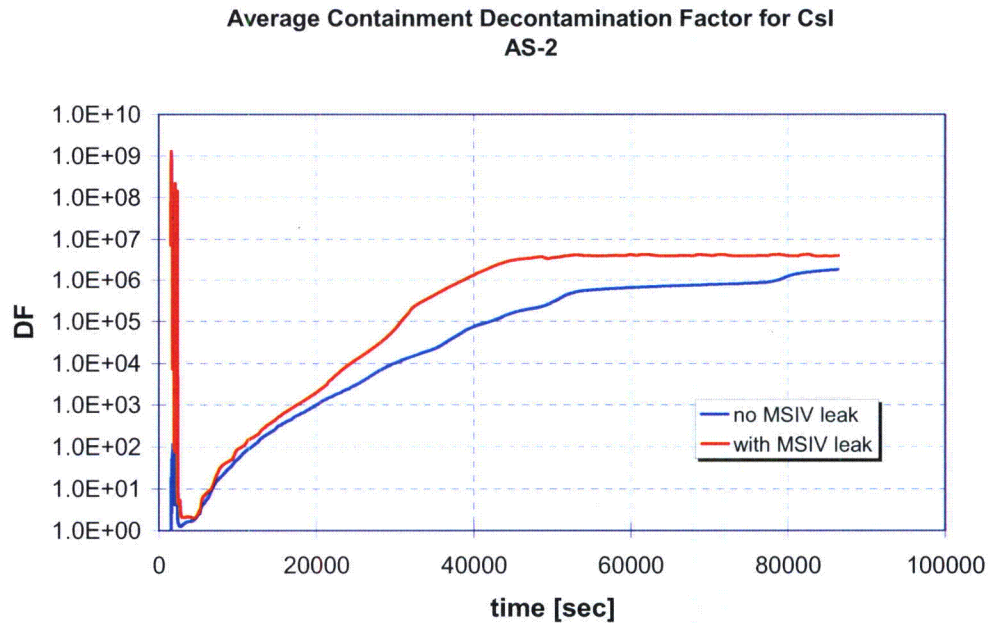


**Figure 94.** Average decontamination factor of CsI in the containment. DF is calculated as cumulative CsI mass released from the RPV into the containment divided by the total airborne CsI mass in the containment. AS-2 with and without MSIV failure and leak.

About 80 % of the CsOH formed in the Wetwell originates from the discharge through the SRV and SRV/ADS valves. The aerosol DF varies from 10 to 1000 during the main discharge phase through SRVs (3000 – 10000 s) (Fig 95). The condensate flow to the Vertical Vent volume contributes, similarly to the AS-1 case the remaining 20 % of the CSOH inventory in the Wetwell pool. Due to initial failure of ADS the SRV flow carries relatively more cesium to the Suppression pool than in AS-1 with ADS. Also due to the same reason the cesium discharge to the Upper Drywell through DPVs is much less than in AS-1 and thus the condensate flow also adds relatively less CsOH to the Wetwell pools. The total CsOH masses in the different water pools in case AS-2 are presented in Fig 96.



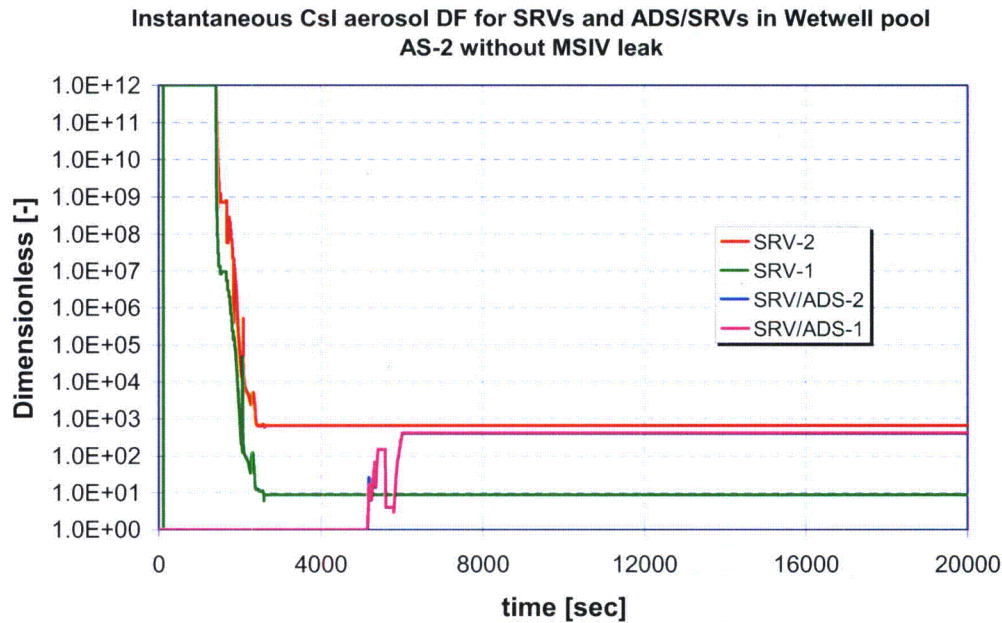


**Figure 95.** Instantaneous decontamination factor of CsI aerosol in the Suppression Pool. AS-2 without MSIV failure and leak.

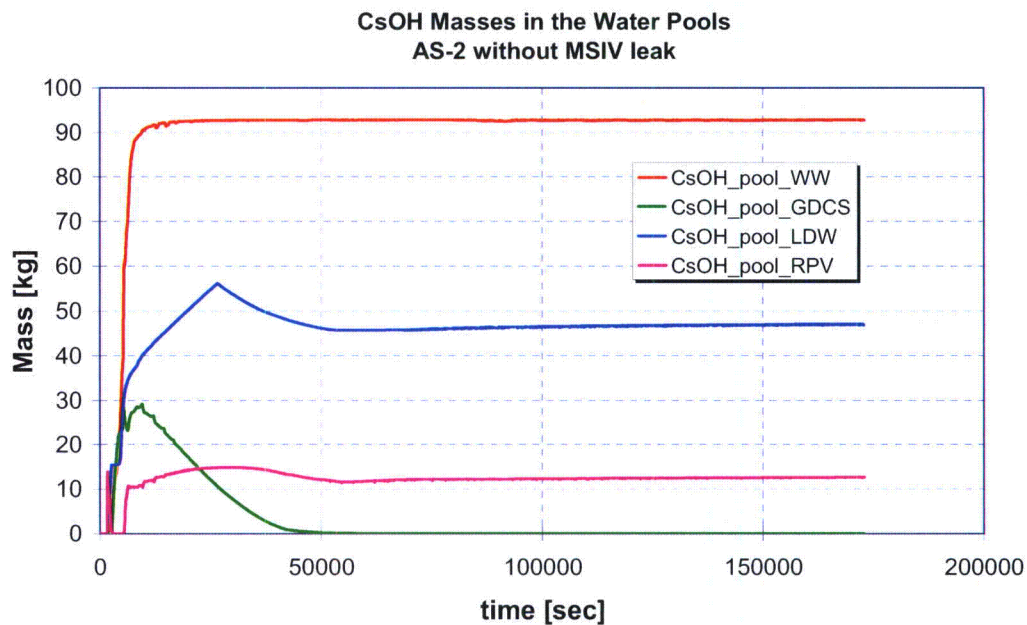


**Figure 96.** CsOH masses in different water pools. Calculation was extended to two days for stable situation. AS-2 without MSIV leak.

### 17.3 Comparison of AS-3 with and without MSIV leak

The differences in the results of case with and without MSIV leak are highest in AS-3. The airborne mass of CsI remains higher in case without MSIV leak than with leak through out the balance of the simulation (Fig. 97). The difference in absolute masses is about an order of magnitude at the end of the calculation. In AS-3 the RPV remains at high pressure for a longer time than in AS-1 and AS-2 and thus a higher pressure difference drives the flow to the MSLs and also the MSIV leak has a higher driving pressure difference.

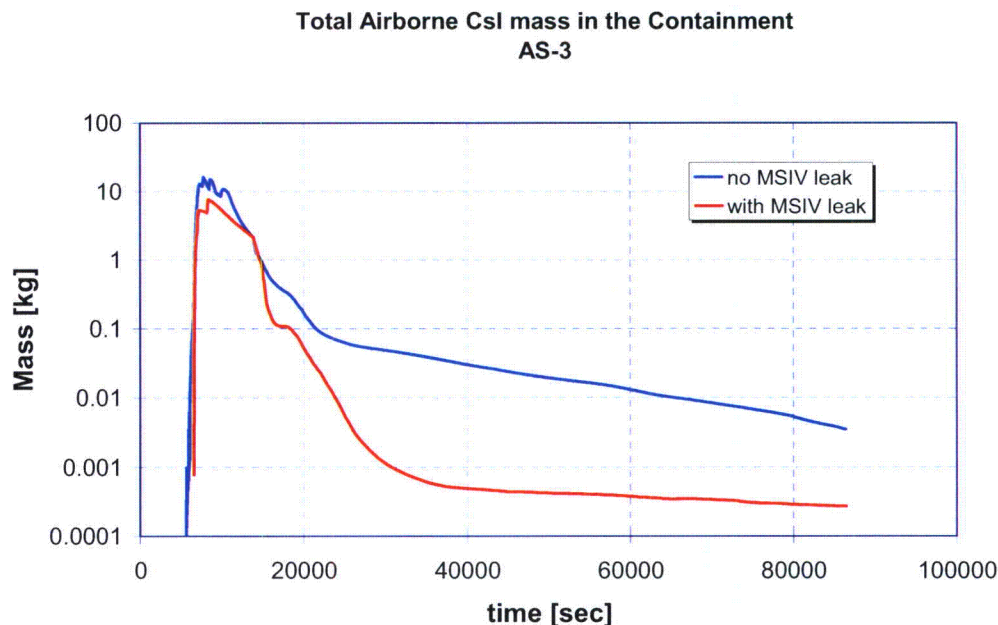


**Figure 97.** Total airborne CsI mass in the containment. AS-3 with and without MSIV leak.

The CsI leak from the containment via nominal leakage is slightly higher in case without MSIV leak than in the case with the leak, but the difference between the total leakages is larger than the respective difference in AS-1 and AS-2 (Fig. 98). Also the airborne CsI mass in the Main Condenser is much higher than the cumulative nominal leakage from the containment. The pressure remains in the Main Condenser below 0.01 MPa. The reason to higher airborne CsI mass in the Condenser is that the gas temperature in the RPV Upper Plenum and consequently in the flow through the MSL is high and CsI enters as gas into the Condenser. The cooling and agglomeration into particles takes more time than in AS-1 and AS-2.

The average decontamination factor in the PCCS is rather similar in AS-3 with and without MSIV leak (Fig. 99). In the early part of the accident prior to reflooding the removal of CsI in the PCCS is higher in case with MSIV leak.

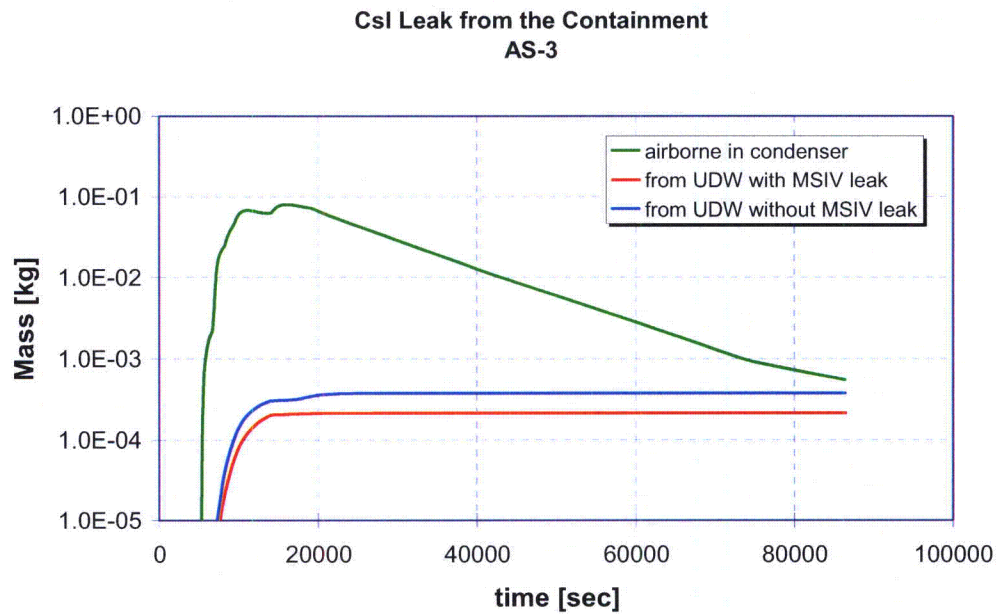


**Figure 98.** CsI mass released from the containment. AS-3 with and without MSIV leak.

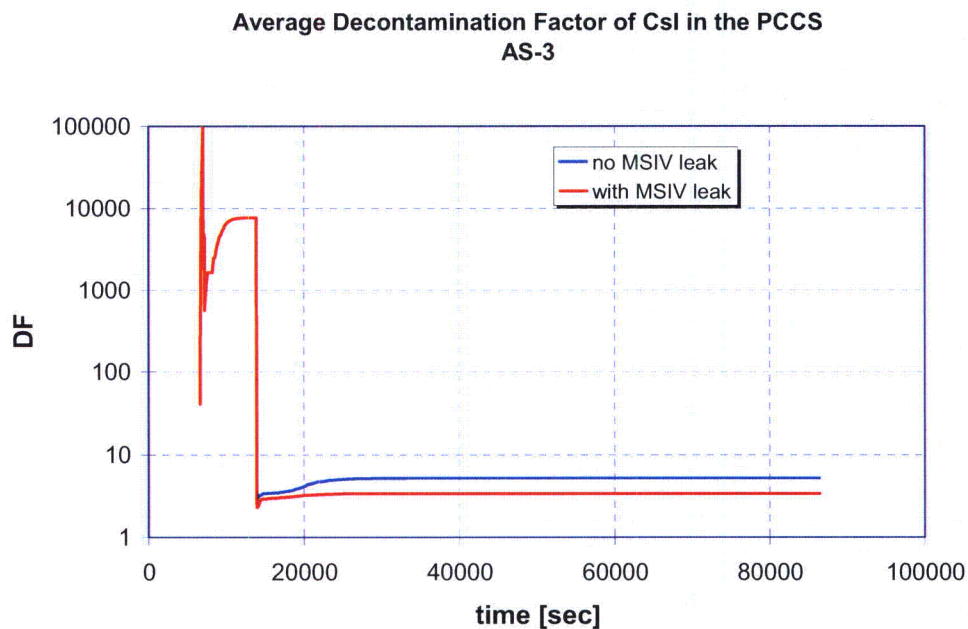


**Figure 99.** Average CsI decontamination factor in the PCCS. DF is calculated as cumulative mass of CsI entering the PCCS (flow junction 233) divided by the sum of cumulative masses of CsI exiting the PCCS through the Vent Line (flow junction 295) and the Drain Line (flow junction 296). AS-3 with and without MSIV failure and leak.

The average decontamination factor of CsI in the containment is about an order of magnitude higher in case with MSIV leak than in the case without MSIV leak (Fig. 100). This is directly addressable to the lower airborne CsI mass in case with MSIV leak, since containment DF is calculated as release from the RPV to the containment divided by total airborne mass.

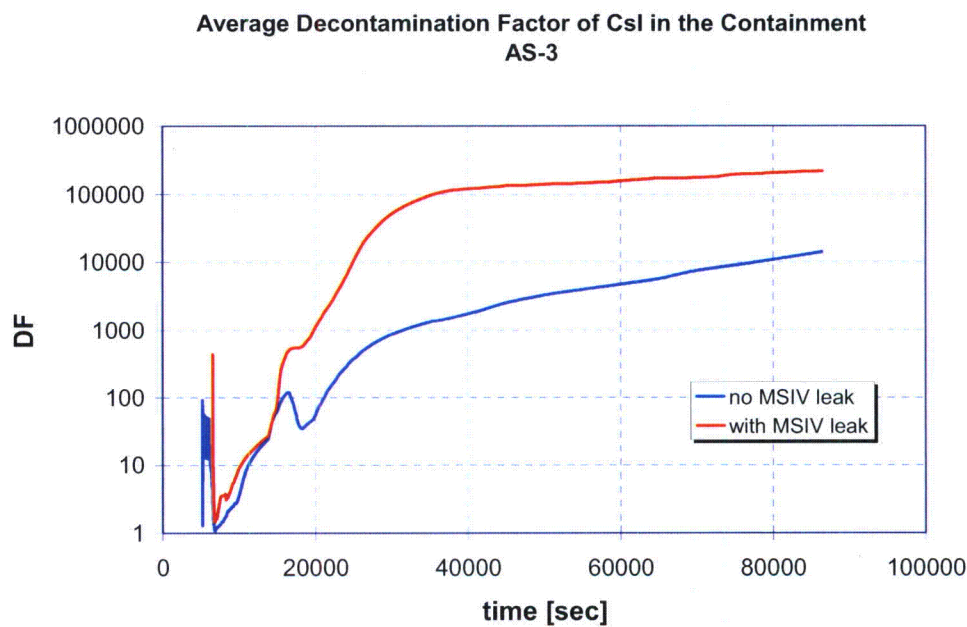


**Figure 100.** Average decontamination factor of CsI in the containment. DF is calculated as cumulative CsI mass released from the RPV into the containment divided by the total airborne CsI mass in the containment. AS-3 with and without MSIV failure and leak.

In AS-3 practically all Cs released from the core is released into the Suppression Pool through SRVs. A total of 297 kg of Cs vapor is blown into Suppression Pool (Fig. 102). The vacuum breakers open at about 4000 s and operate till about 18500 s. A total of 215 kg is collected into the Wetwell pool by fall-out and condensate flow. Only a small amount of CsOH is carried over to the Lower Drywell by the condensate flow from the Upper and Middle Drywells. The Cs vapor is not scrubbed directly during discharge through SRVs because Cs is in vapor form due to high gas temperature in the RPV Upper Plenum. In the current version of MELCOR pool scrubbing is not calculated for other vapors but elemental iodine. For aerosol the pool scrubbing DF is relatively high ranging from 100 to 100000 (Fig. 101).



**Instantaneous aerosol DF for SRVs and SRV/ADS in Wetwell Pool  
AS-3 without MSIV leak**

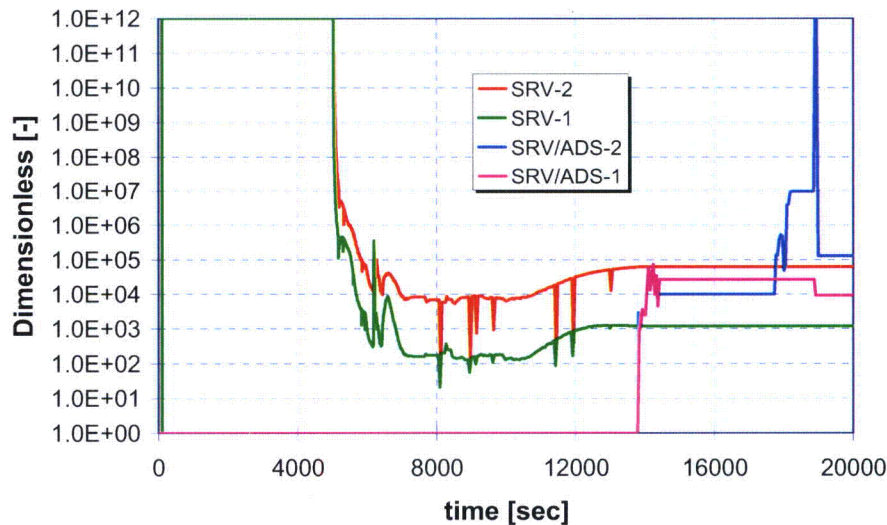


**Figure 101.** Instantaneous decontamination factor of CsI aerosol in the Suppression Pool. AS-3 without MSIV failure and leak.

**CsOH Masses in the Water Pools  
AS-3 without MSIV leak**

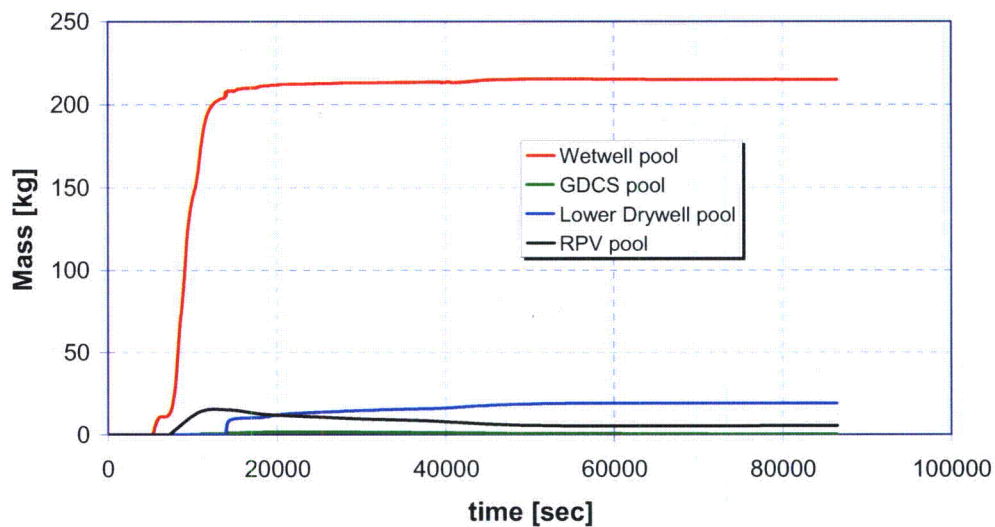


**Figure 102.** CsOH masses in different water pools. AS-3 without MSIV leak.

## 18 Summary And Conclusions

The sensitivity of pH in the containment pools to the anticipated mass of CsOH was estimated with ChemSheet code and the fission product Source Term accounting for the Main Steam Line leak path was estimated with MELCOR 1.8.6YN code to support GE's response to selected questions of the Letter RAI No. 90. The studied accident scenarios were Bottom Drain Line LOCA with ADS (AS-1) and with failure of ADS (AS-2) and Loss of Preferred Power (AS-3) with recovery of core cooling prior to pressure vessel failure. These are the same accident scenarios that are investigated in the FR Parts 1 and 2 [1], [2].

The CsOH mass entering the containment pools was varied to be 100 %, 50 %, 25 %, 10 % and 0 % of the maximum amount of CsOH released to containment as predicted by MELCOR under the assumptions that all iodine forms CsI and the rest of Cs released from the core forms CsOH. This sensitivity study is aimed at addressing an uncertainty if Cs formed also other compounds than cesium hydroxide that may not be as strong bases as CsOH.

The Wetwell pool remains basic in all three scenarios with 100 % and 50 % of the maximum available CsOH mass. With values less than or equal to 25 % of maximum CsOH the Suppression Pool becomes acidic in Scenarios 1 and 2. The Lower Drywell pool becomes acidic in all three accident scenarios during the balance of the simulation. In the worst case, with 0 % CsOH of the maximum value in Scenario 3, the Lower Drywell Pool turns acid at 8.4 days from the beginning of the accident. Reactor Pressurized Vessel (RPV) becomes acidic in scenarios 1 and 2 but not in scenario 3.

The GDSCS pool becomes acidic at an earlier time. AS-2 shows the earliest change to acidic, with 100 % CsOH at about 11.6 hr into the accident and with values less than or equal to 25 % of maximum CsOH the GDSCS pool is always acidic.

The key factor to keep pH of the pools alkaline is the distribution of sodium borate buffer between the pools. In scenario 3 less buffer solution goes to Lower Drywell than in scenarios 1 and 2 and therefore the pool pH turns acidic earlier in scenario 3. In scenario 3 also enough buffer solution goes Suppression Pool to keep it alkaline all the time.

In the analyses of CsI retention to MSL leak path, the average total removal fraction to the MSL leak path section between MSIV-1 and the Main Condenser inlet was in 63.7 % in AS-1, 89.4 % in AS-2, 91.0 % in AS-3 and 53.3 % in MSL Guillotine Break (AS-4). The average decontamination factors of CsI were higher in cases with MSIV leak than without. The highest airborne CsI masses in the containment are obtained in AS-2 with and without MSIV leak. The highest containment nominal leakage fractions, which are defined as the cumulative leaked mass divided by the mass released from RPV to the containment, are obtained in AS-1 with and without MSIV leak.

## 19 References

1. I. Lindholm, A. Auvinen, Y. Enqvist, K. Penttilä, T. Sevón, R. Zilliacus, Estimation and Modeling of Effective Fission Product Decontamination Factor for ESBWR Containment – Part 1, VTT Research Report VTT-R-04413-06, 16.10.2006, 123 p.
2. I. Lindholm, A. Auvinen, Y. Enqvist, K. Penttilä, T. Sevón, R. Zilliacus, Estimation and Modeling of Effective Fission Product Decontamination Factor for ESBWR Containment – Part 2, VTT Research Report VTT-R-04413-06, 21.12.2006, 82 p.
3. Los Alamos National Laboratory, X-5 Monte Carlo Team, MCNP - A General Monte Carlo N-Particle Transport Code, Version 5, Volume 1: Overview and Theory, LA-UR-03-1987 & Volume II: User's Guide, LA-CP-03-0245, April 24, 2003 (Revised 10/3/05).
4. Seiler, J.M., Tourniaire, B., Defoort, F., Froment, K., Consequences of material effects on in-vessel retention, Nucl. Eng. & Des. 237 (2007) pp. 1752 – 1758.
5. RASCAL 3.0.5 Workbook, 2007. Radiological Assessment System for Consequence Analysis. NUREG-1889.
6. Eckerman K. F., Ryman J. C. 1993. External exposure to radionuclides in air, water and soil. Federal Guidance Report No. 12. EPA-402-R-93-081. Oak Ridge National Laboratory.
7. Los Alamos National Laboratory, MCNPDATA: Standard Neutron, Photon and Electron Data Libraries for MCNP4C. Oak Ridge National Laboratory, RSICC Data Library Collection DLC-200.
8. E.C. Beahm, R.A. Lorenz, C.E. Weber, Iodine Evolution and pH Control, NUREG/CR-5950, ORNL/TM-12242.
9. Lindholm, I. Penttilä, K., Estimation and Modeling of Effective Fission Product Decontamination Factor for ESBWR Containment – Part 3 rev 1, VTT Research Report VTT-R-06671-07, 10.09.2007, 155 p.
10. <http://www.matweb.com/search/SpecificMaterial.asp?bassnum=CSKAM015>
11. [http://www.jm.com/insulation/performance\\_materials/products/ci125\\_t12.pdf](http://www.jm.com/insulation/performance_materials/products/ci125_t12.pdf)
12. <http://www.insulite.co.za/product.html#2>



## 20 APPENDIX A: Dose rates due to three accident sequences (AS-1, AS-2, AS-3) in four water pools (WW, GDCS, DW, RPV).

<b>AS-1</b>		[Rad/h]									
Time [s]	0	2500	3600	6052	7200	10800	14400	21600	28800	43200	86400
WW	0	8,79E+03	8,24E+03	4,27E+04	5,56E+04	1,57E+05	6,29E+04	5,92E+04	5,28E+04	5,41E+04	4,34E+04
GDCS	0	1,93E+04	1,93E+04	8,92E+04	9,24E+04	7,99E+04	8,03E+04	7,59E+04	6,33E+04	3,87E+04	8,68E+02
DW	0	6,65E+02	5,95E+03	1,01E+05	1,57E+05	1,55E+05	1,12E+05	9,21E+04	8,04E+04	9,66E+04	8,51E+04
RPV	0	1,30E+01	1,42E+03	1,62E+04	4,39E+04	6,90E+04	6,44E+04	6,51E+04	6,12E+04	5,44E+04	6,68E+04
Time [s]	172800	259200	345600	432000	720000	1080000	1440000	1800000	2160000	2520000	2592000
WW	2,10E+04	1,62E+04	1,39E+04	1,26E+04	1,05E+04	9,48E+03	8,94E+03	8,61E+03	8,37E+03	8,20E+03	7,13E+03
GDCS	4,23E+02	3,26E+02	2,81E+02	2,55E+02	2,14E+02	1,93E+02	1,82E+02	1,75E+02	1,71E+02	1,67E+02	1,46E+02
DW	4,20E+04	3,27E+04	2,83E+04	2,57E+04	2,17E+04	1,96E+04	1,86E+04	1,79E+04	1,74E+04	1,71E+04	1,50E+04
RPV	3,30E+04	2,56E+04	2,22E+04	2,02E+04	1,70E+04	1,54E+04	1,46E+04	1,40E+04	1,37E+04	1,34E+04	1,17E+04
<b>AS-2</b>		[Rad/h]									
Time [s]	0	2500	3600	6052	7200	10800	14400	21600	28800	43200	86400
WW	0	1,02E+04	1,07E+04	5,08E+04	5,30E+04	4,99E+04	4,77E+04	4,63E+04	4,44E+04	4,11E+04	3,13E+04
GDCS	0	2,93E+01	5,50E+03	4,93E+04	5,36E+04	5,69E+04	5,77E+04	5,35E+04	4,81E+04	2,02E+04	1,97E+03
DW	0	9,26E+03	9,01E+03	4,59E+05	3,76E+05	2,33E+05	1,76E+05	1,53E+05	1,38E+05	1,34E+05	1,06E+05
RPV	0	0,00E+00	0,00E+00	3,04E+04	2,69E+04	2,87E+04	3,31E+04	3,86E+04	4,23E+04	6,08E+04	1,18E+05
Time [s]	172800	259200	345600	432000	720000	1080000	1440000	1800000	2160000	2520000	2592000
WW	1,46E+04	1,10E+04	9,33E+03	8,35E+03	6,81E+03	6,04E+03	5,65E+03	5,41E+03	5,24E+03	5,12E+03	4,37E+03
GDCS	9,20E+02	6,93E+02	5,87E+02	5,25E+02	4,28E+02	3,80E+02	3,55E+02	3,40E+02	3,29E+02	3,21E+02	2,74E+02
DW	5,04E+04	3,83E+04	3,26E+04	2,93E+04	2,41E+04	2,15E+04	2,02E+04	1,94E+04	1,88E+04	1,84E+04	1,58E+04
RPV	5,52E+04	4,17E+04	3,55E+04	3,18E+04	2,60E+04	2,32E+04	2,17E+04	2,08E+04	2,01E+04	1,97E+04	1,68E+04
<b>AS-3</b>		[Rad/h]									
Time [s]	0	2500	3600	6052	7200	10800	14400	21600	28800	43200	86400
WW	0	0,00E+00	0,00E+00	6,13E+03	7,55E+03	8,83E+04	9,18E+04	8,77E+04	8,41E+04	7,93E+04	6,34E+04
GDCS	0	0,00E+00	0,00E+00	6,22E-04	5,01E+00	3,47E+02	1,61E+03	1,10E+04	1,27E+04	1,00E+04	3,60E+03
DW	0	0,00E+00	0,00E+00	0,00E+00	0,00E+00	0,00E+00	8,85E+06	4,36E+05	2,18E+05	1,51E+05	7,36E+04
RPV	0	0,00E+00	0,00E+00	2,22E+04	6,21E+04	2,79E+05	5,20E+04	2,58E+04	2,20E+04	2,06E+04	1,46E+04
Time [s]	172800	259200	345600	432000	720000	1080000	1440000	1800000	2160000	2520000	2592000
WW	3,01E+04	2,29E+04	1,95E+04	1,76E+04	1,45E+04	1,30E+04	1,22E+04	1,17E+04	1,13E+04	1,11E+04	9,55E+03
GDCS	1,70E+03	1,29E+03	1,10E+03	9,89E+02	8,15E+02	7,28E+02	6,83E+02	6,56E+02	6,37E+02	6,23E+02	5,36E+02
DW	3,51E+04	2,68E+04	2,29E+04	2,07E+04	1,71E+04	1,53E+04	1,44E+04	1,38E+04	1,34E+04	1,32E+04	1,14E+04
RPV	7,00E+03	5,35E+03	4,58E+03	4,14E+03	3,43E+03	3,08E+03	2,90E+03	2,79E+03	2,71E+03	2,65E+03	2,30E+03

## 21 APPENDIX B: Sensitivity Analysis for LDW mixing

The base case calculation for AS-1 with LDW mixing with RPV and UDW (with 100 % CsOH) is compared with case where there is no LDW mixing after 24 hours (Figs B-1 and B-2). RPV pH stays over 7 all the time after 24 hours and LDW becomes less than seven 43.3 hours earlier without mixing.

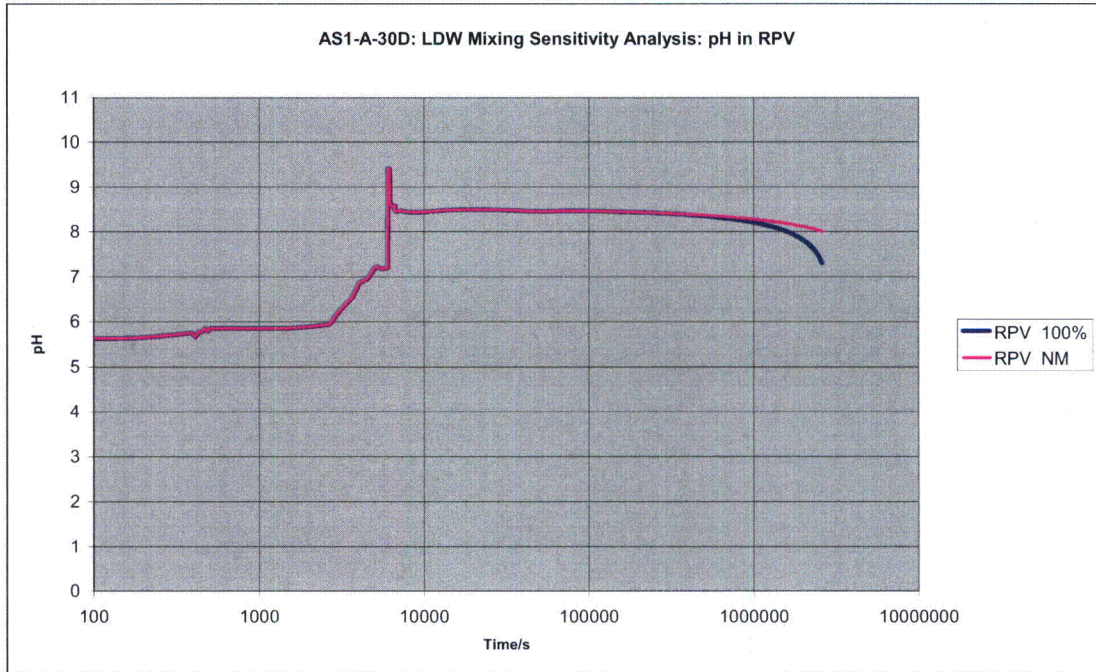


**Figure B-1.** *pH in RPV with and without mixing of LDW. Scenario AS-1.*

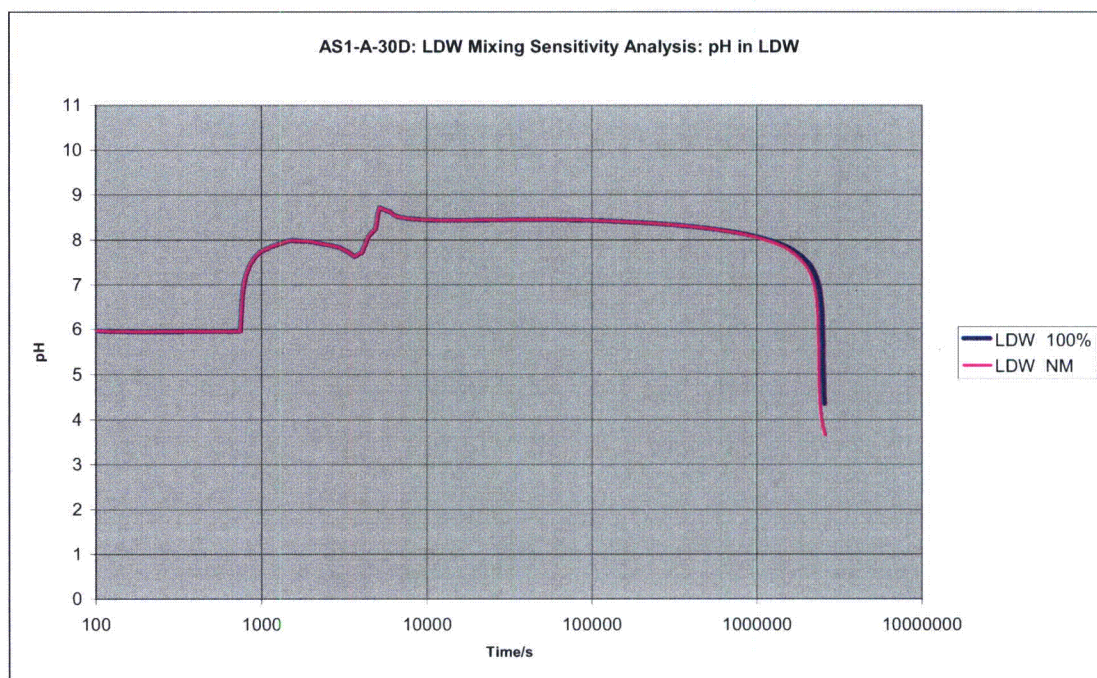


**Figure B-2.** *pH in LDW with and without mixing of LDW. Scenario AS-1.*

The base case calculation for AS-2 with LDW mixing with RPV and UDW (with 100 % CsOH) is compared with case where there is no LDW mixing after 24 hours (Figs. B-3 and B-4). RPV pH becomes less than seven 45.3 hours earlier without mixing and LDW becomes less than seven 12.7 hours later without mixing.

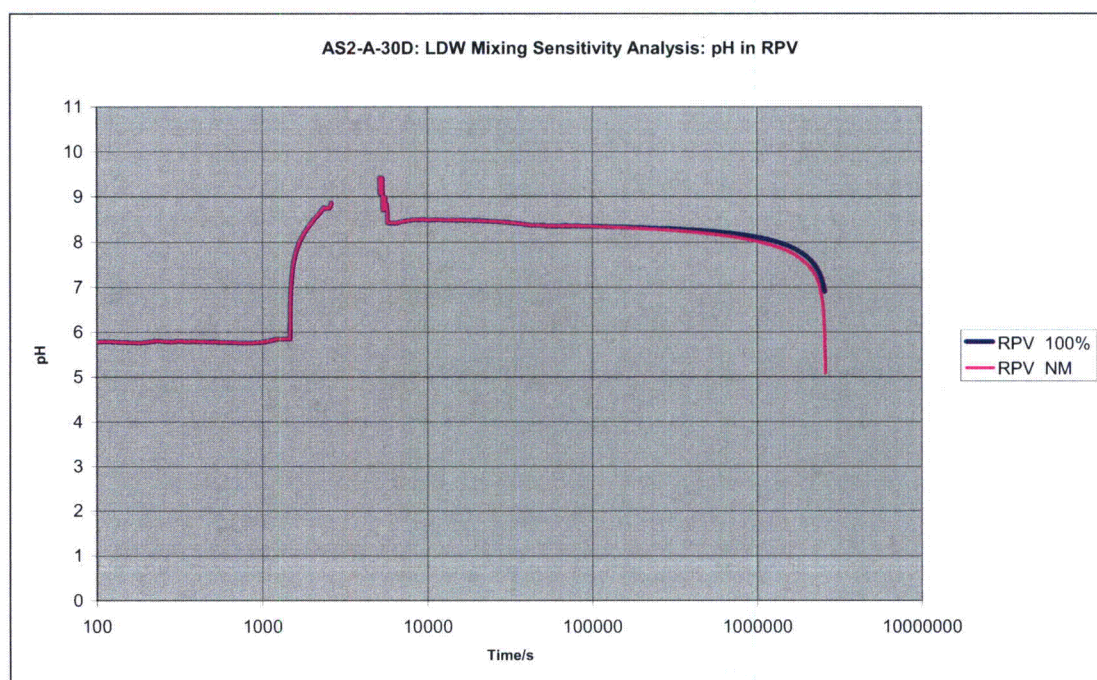


**Figure B-3.** *pH in RPV with and without mixing of LDW. Scenario AS-2.*



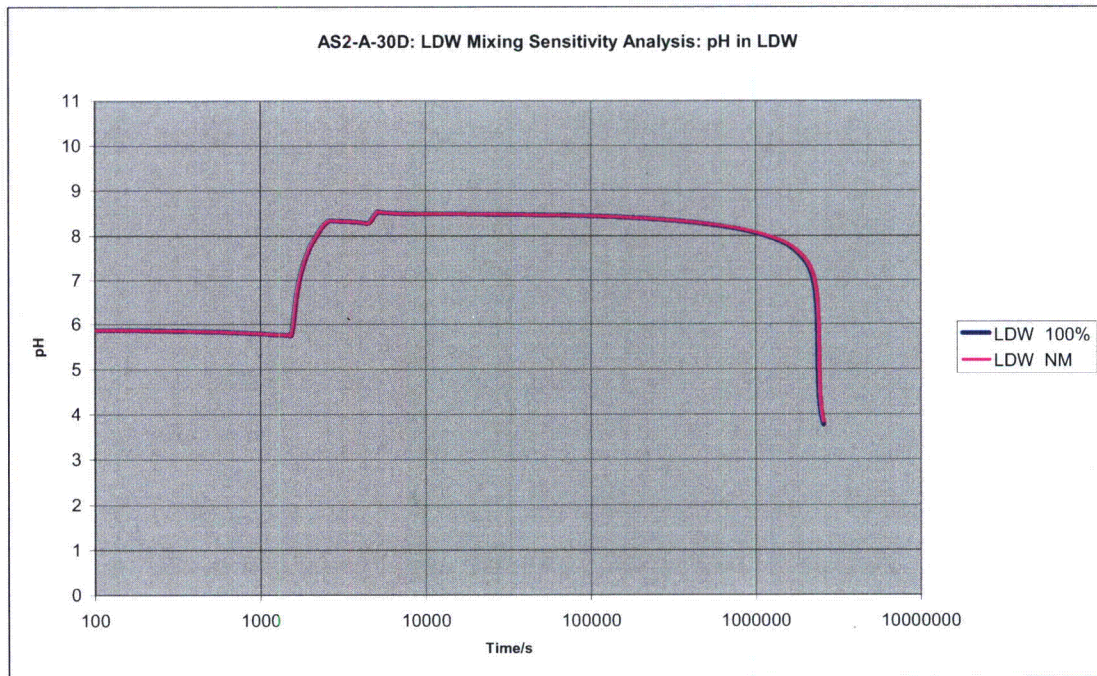
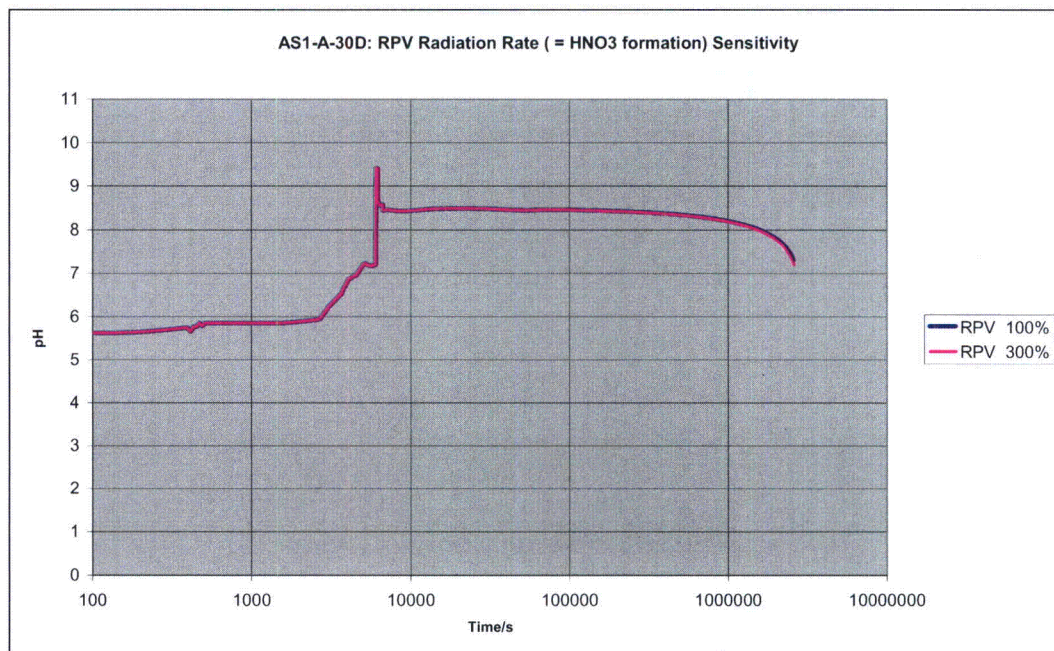


Figure B-4. pH in LDW with and without of LDW. Scenario AS-2.

## 22 APPENDIX C: Sensitivity Analysis of pH with Including Radiation from the Core Melt Pool in the Lower Head

Radiation rate that was used to calculate  $\text{HNO}_3$  formation in RPV pool was scaled so that about 80 moles more of  $\text{HNO}_3$  in RPV was generated. In the case of AS-1 this caused an up-scaling by 300 % of the  $\text{HNO}_3$  production in the RPV pool caused by dissolved fission products (40 mole of  $\text{HNO}_3$  vs. 120 moles). The pH in LDW becomes permanently less than 7 about 0.3 % earlier with scaled radiation (Figs. C-1 and C-2). The pH in the other pools did not go below 7. The dose rate estimates from the Lower Head melt pool, however, were obtained with highly conservative assumptions.

Radiation dose rate that was used to calculate  $\text{HNO}_3$  formation in RPV was scaled so that about 80 mole more of  $\text{HNO}_3$  in RPV was formed. In AS-2 the scaling factor was 230 % for  $\text{HNO}_3$  production in the RPV pool. The  $\text{HNO}_3$  production due to radiation of dissolved fission products in the RPV pool was 62.4 moles and with additional dose rate from the Lower head Melt pool accounted for the  $\text{HNO}_3$  production is 142.4 moles. The pH in the RPV becomes permanently less than 7 about 3 % and in LDW about 1.4 % earlier than in the base case with only dissolved fission products considered in the calculation of the dose rate in the RPV pool (Figs. C-3 and C-4).



**Figure C-1.** pH in RPV with 100 % and 300 % radiation dose rate in RPV. Scenario AS-1.



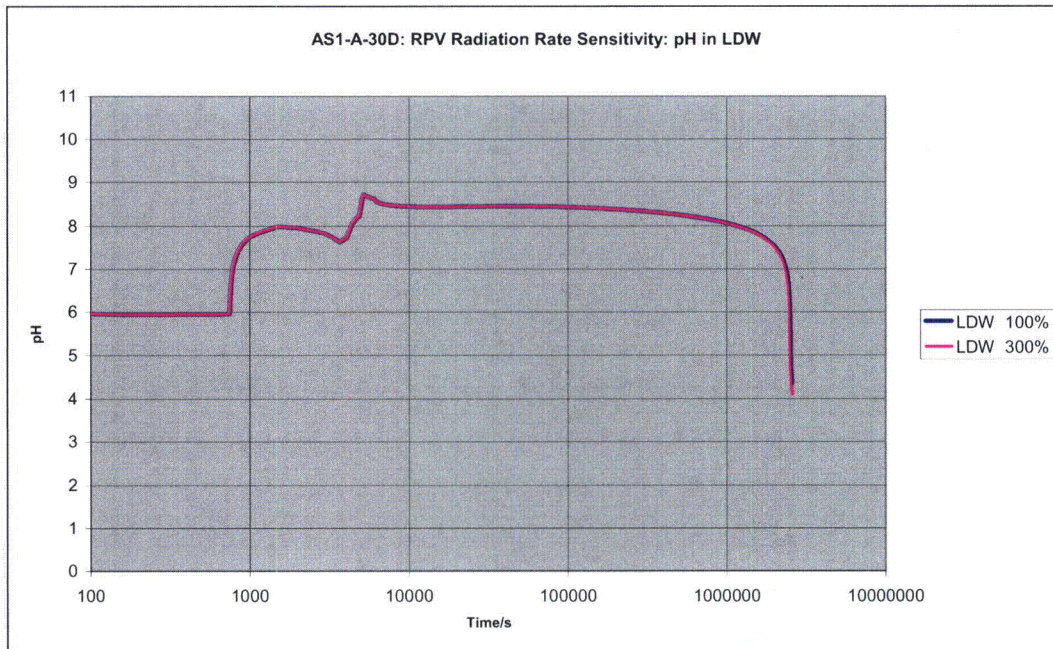


**Figure C-2.** pH in LDW with 100 % and 300 % radiation rate in RPV. Scenario AS-1.

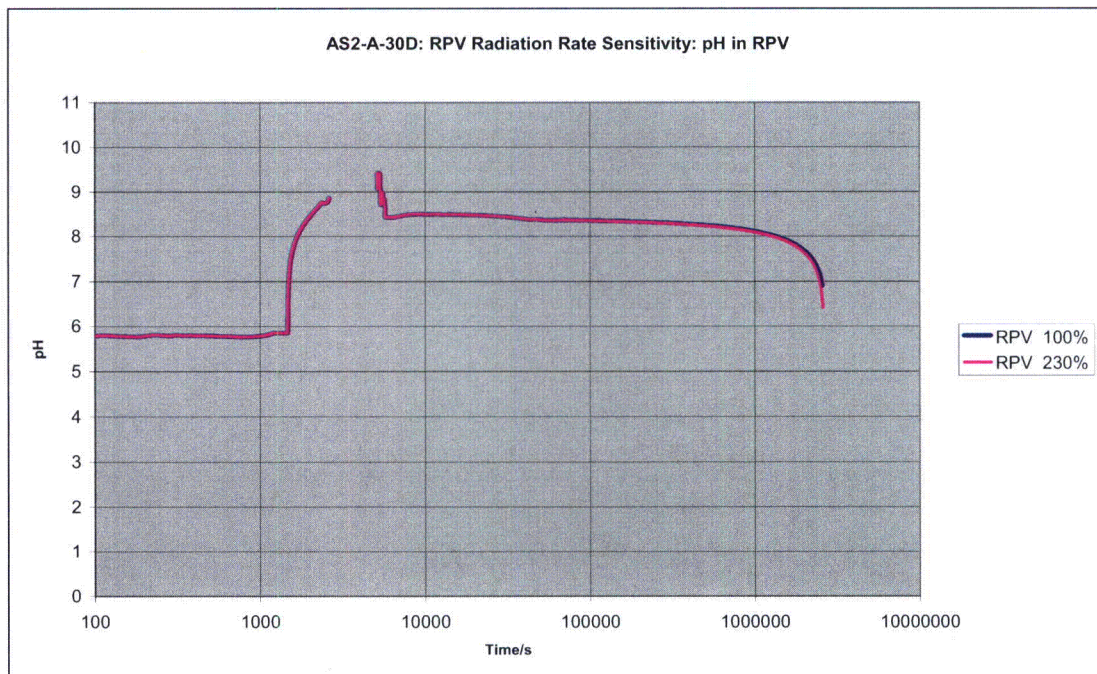


**Figure C-3.** pH in RPV with 100 % and 230 % radiation rate in RPV. Scenario AS-2.

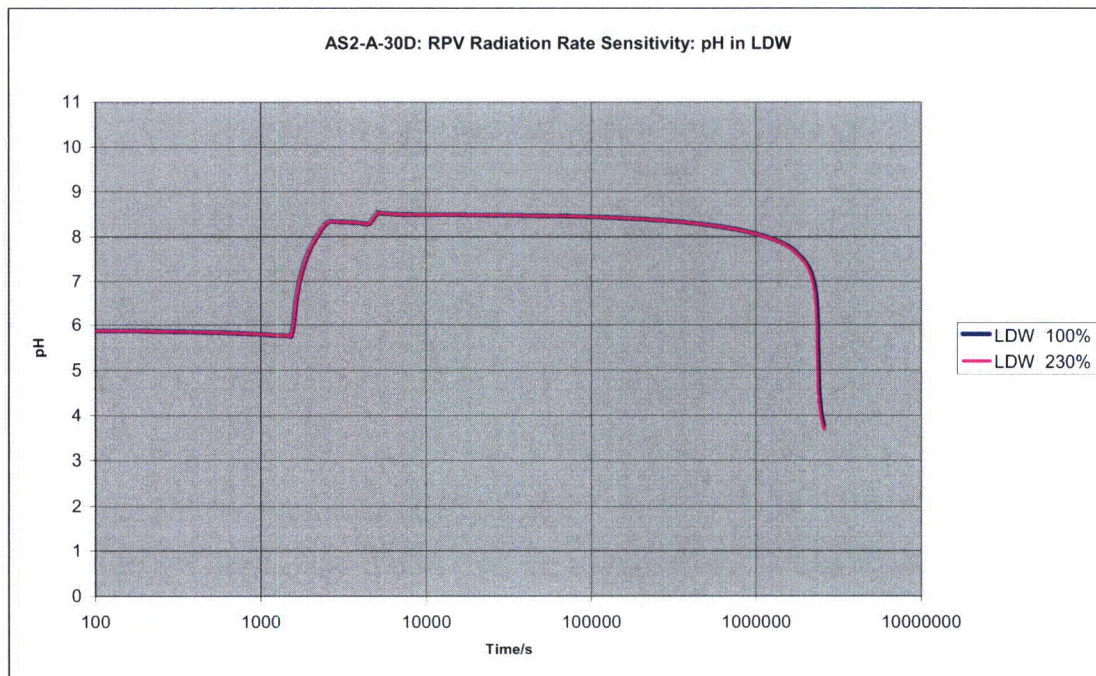


**Figure C-4.** *pH in LDW with 100 % and 230 % radiation rate in RPV. Scenario AS-2.*

Radiation rate that was used to calculate  $\text{HNO}_3$  formation in RPV was scaled so that about 80 mole more of  $\text{HNO}_3$  in RPV was formed. In AS-3 the scaling factor was 680 % compared to the base case with dose rate calculated from the dissolved fission products in the RPV pool (13.75 moles in the base case vs. 83.75 moles if radiation of the melt pool is taken into account). The pH in LDW becomes permanently less than 7 about 0.3 % earlier with the up-scaled dose rate in the RPV (Fig. C-5). The pH in the other pools remained above seven during the balance of the simulation (30 days). The pH in the LDW pool is shown in Fig. C-6.

It can be concluded that the effect of the radiation from the RPV Lower Head melt pool is small. Considering further that the dose rate from the melt pool was calculated with conservative assumptions assuming the whole core inventory in the melt without reducing the effect of volatile, released fission products, it is justified to simplify the estimation of  $\text{HNO}_3$  production in the RPV by calculating the dose rate in the RPV only from the dissolved fission products.



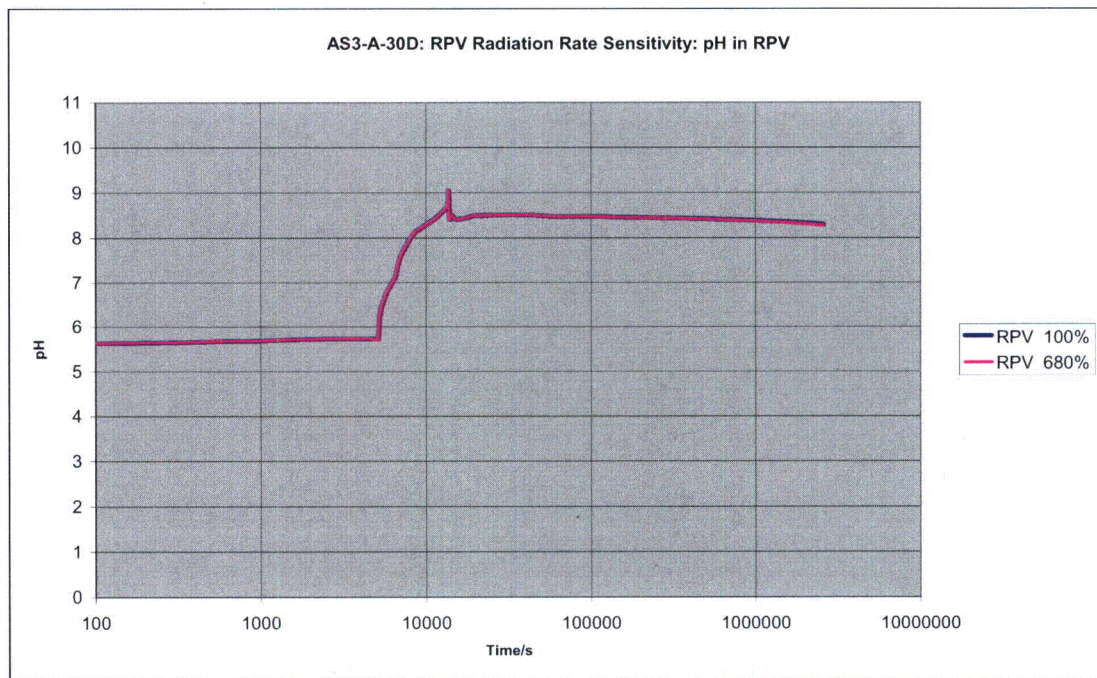


Figure C-5. pH in RPV with 100 % and 680 % radiation rate in RPV. Scenario AS-3.

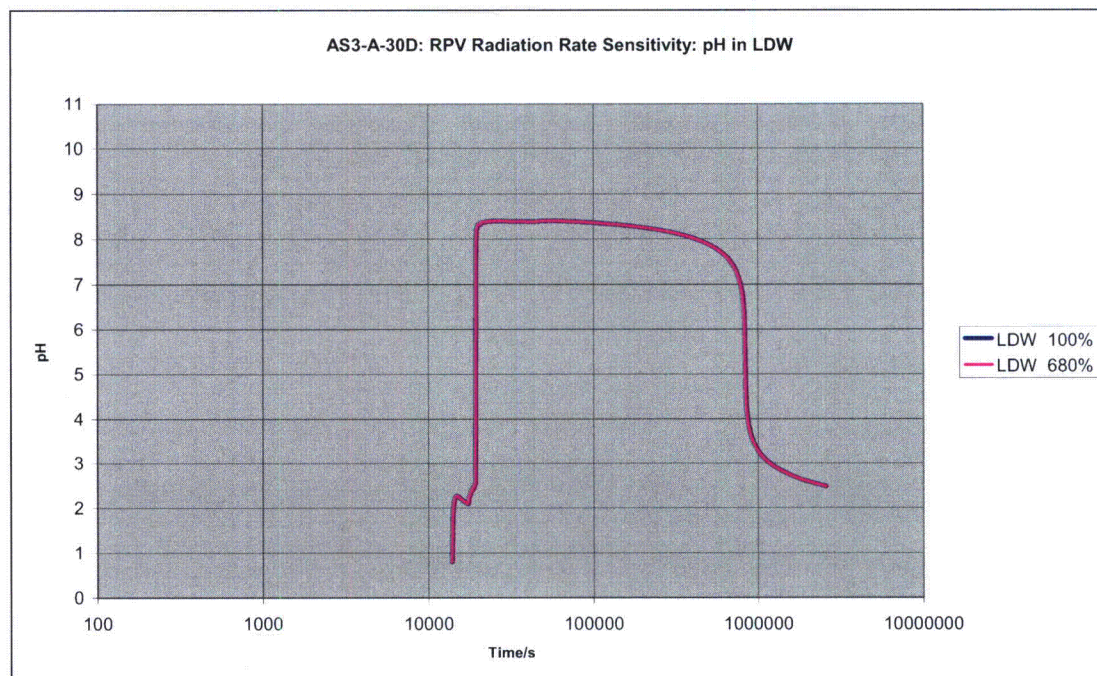


Figure C-6. pH in LDW with 100 % and 680 % radiation rate in RPV. Scenario AS-3.

## 23 APPENDIX D: Concentration Tables for Sensitivity Calculations

Concentration tables were made to show the compositions in RPV, LDW, GDCS and WW at selected time steps. Values in the tables are:

Time	Time when the equilibrium composition was saved
T	Temperature (K)
P	Pressure (Pa)
V	Mass of water in pool (kg)
HCl	From Cl <sup>-</sup> in water (mol/kg-water)
HNO <sub>3</sub>	From sum of HNO <sub>3</sub> (a)-, NO <sub>2</sub> (-a), NO <sub>3</sub> (-a) in water (mol/kg-water)
CsOH	From Cs(+a) minus I(-a) in water (mol/kg-water) (if positive) (mol/kg-water)
HI	From I(-a) minus Cs(+a) in water (mol/kg) (if positive) (mol/kg-water) (if there is more I- than Cs+ it is assumed as HI)
B(OH) <sub>3</sub>	From sum of B(OH) <sub>3</sub> , B(OH) <sub>4</sub> (-a) in water (mol/kg-water)
NaOH	From Na(+a) in water (sodium pentaborate must be given as boric acid and sodium hydroxide)
pH1	pH1 is calculated using the values in the table (with ChemSheet)
pH2	pH2 is calculated using the original equilibrium composition (with ChemSheet). This is also the pH calculated during the simulation.

Tables D-1 thru D-20 are for scenario AS-1, Tables D-21 thru 40 for scenario AS-2 and Tables D-41 thru D-60 for scenario AS-3.

[[

































## 24 APPENDIX E: Validation of Thermodynamic System

The thermodynamic system (see Table 2) used in the ChemSheet pH model was validated with experimental pH data found in the literature. The data values are listed in Table E-1. Experimental data covers pH values between 5.1 and 12, temperature between 25 °C (298 K) and 90 °C (363 K) and ionic strengths up to 0.299. Potassium was not included in the used system so respective sodium species were used.

Table E-1. Experimental data.

Solutes	Min.pH	Max.pH	Min.T C	Max.T C	Min.I <sub>m</sub> mol/L	Max.I <sub>m</sub> mol/L	Reference
0.05M Na <sub>2</sub> HPO <sub>4</sub> + 0.1M NaOH	10.900	12.000	25	25	0.157	0.173	1
0.1M Na <sub>2</sub> HPO <sub>4</sub> + 0.1M HCl	7.000	9.000	25	25	0.203	0.299	1
0.025M KH <sub>2</sub> PO <sub>4</sub> + 0.025M Na <sub>2</sub> HPO <sub>4</sub>	6.830	6.880	25	90	0.050	0.050	2
0.008695M KH <sub>2</sub> PO <sub>4</sub> + 0.03043M Na <sub>2</sub> HPO <sub>4</sub>	7.385	7.416	25	50	0.050	0.050	2
0.025M Borax + 0.1M NaOH	9.200	10.800	25	25	0.051	0.066	1
0.025M Borax + 0.1M HCl	8.000	9.100	25	25	0.035	0.048	1
0.01M Borax	8.850	9.182	25	90	0.020	0.020	3
0.05M Borax + 0.1M NaOH	8.860	9.670	40	70	0.100	0.100	4
0.05M Borax + 0.1M HCl	7.950	9.080	40	70	0.057	0.100	4
0.1M H <sub>3</sub> BO <sub>3</sub>	5.100	5.100	20	20	6.660E-06	6.660E-06	5

Figures E-1 thru E-5 show the differences between the measured and calculated pH values. Most of the calculated values are within 0.1 pH unit and all values except one (0.34) are within 0.22 pH unit.

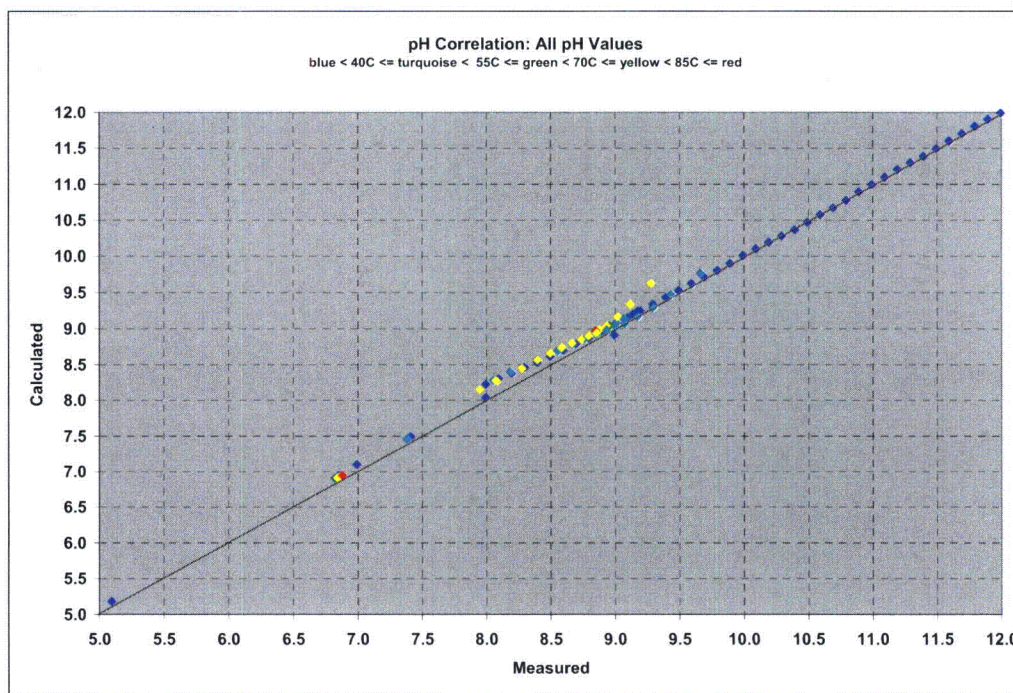


Figure E-1. The differences between all the measured and calculated pH values. Experiments done at different temperature ranges are indicated by the color of the points.



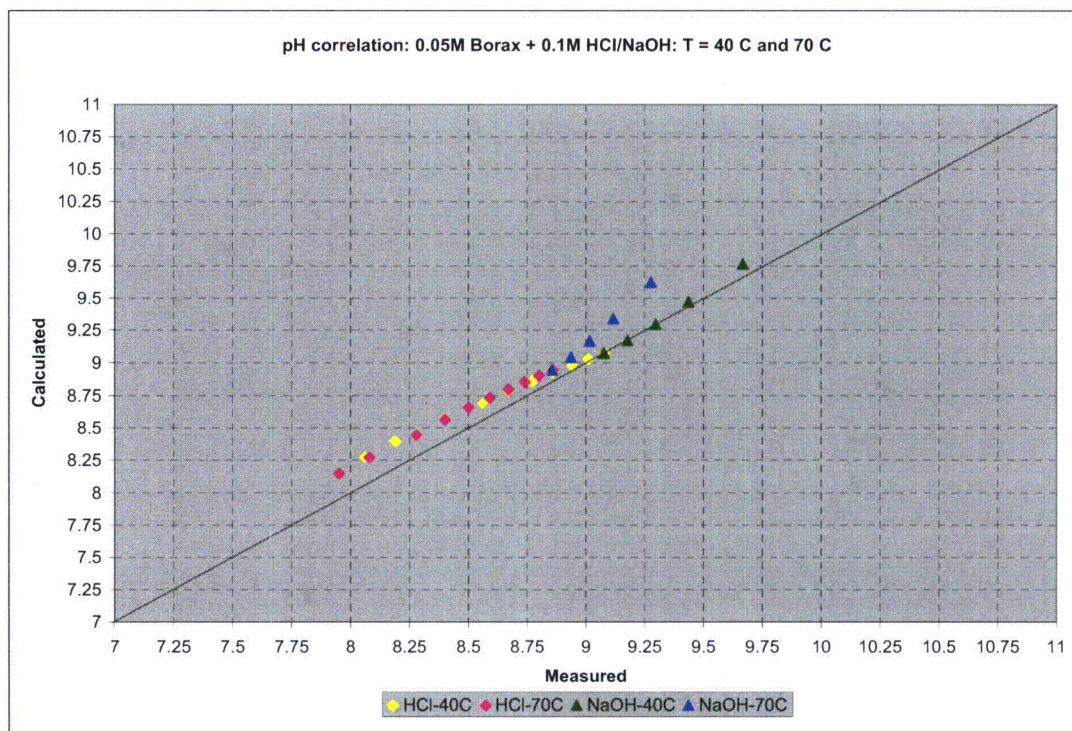


Figure E-2. The differences between measured and calculated pH values in Borax + HCl/NaOH at 40 °C (313 K) and 70 °C (343 K)..

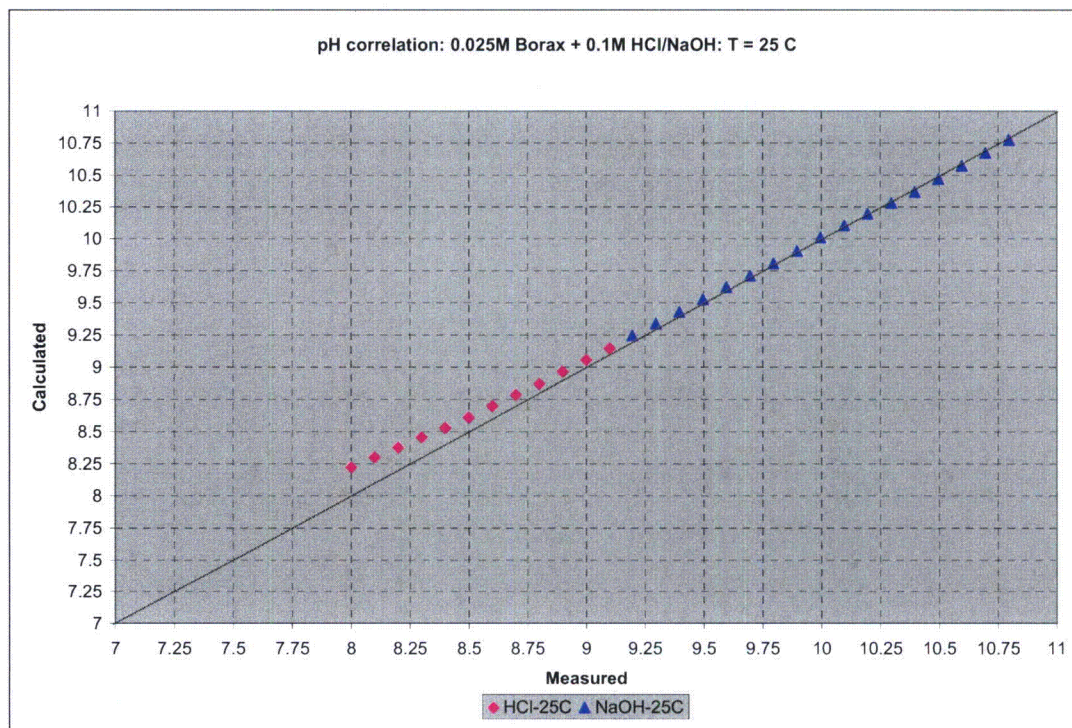


Figure E-3. The differences between measured and calculated pH values in Borax + HCl/NaOH at 25 °C (298 K).



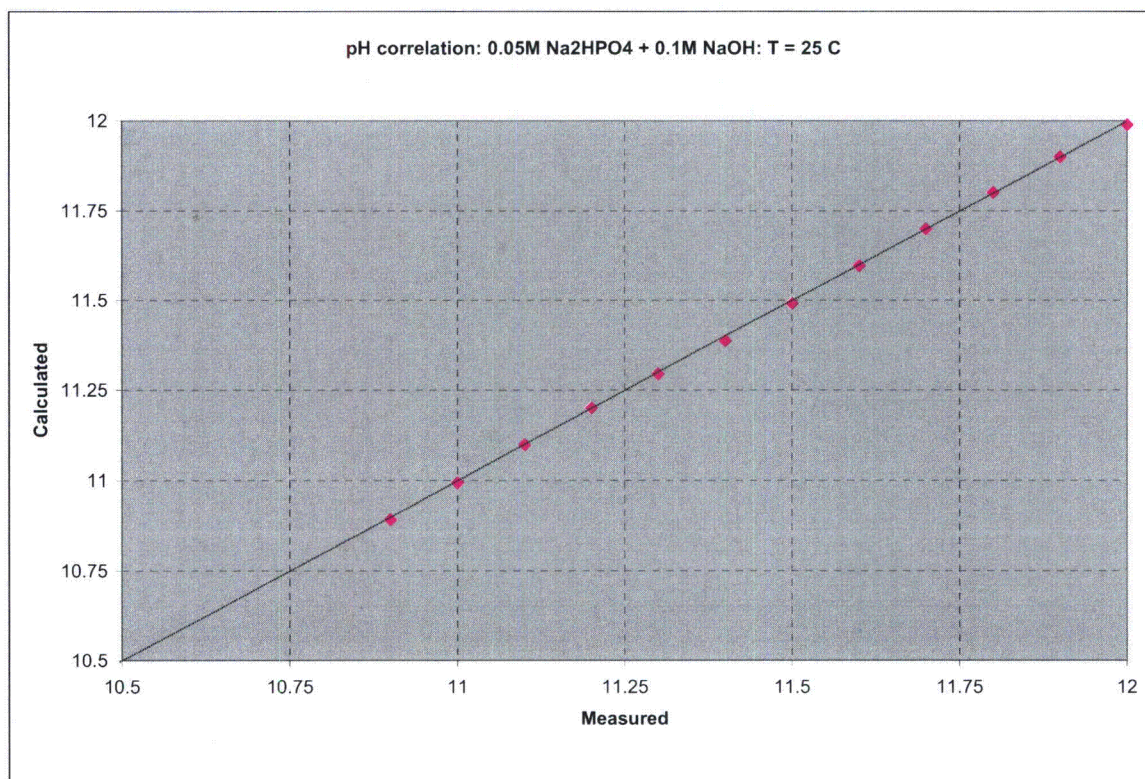


Figure E-4. The differences between measured and calculated pH values in Na<sub>2</sub>HPO<sub>4</sub> + NaOH at 25 °C.

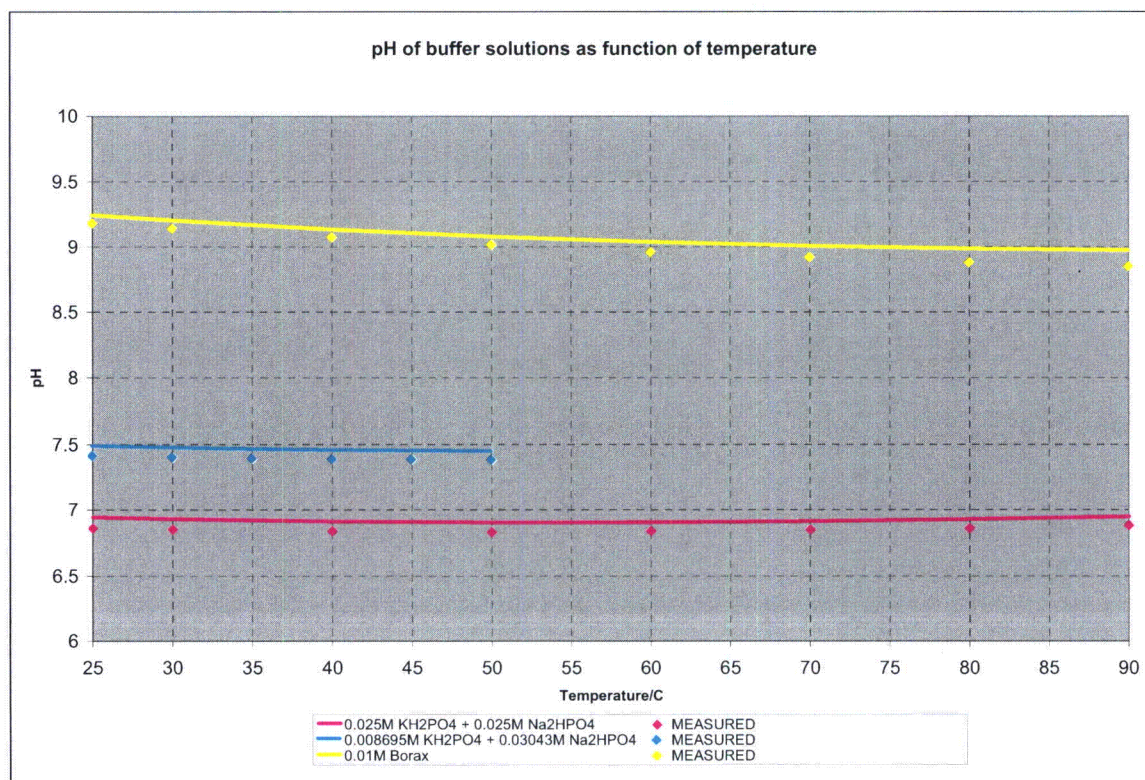


Figure E-5. The pH of the buffer solutions as a function of the temperature.



Table E-2 shows the active species in the thermodynamic system. Species colored red are phosphate species that are not yet used in the pH simulations. They are used in the validation calculations in case they are needed in the future (for  $\text{Na}_3\text{PO}_3$  buffer added to pools).

Table E-2. Thermodynamic System.

Phase	Constituent	Element									
		B	Cl	Cs	H	I	N	Na	O	P	e-
Gas	H2O(g)				2				1		
	Cl2(g)		2								
	CsOH(g)			1	1				1		
	H(g)				1						
	H2(g)				2						
	HCl(g)		1		1						
	HI(g)				1	1					
	I(g)					1					
	I2(g)					2					
	IO(g)					1			1		
	N2(g)						2				
	NO2(g)						1		2		
O2(g)								2			
Water	H2O				2				1		
	B(OH)3(a)	1			3				3		
	B(OH)4(-a)	1			4				4		1
	Cl(-a)		1								1
	Cs(+a)			1							-1
	CsOH(a)			1	1				1		
	H(+a)				1						-1
	I(-a)					1					1
	I2(a)					2					
	Na(+a)							1			-1
	OH(-a)				1				1		1
	N2(a)						2				
	HNO3(a)				1		1		3		
	NO2(-a)						1		2		1
	NO3(-a)						1		3		1
	H2PO4(-a)				2				4	1	1
	HPO4(-2a)				1				4	1	2
	PO4(-3a)								4	1	3
	H3PO4(a)				3				4		
Solids	CsI			1		1					
	CsOH			1	1				1		
	Na2O*2B2O3*10H2O	4			20			2	17		
	Na2O*5B2O3*10H2O	10			20			2	26		
	NaCl		1					1			
	NaOH				1			1	1		
	Na3PO4							3	4	1	
	Na2HPO4				1			2	4	1	
	NaH2PO4				2			1	4	1	

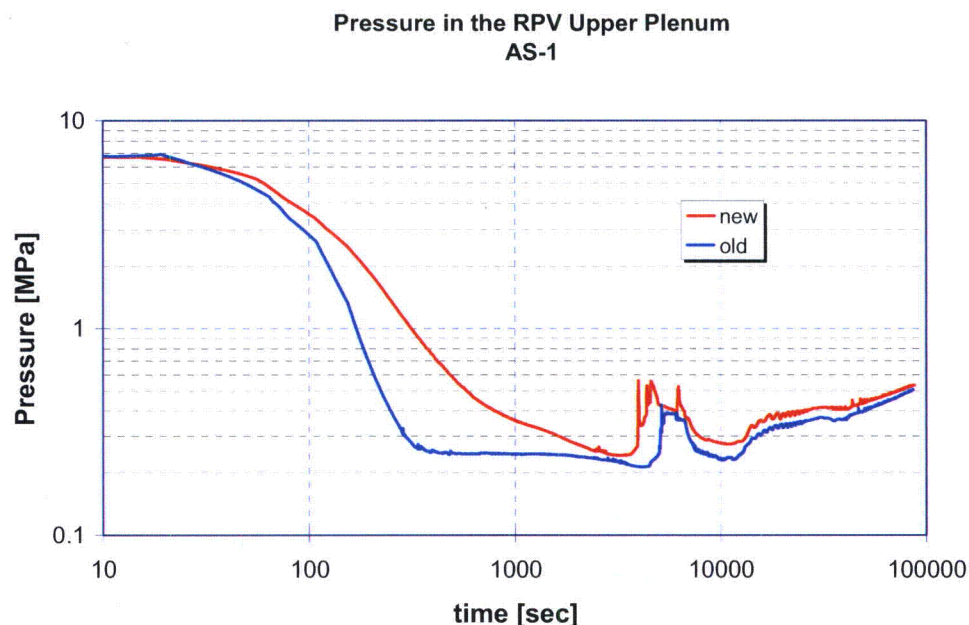


## 25 APPENDIX F: Comparison of results : AS-1 without MSIV leak of FR Part 2 and FR Part 3

In all following plots the curve indicated as "new" is a result calculated with the updated MELCOR input (MSL, MSDL and Main Condenser and SRVs, SRV/ADS and DPV models, The IC vent line always closed) and with code version 1.8.6YH. "old" is FR Part 2 result.

The comparison of the results of AS-1 showed that:

1. The average decontamination factor of CsI in the containment is the same or higher in the "new" runs than in the "old" runs. Thus the results of FR Part 2 are conservative in respect to the updated analyses.
2. The average decontamination factor of CsI in the PCCS is the same or higher in the "new" runs than in the "old" runs. Thus the results of FR Part 2 are conservative in respect to the updated analyses.
3. The total airborne CsI mass in the containment is the same or lower in the "new" runs than in the "old" runs. Thus the results of FR Part 2 are conservative in respect to the updated analyses.
4. The masses of CsOH in the containment water pools are higher in the "new" runs than in the "old" runs. Thus the "old" runs are conservative in respect to pool pH in all pools.
5. Containment pressure is higher in the "new" runs than in the "old" runs due to larger H<sub>2</sub> production in the core in the "new" run.
6. The CsI leakage from containment via nominal leakage path is 15.7 % higher in the "new" results than in the "old" results of FR Part 2. This is due to higher containment pressure and consequently higher driving pressure difference for the nominal leak path.



7.  
Figure F-1. Pressure in the RPV, AS-1

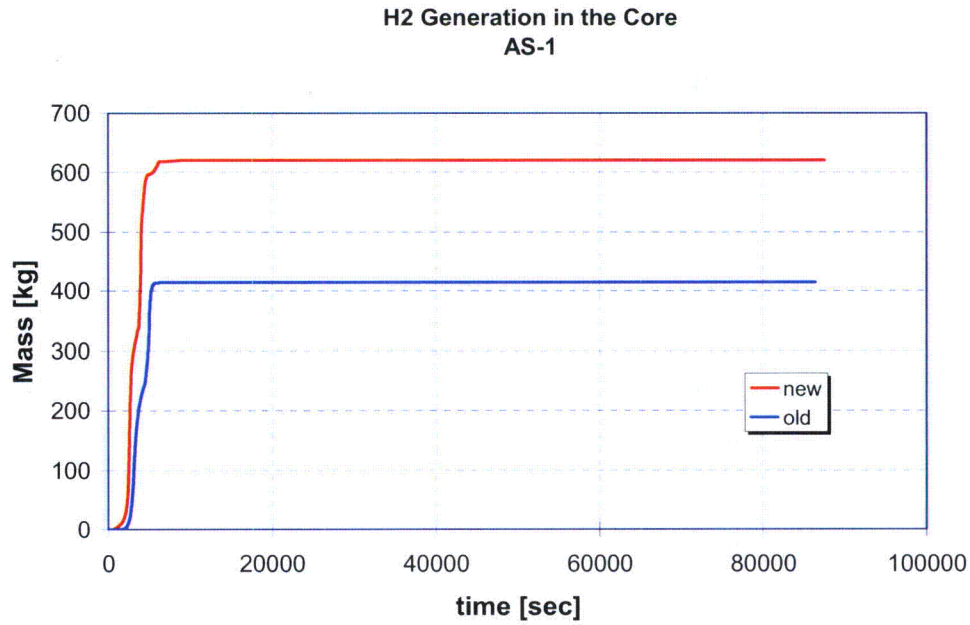


**Figure F-2.** *Hydrogen generation in the core. AS-1.*

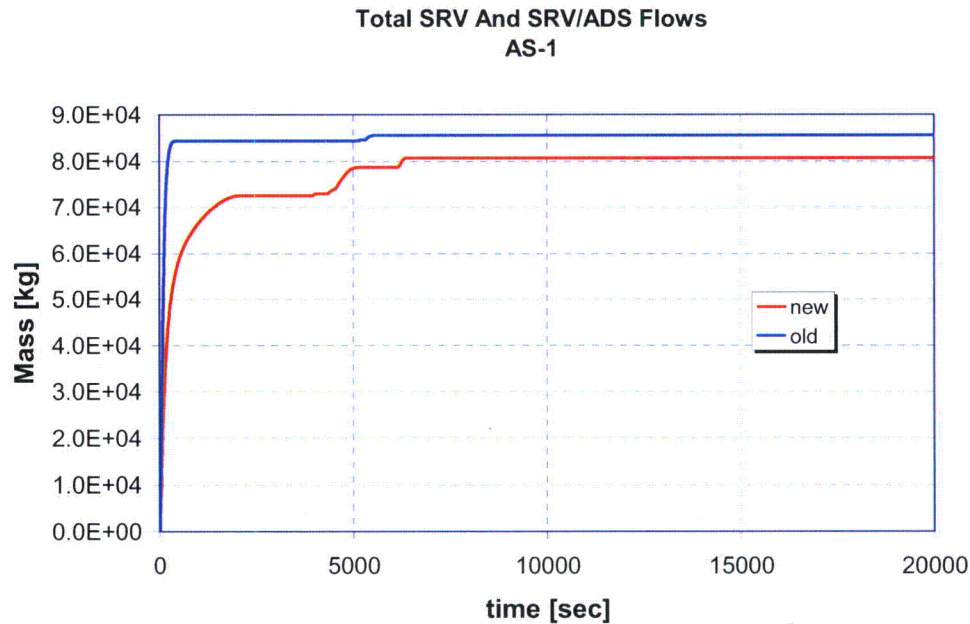


**Figure F-3.** *Total steam flows through SRVs and SRV/ADS valves. AS-1.*

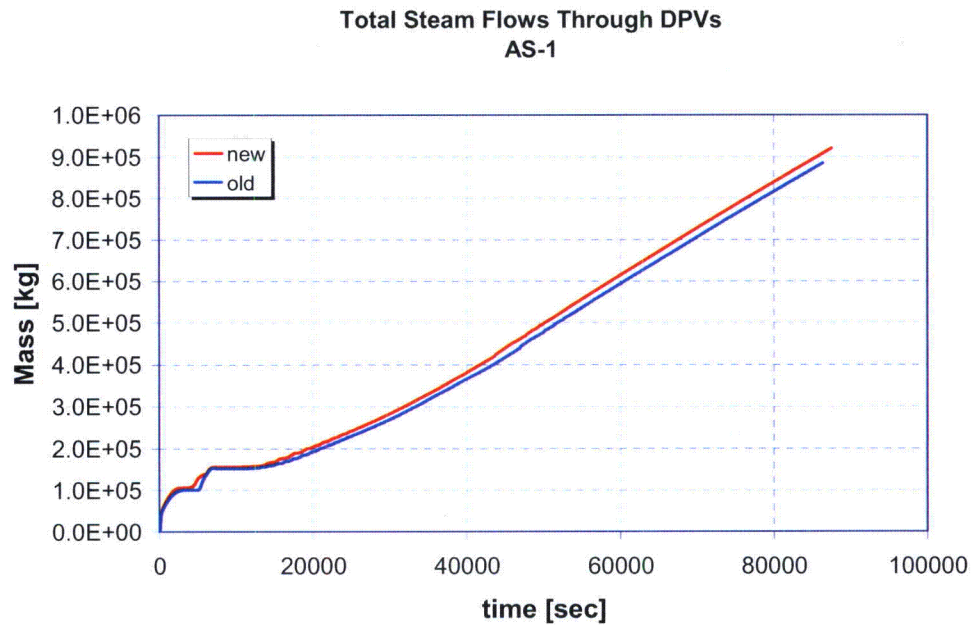


Figure F-4. Total steam flow through DPVs. AS-1.

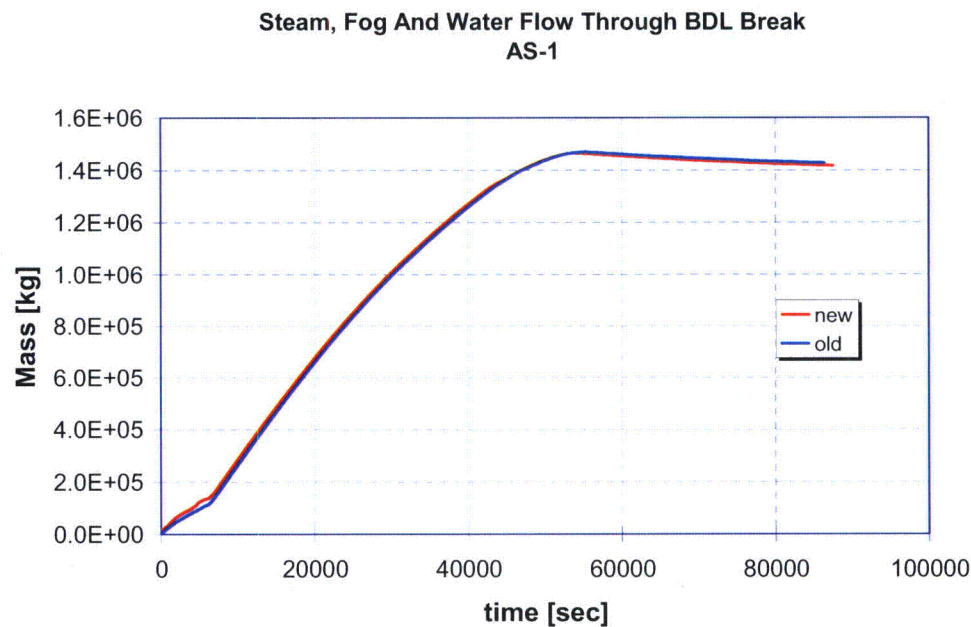
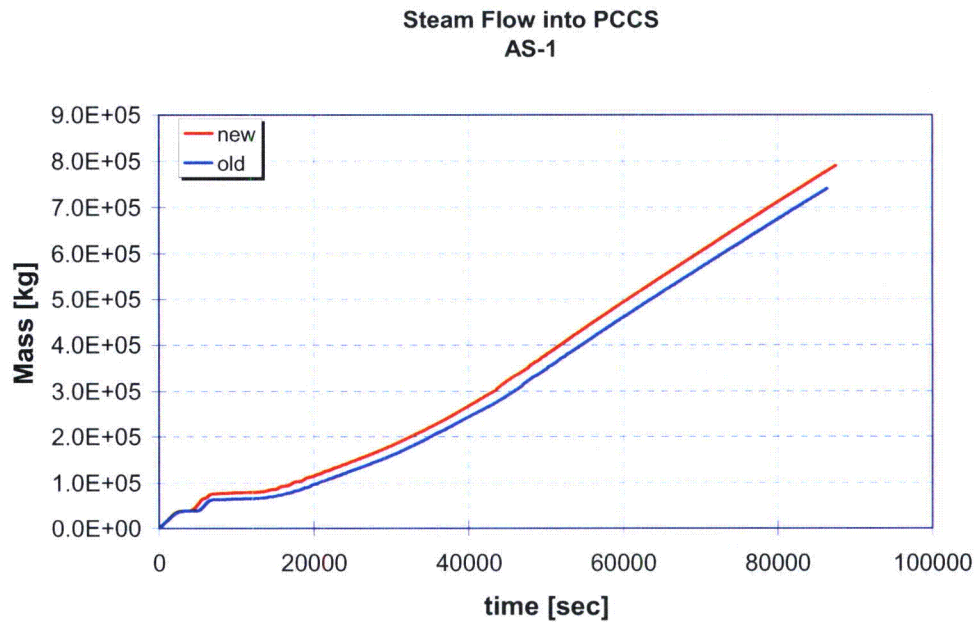
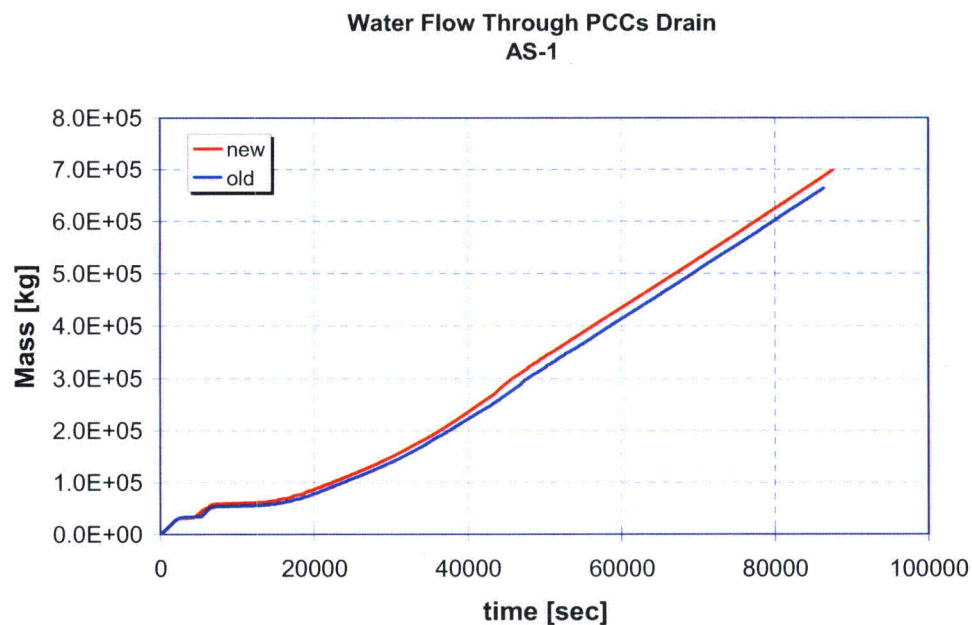


Figure F-4. Total steam, fog and water flow through the BDL break. AS-1.



**Figure F-5.** Cumulative steam flow in to the PCCS. AS-1.



**Figure F-6.** Cumulative water flow through the PCCS Drain Line. AS-1.

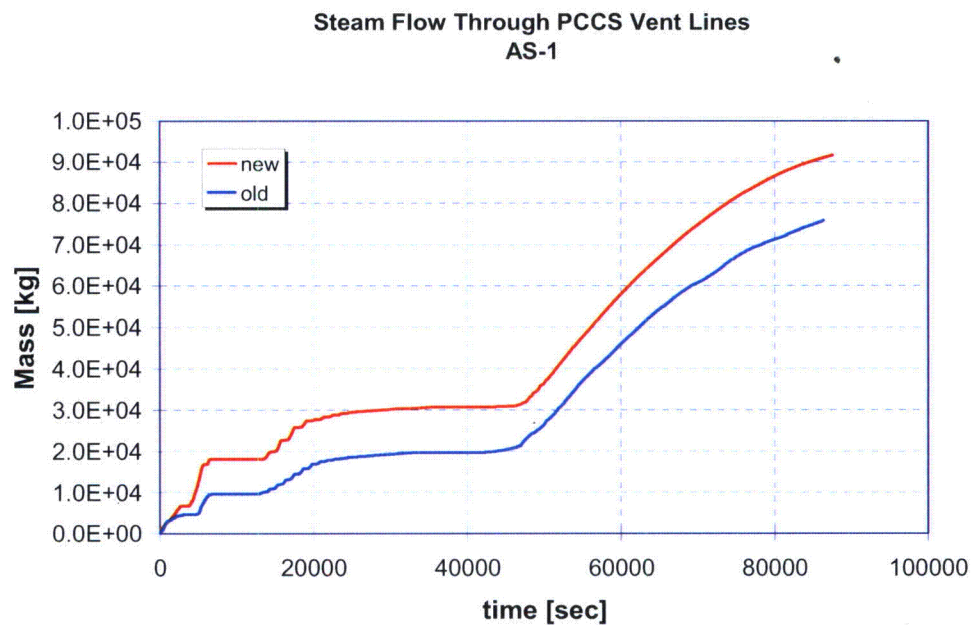


Figure F-7. Cumulative steam flow through the PCCS Vent Line. AS-1.

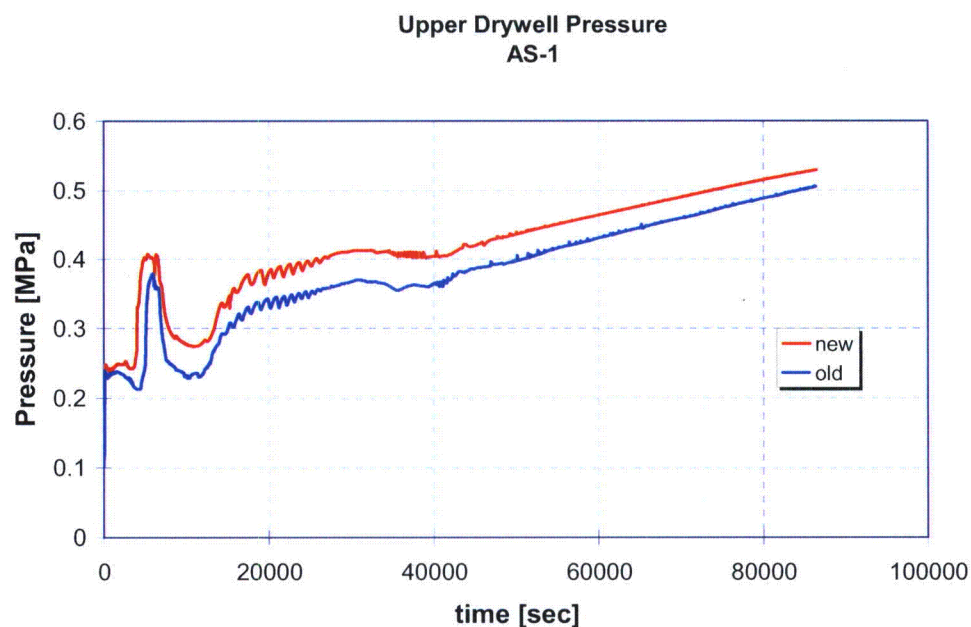


Figure F-8. Pressure in the Upper Drywell. AS-1.



### Partial Pressure of Hydrogen in Upper Drywell AS-1

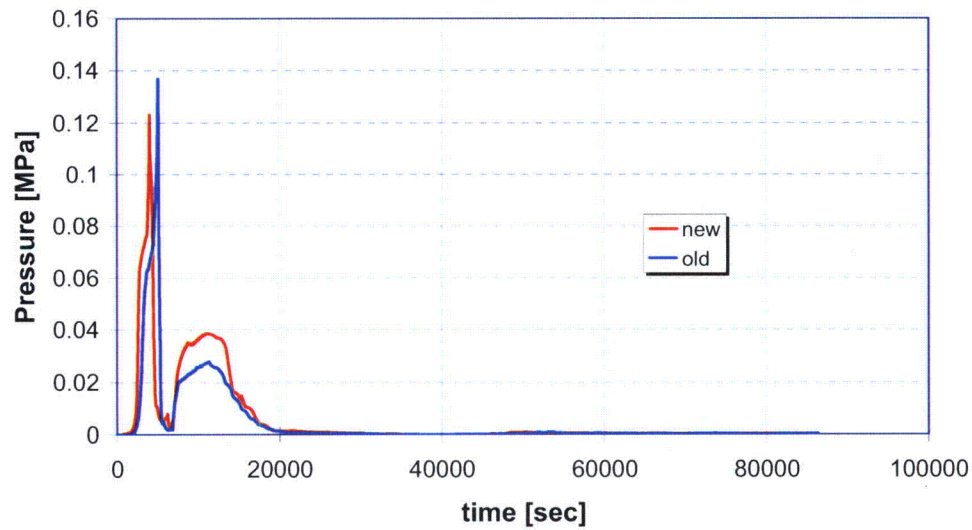


Figure F-9. Partial pressure of hydrogen in the Upper Drywell. AS-1.

### Water Mass in the GDCS Pool AS-1

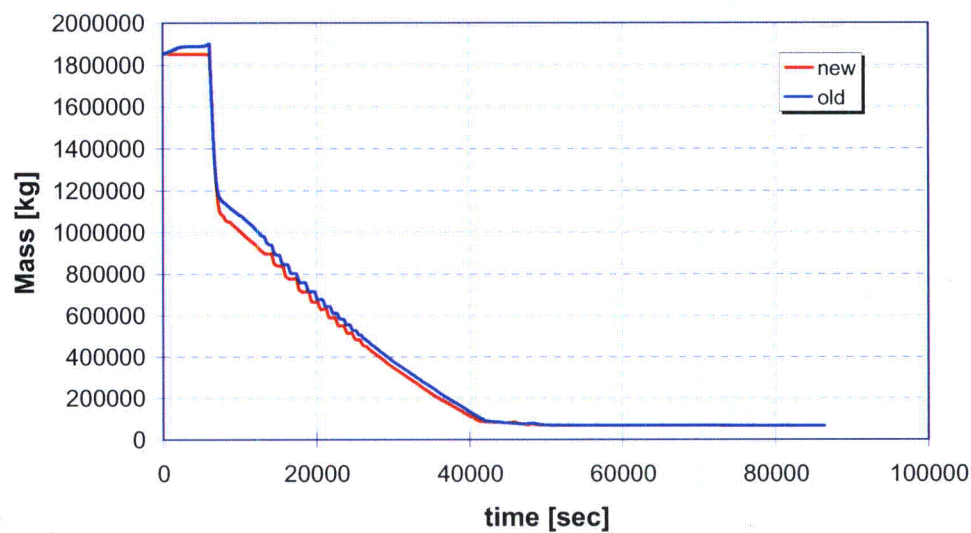


Figure F-10. Water mass in the GDCS pool. AS-1.



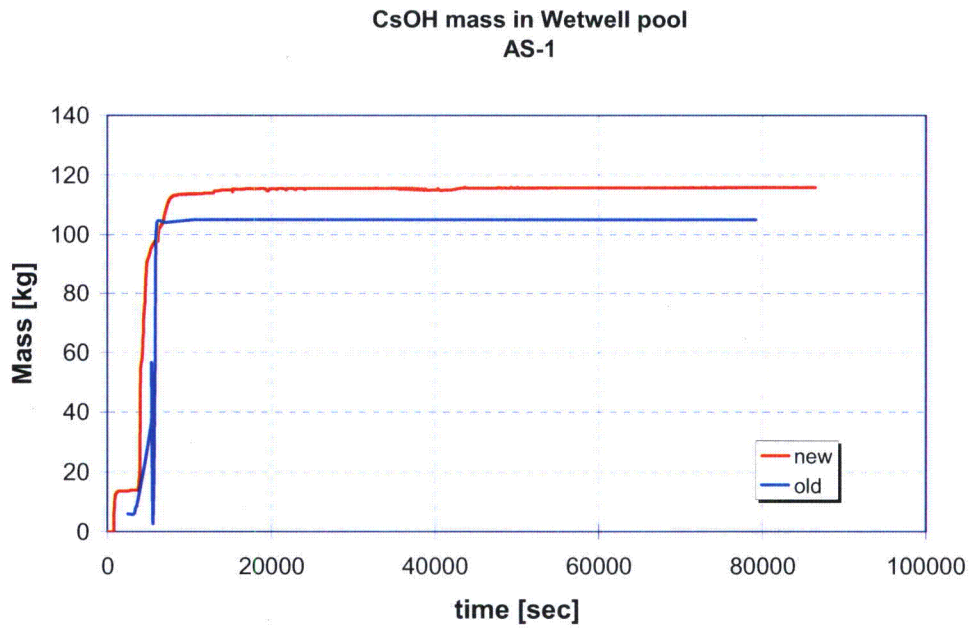


Figure F-11. CsOH mass in the Wetwell pool. AS-1.

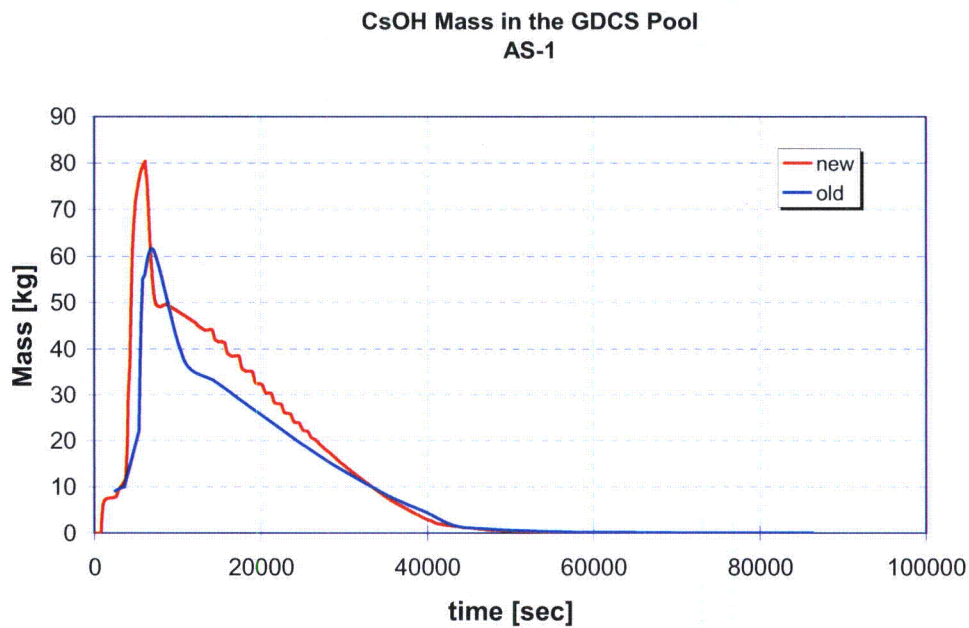


Figure F-12. CsOH mass in the GDCS pool. AS-1.

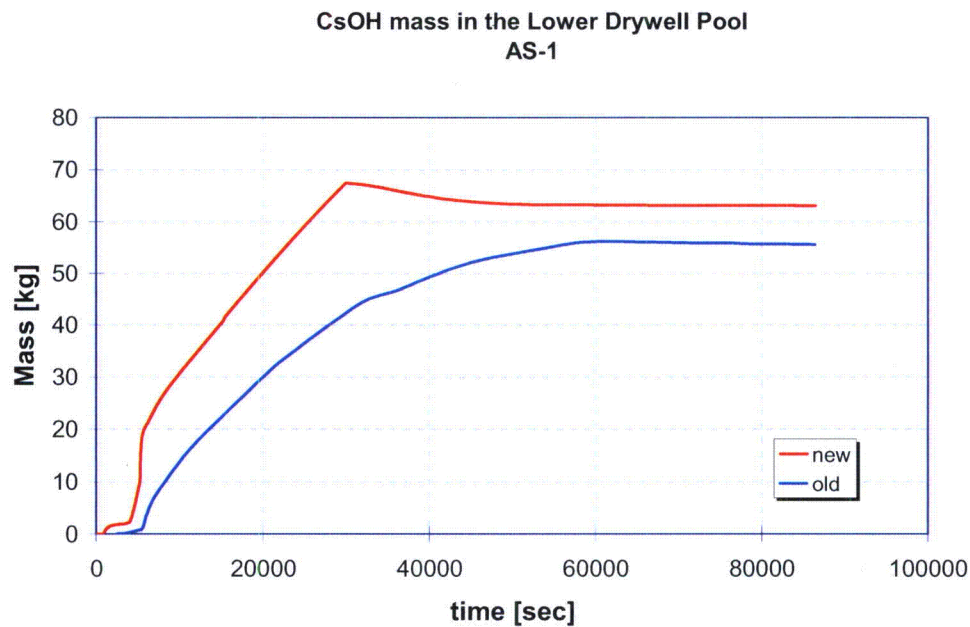


Figure F-13. CsOH mass in the Lower Drywell pool. AS-1.

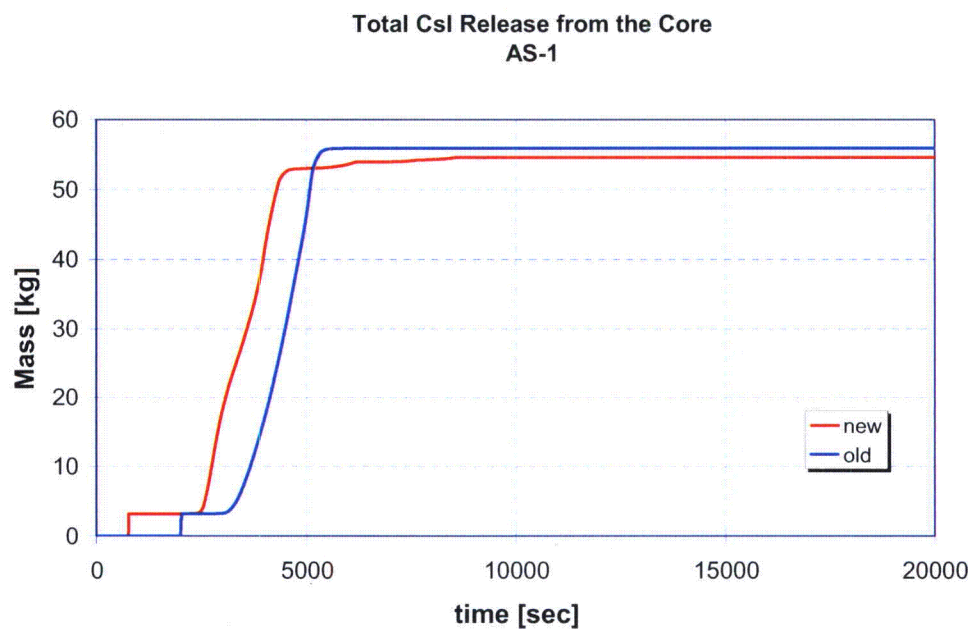


Figure F-14. Total release of CsI from the core. AS-1.

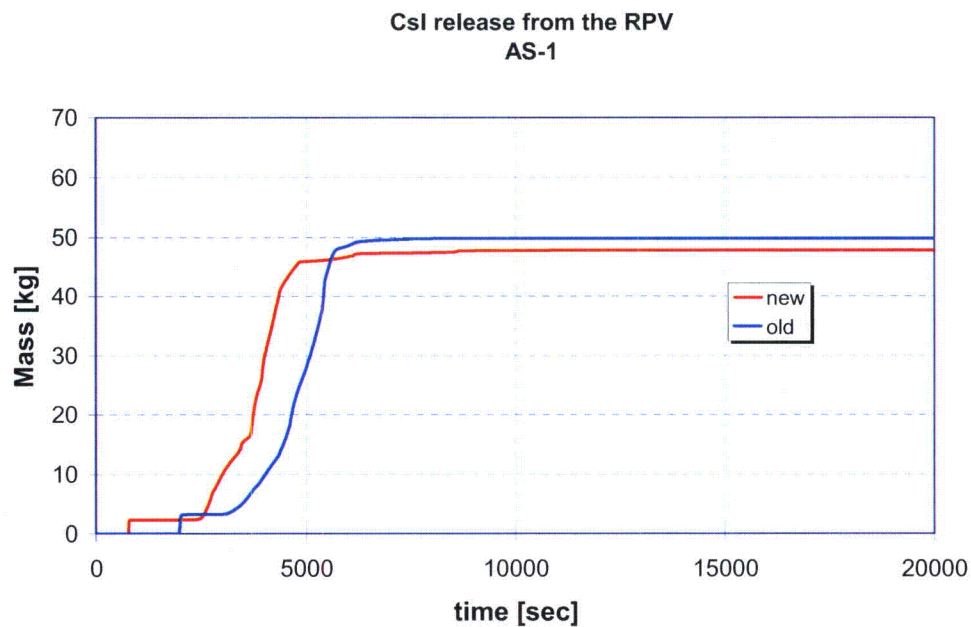


Figure F-15. Total release of CsI from the RPV to the containment. AS-1.

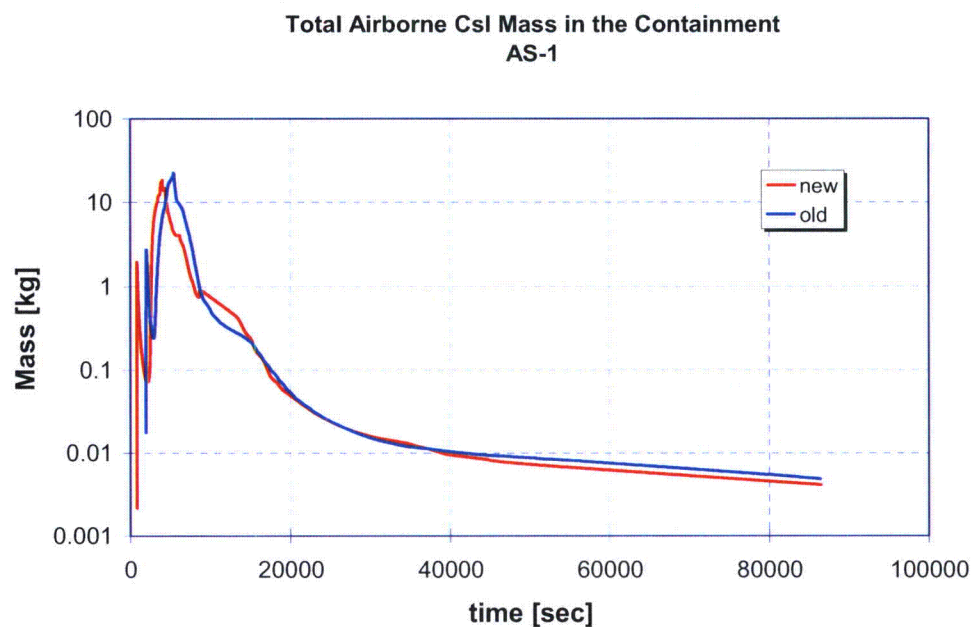


Figure F-16. Total airborne CsI mass in the containment. AS-1.

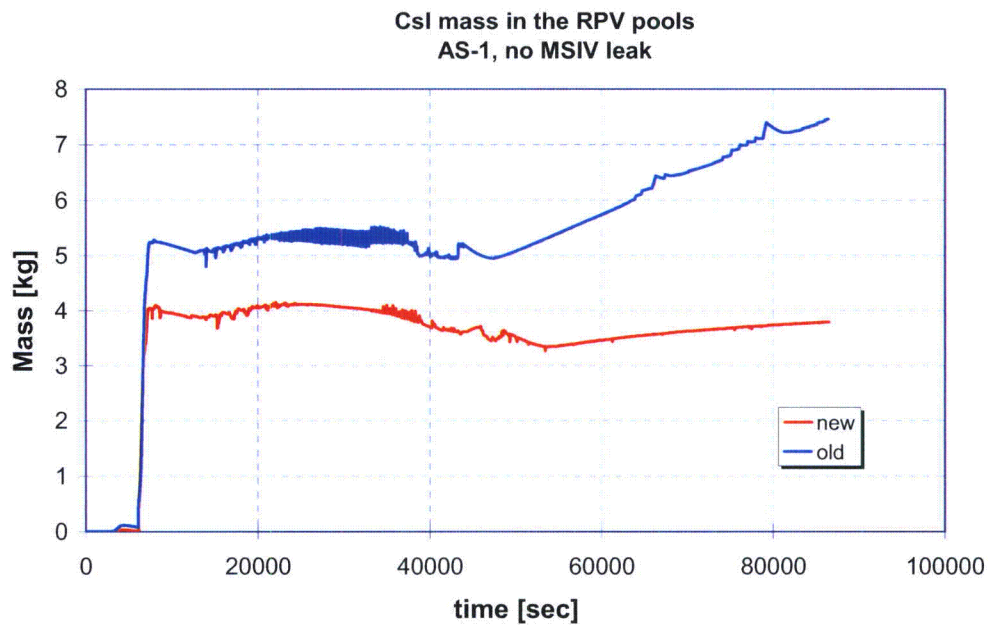


Figure F-17. CsI mass in the RPV water pools. AS-1.

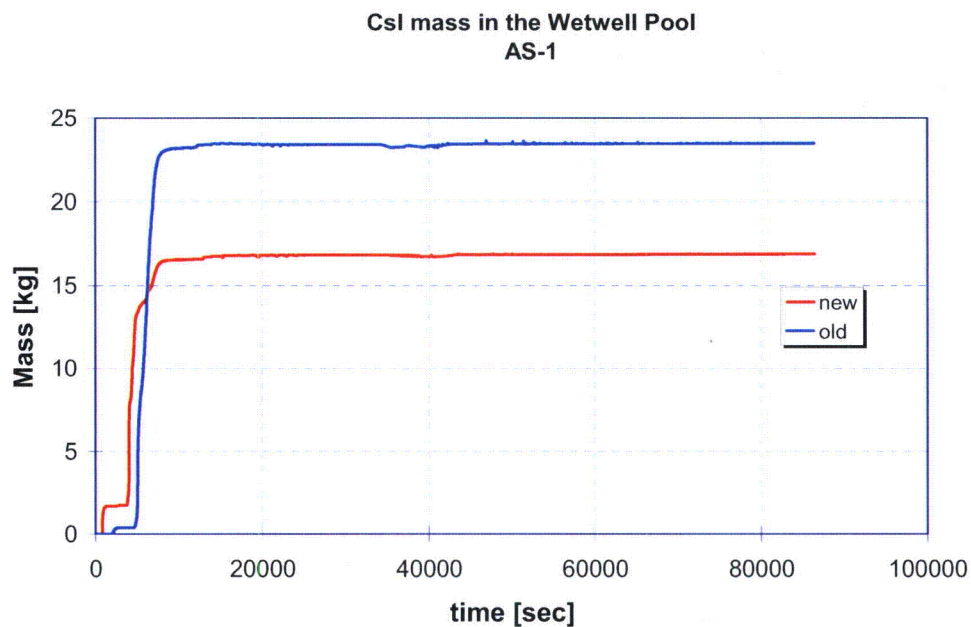


Figure F-18. Total mass of CsI in the Wetwell pool. AS-1.

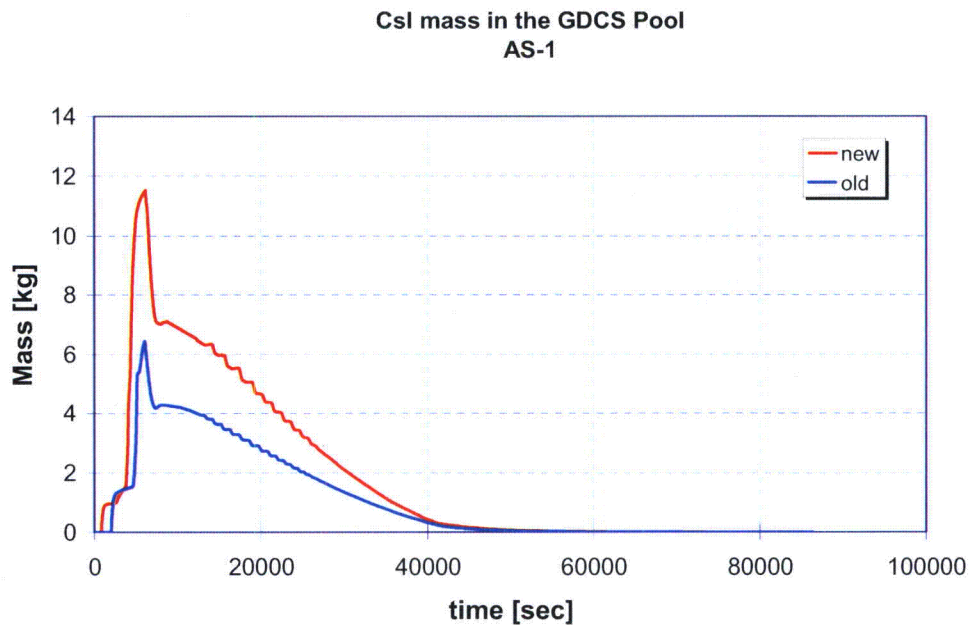


Figure F-19. Total CsI mass in the GDCS pool. AS-1.

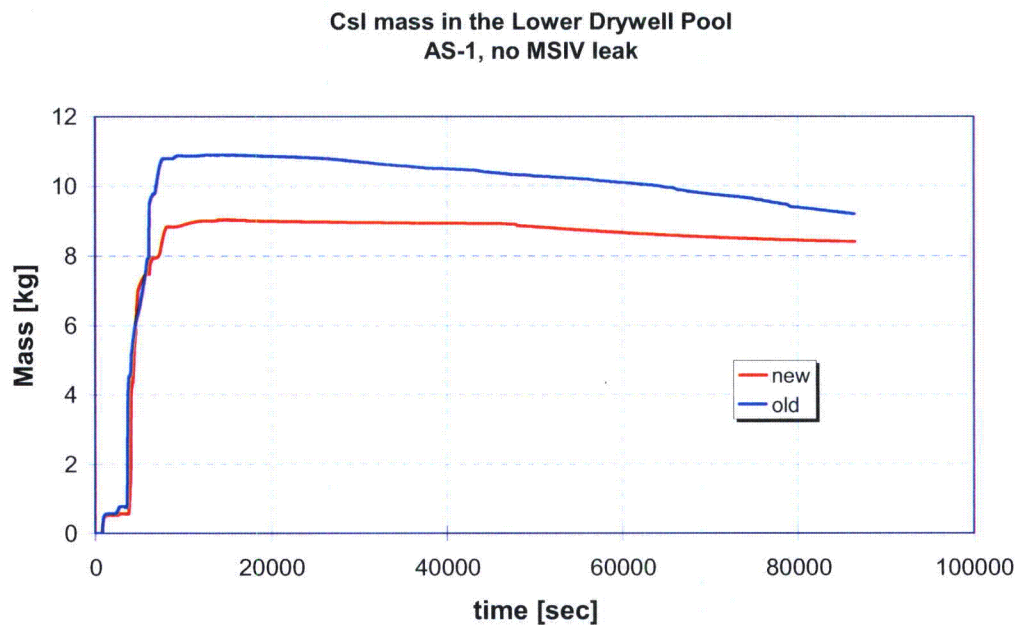
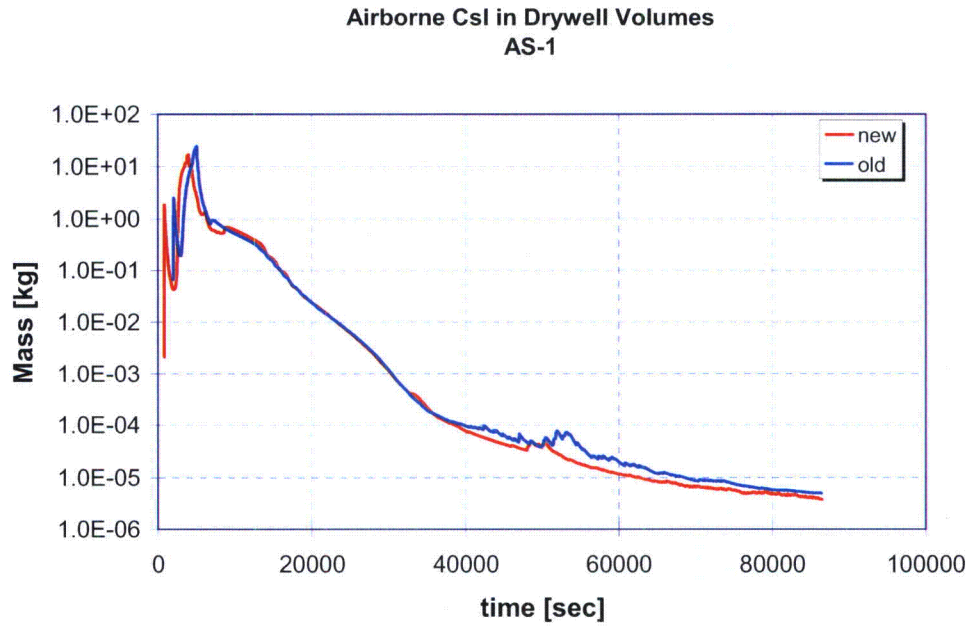
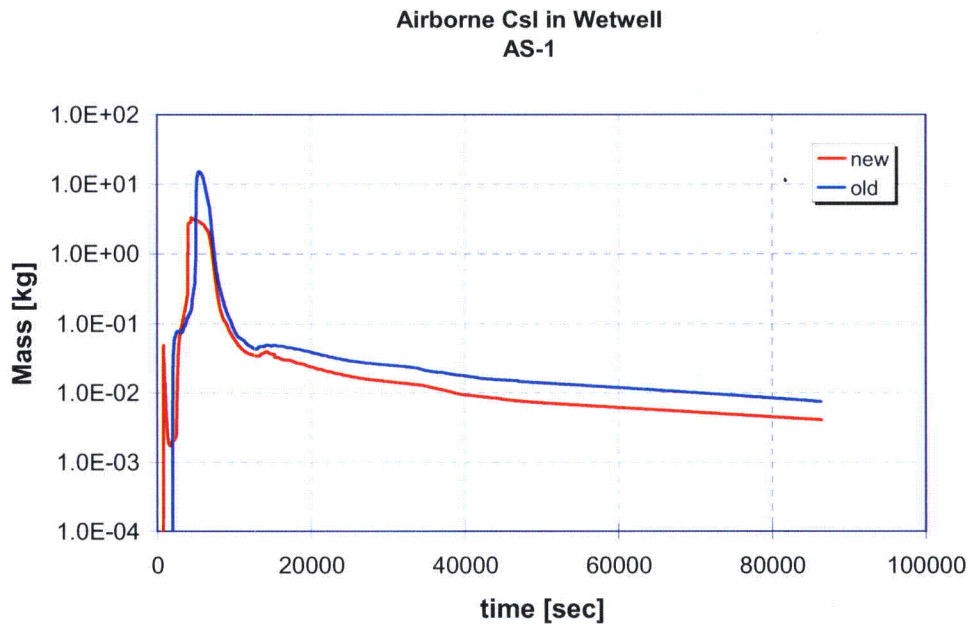


Figure F-20. Total CsI mass in the Lower Drywell pool. AS-1.



**Figure F-21.** Total airborne CsI in the Drywell volumes. AS-1.



**Figure F-22.** Total airborne CsI mass in the Wetwell. AS-1.



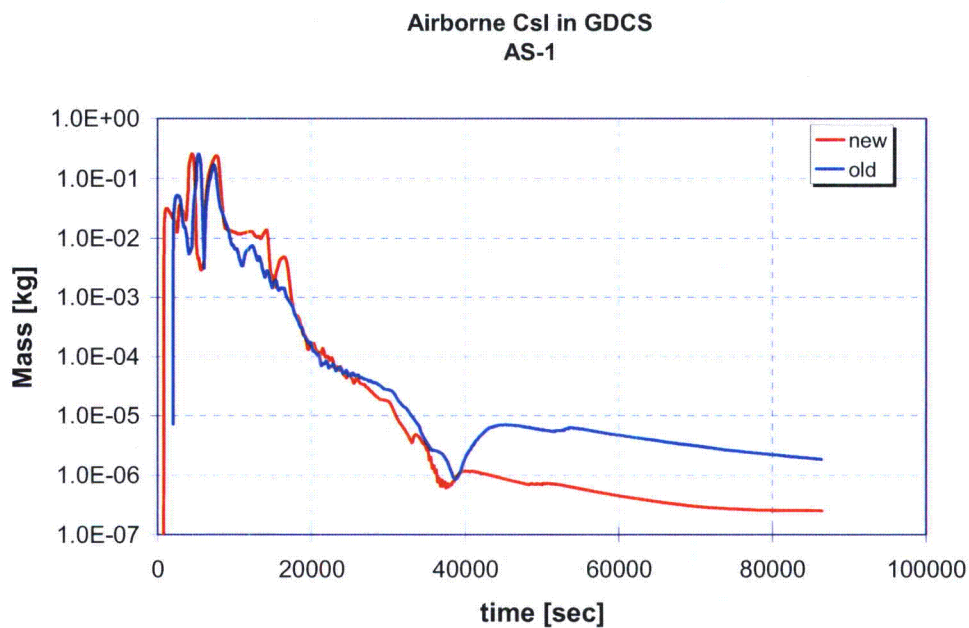


**Figure F-23.** Total airborne CsI mass in the GDCS. AS-1.

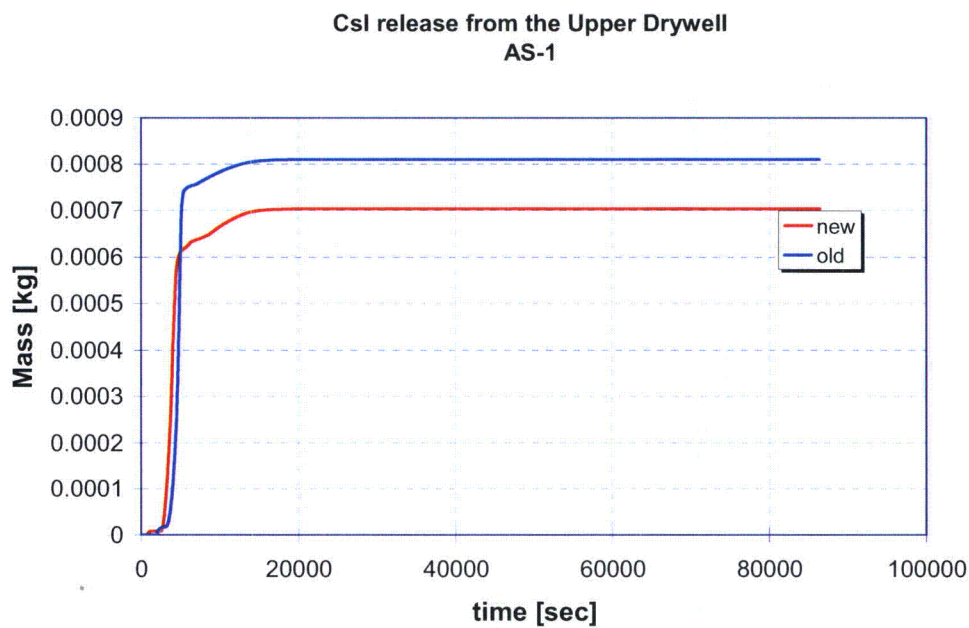


**Figure F-24.** Total CsI release from the Upper Drywell via containment nominal leakage path. AS-1.

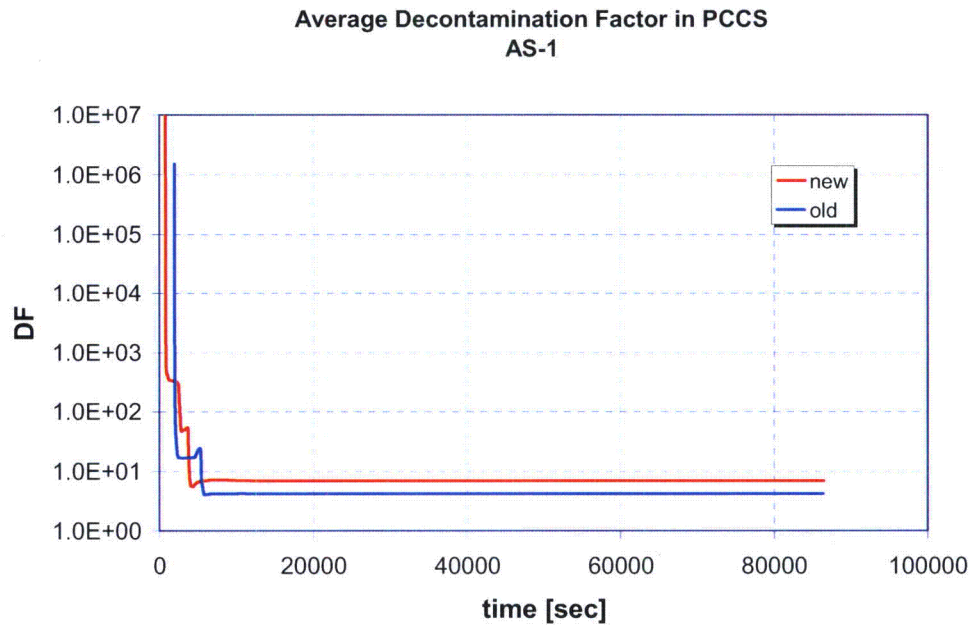


**Figure F-25.** Average decontamination factor of CsI in the PCCS. Calculated as CsI flow in to the PCCS divided by the sum of CsI flow through the PCCS Drain Lines and Vent Lines. AS-1.

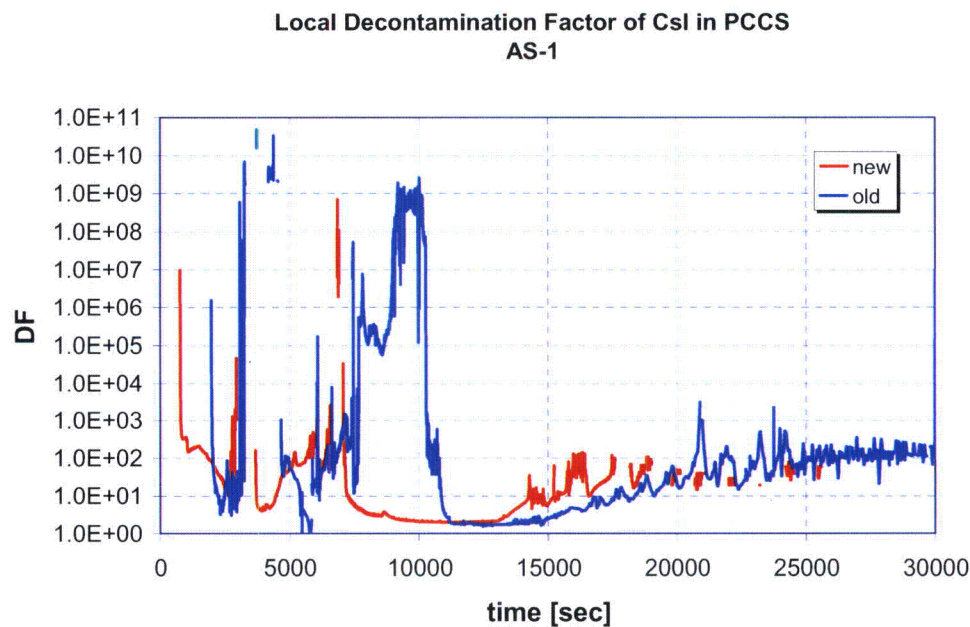


**Figure F-26.** Decontamination factor of CsI in the PCCS calculated over a MELCOR plot file time step as the incoming CsI mass over a time step divided by the outgoing CsI mass (Drain Lines+Vent Line) over a time step. AS-1.

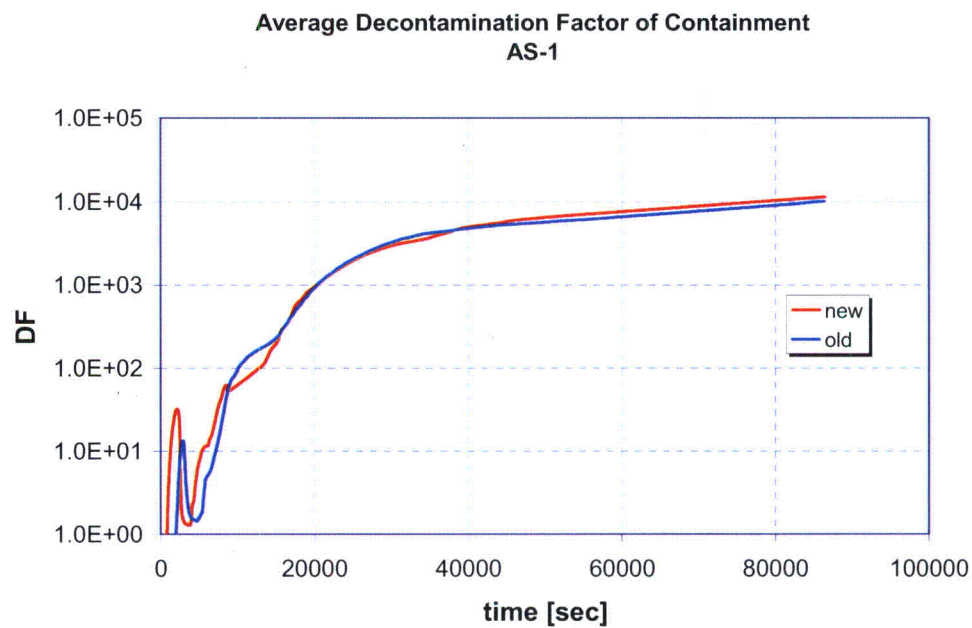


**Figure F-27.** Average CsI decontamination factor in the containment calculated as total CsI release from RPV to containment divided by total airborne mass of CsI in the containment. AS-1.

## 26 APPENDIX G: Comparison of results: AS-2 without MSIV leak of FR Part 2 and FR Part 3

In all following plots the curve indicated as "new" is a result calculated with the updated MELCOR input (MSL, MSDL and Main Condenser and SRVs, SRV/ADS and DPV models, the IC vent line always closed) and with code version 1.8.6YH. "old" is FR Part 2 result.

The comparison of the results of AS-2 showed that:

1. The average decontamination factor of CsI in the containment is higher in the "new" runs than in the "old" runs. Thus the results of FR Part 2 are conservative in respect to the updated analyses.
2. The average decontamination factor of CsI in the PCCS is practically the same in the "new" runs than in the "old" runs. Thus the results of FR Part 2 are conservative in respect to the updated analyses.
3. The total airborne CsI mass in the containment is lower in the "new" runs than in the "old" runs. Thus the results of FR Part 2 are conservative in respect to the updated analyses.
4. The masses of CsOH in the containment water pools are higher in the "new" runs than in the "old" runs. Thus the "old" runs are conservative in respect to pool pH in all pools.
5. Containment pressure is higher in the "new" runs than in the "old" old runs due to larger H<sub>2</sub> production in the core in the "new" run.
6. The CsI leakage through nominal leakage path is 31 % higher in the "new" calculations than in the "old" results. This is due to a higher containment pressure and thus higher driving pressure difference in the "new" runs.

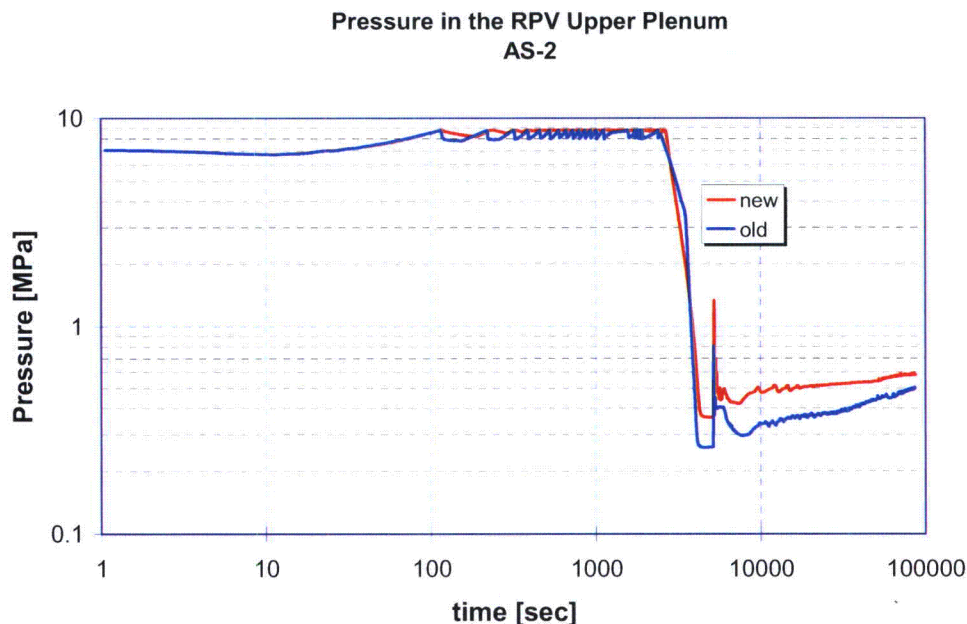


**Figure G-1.** *Pressure in the Upper Plenum. AS-2.*

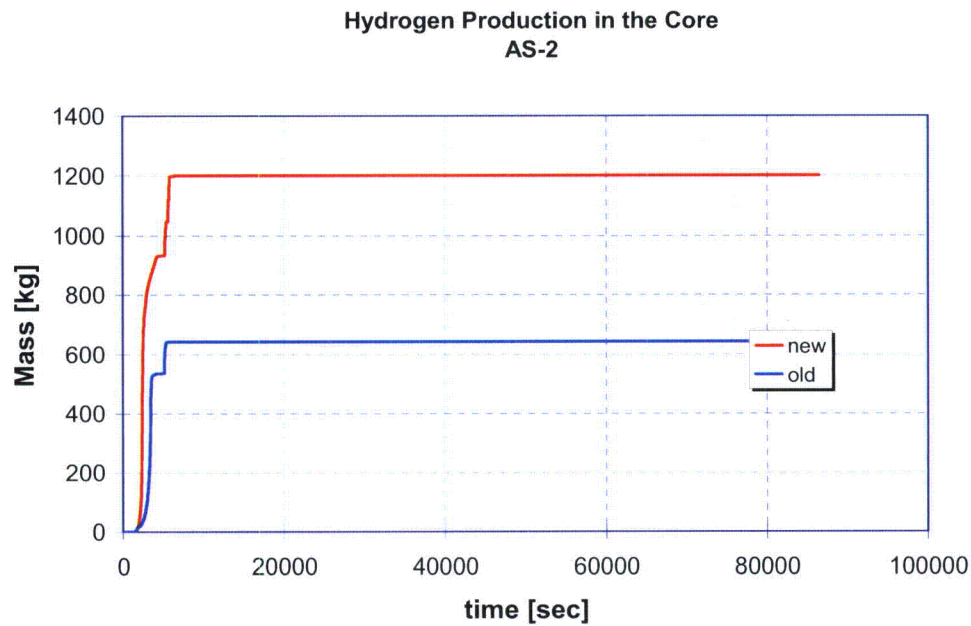


**Figure G-2.** Total hydrogen production in the core. AS-2.

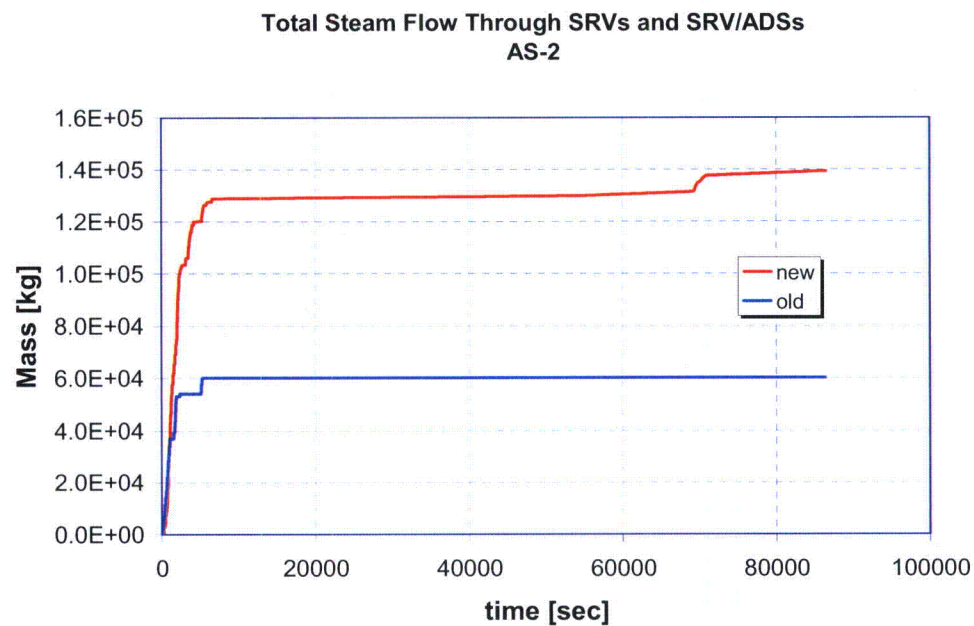


**Figure G-3.** Cumulative steam flow through SRVs and SRV/ADS valves. AS-2.



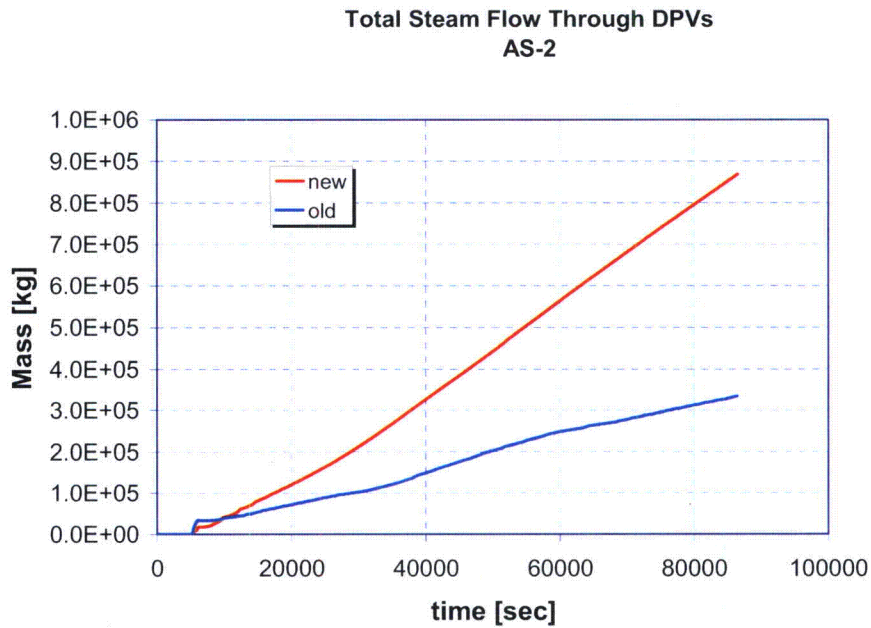


**Figure G-4.** Cumulative steam flow through DPVs. AS-2.

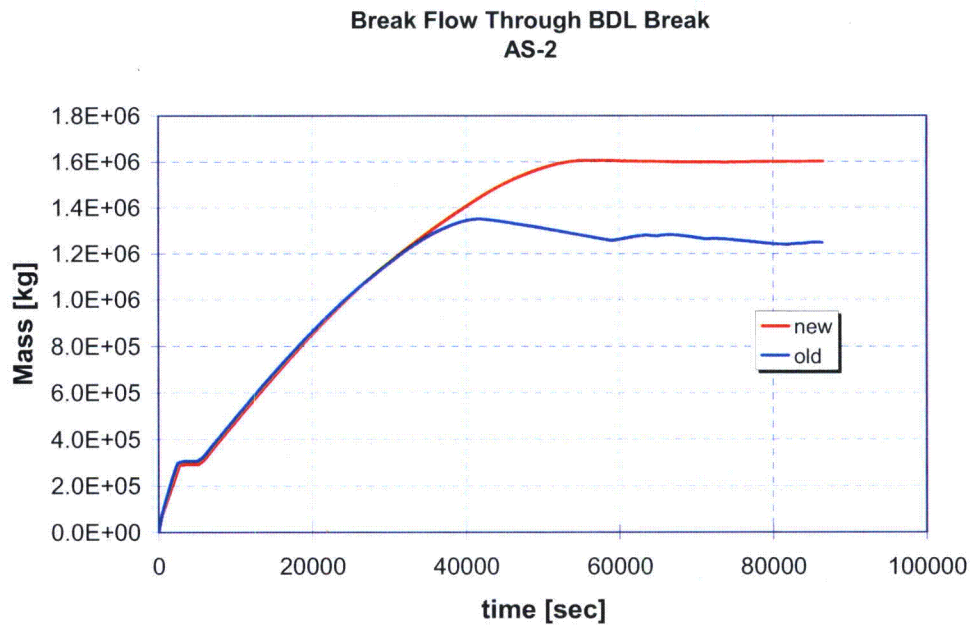


**Figure G-5.** Cumulative steam, fog and water flow through BDL break. AS-2.



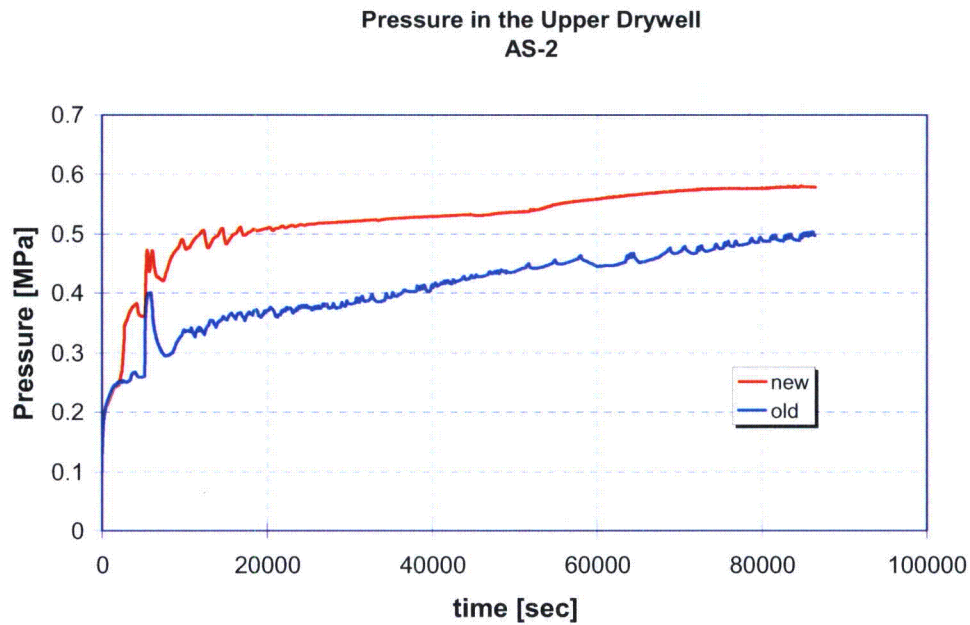


**Figure G-6.** *Pressure in the Upper Drywell. AS-2.*

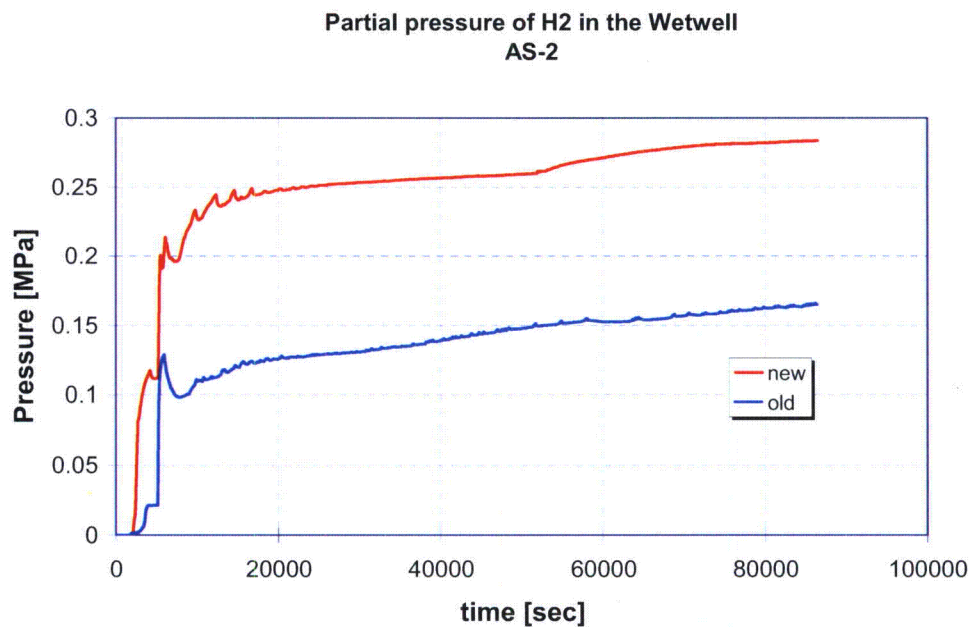


**Figure G-7.** *Partial pressure in the Wetwell. AS-2.*

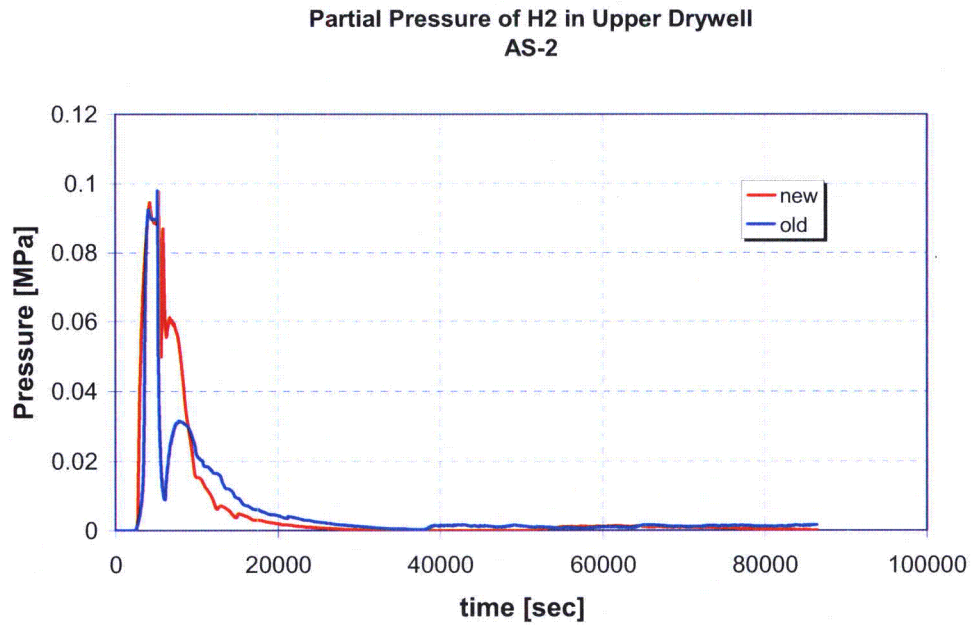


**Figure G-8.** *Partial pressure of hydrogen in the Upper Drywell. AS-2.*

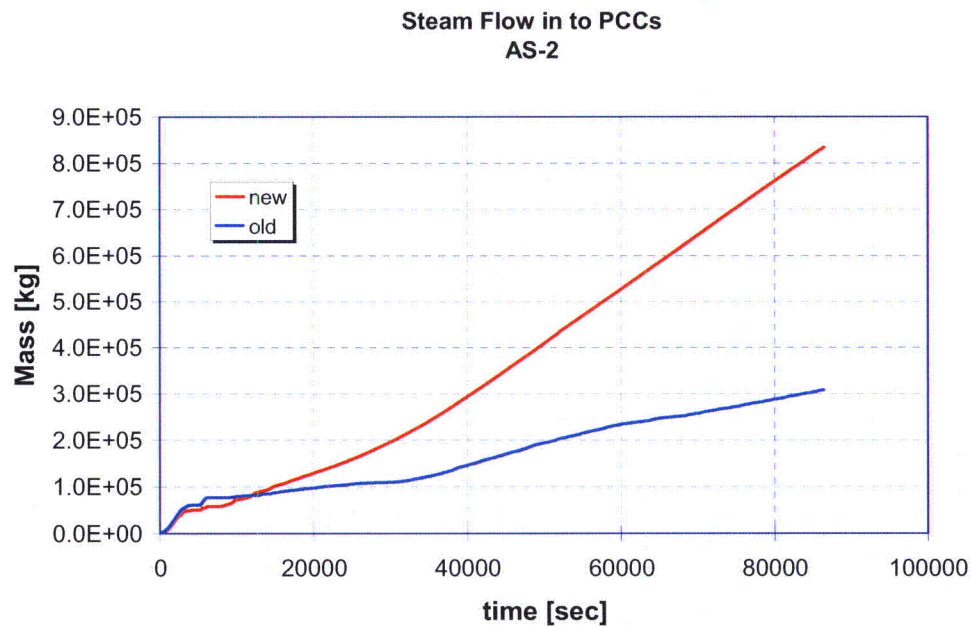


**Figure G-9.** *Cumulative steam flow in to the PCCS. AS-2.*

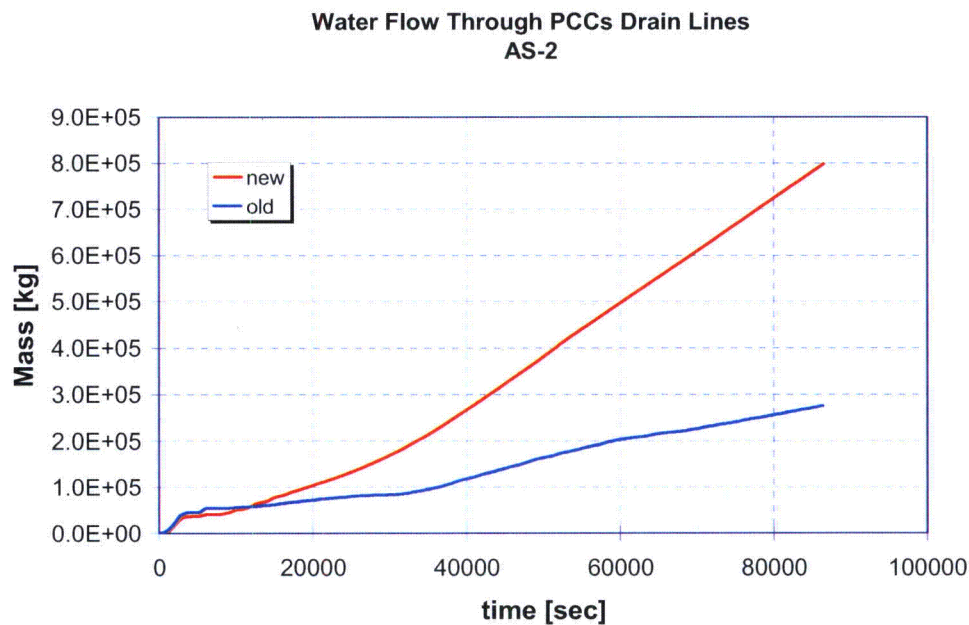


**Figure G-10.** Cumulative water flow through the PCCS Drain Lines. AS-2.

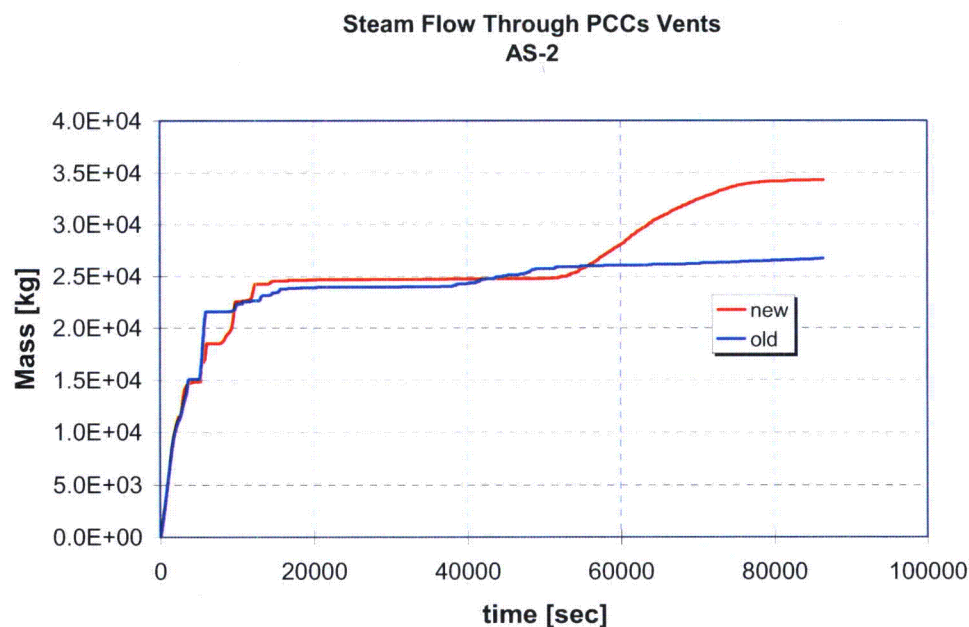


**Figure G-11.** Cumulative steam flow through PCCS Vent Lines. AS-2.

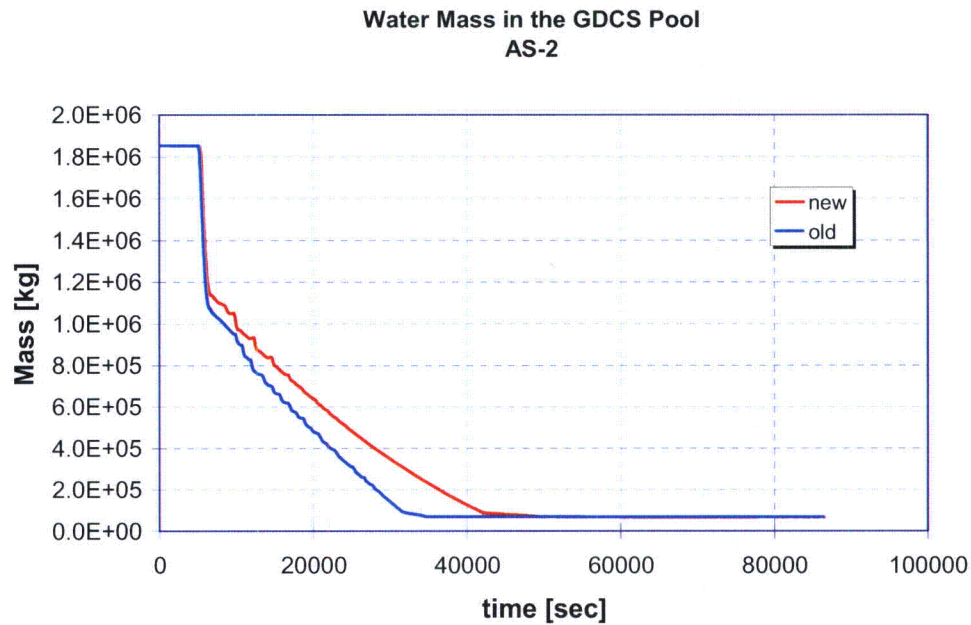


**Figure G-12.** *Water mass in the GDCS pool. AS-2.*

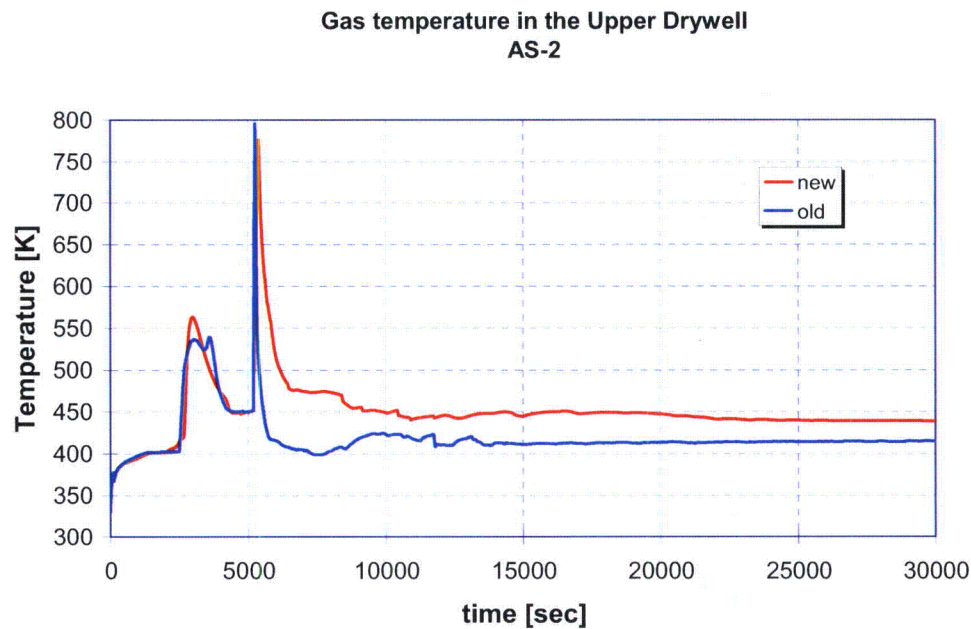


**Figure G-13.** *Gas temperature in the Upper Drywell. AS-2.*

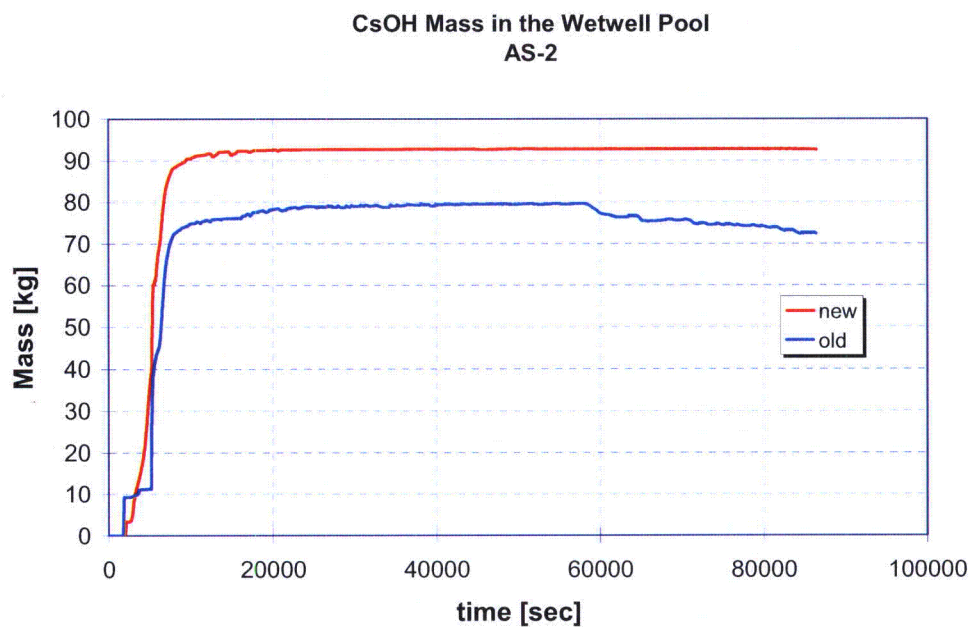


**Figure G-14.** *CsOH mass in the Wetwell pool. AS-2.*

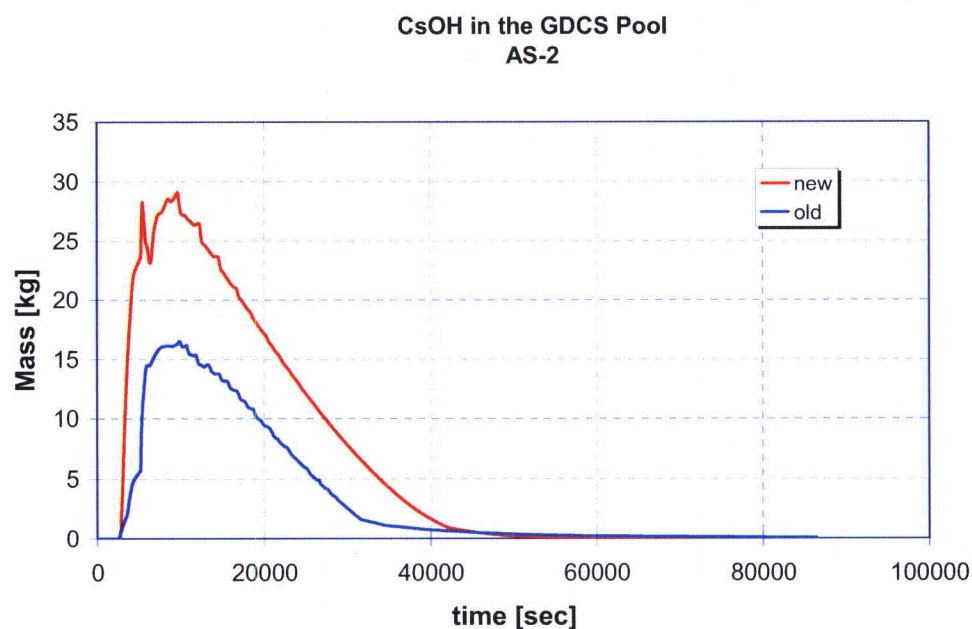


**Figure G-15.** *CsOH mass in the GDCS pool. AS-2.*

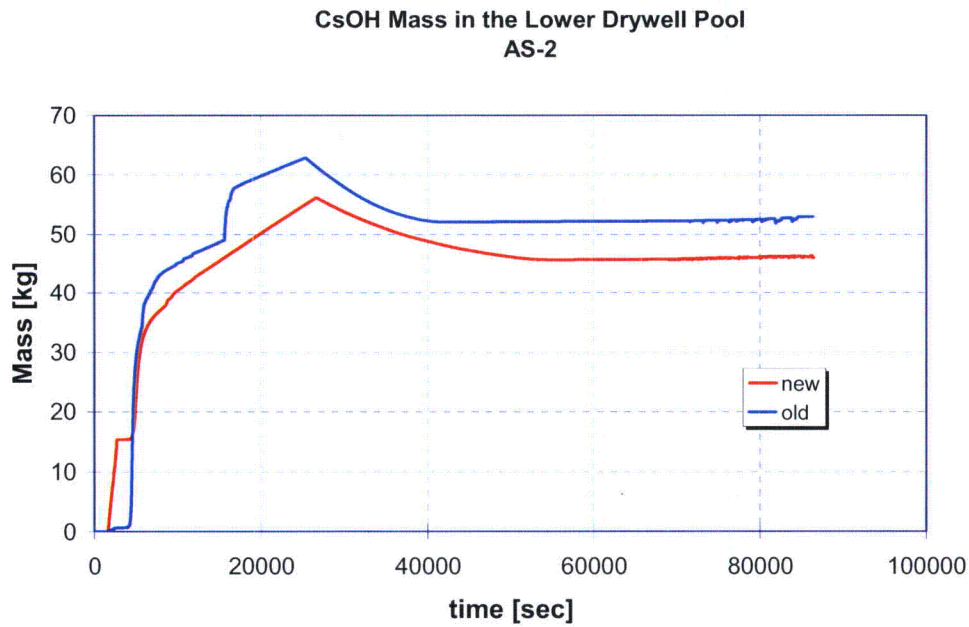


Figure G-16. CsOH mass in the Lower Drywell pool. AS-2.

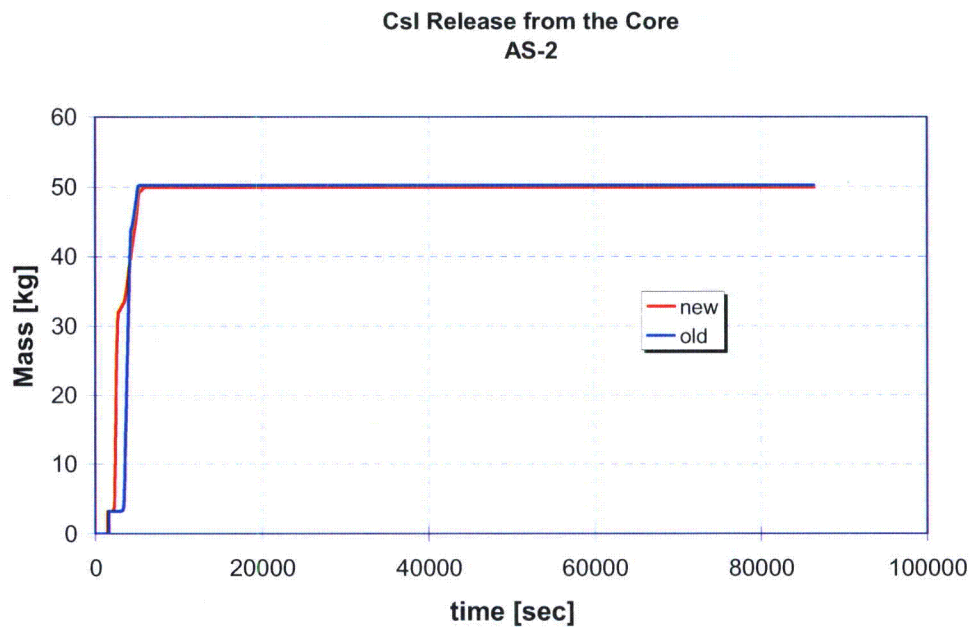


Figure G-17. Total release of CsI from the core to the RCS. AS-1.



### CsI Release from the RCS to Containment AS-2

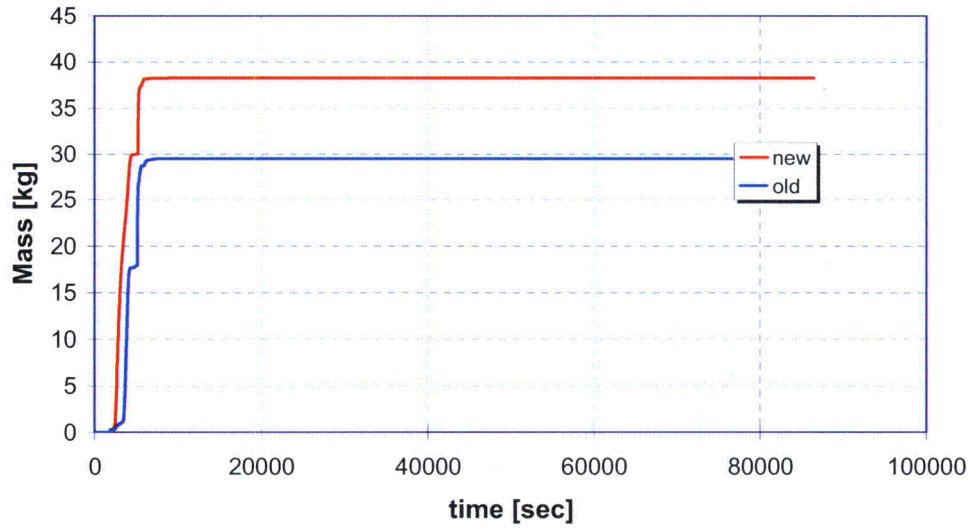


Figure G-18. Total CsI release from the RPV to the containment. AS-2.

### CsI mass in the RPV pool AS-2, no MSIV leak

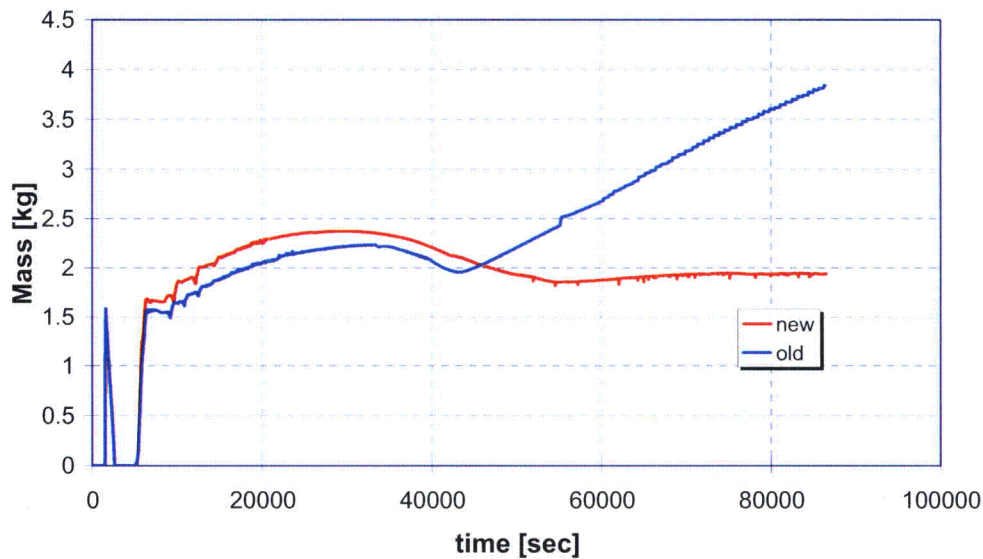
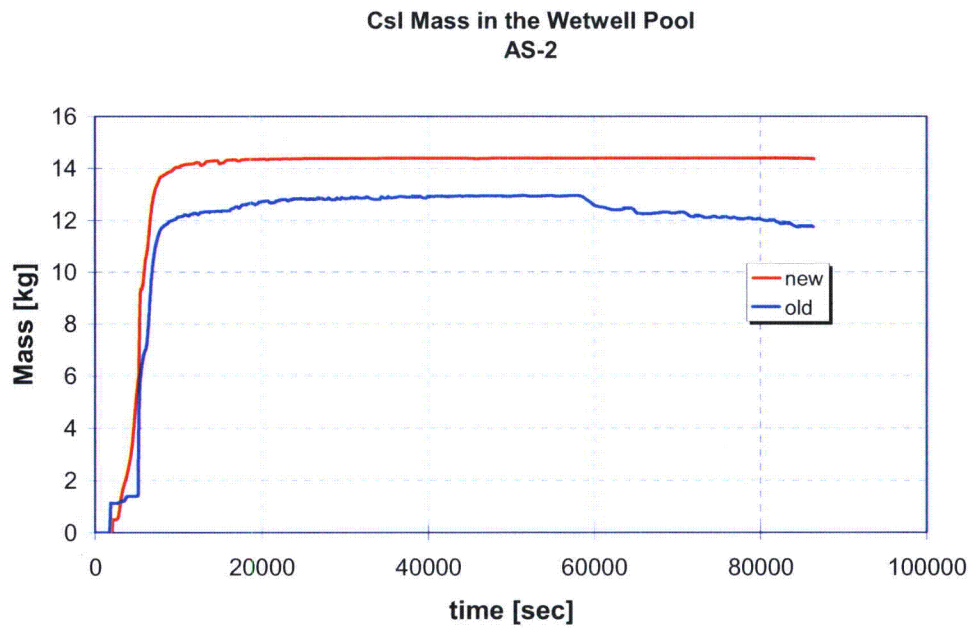
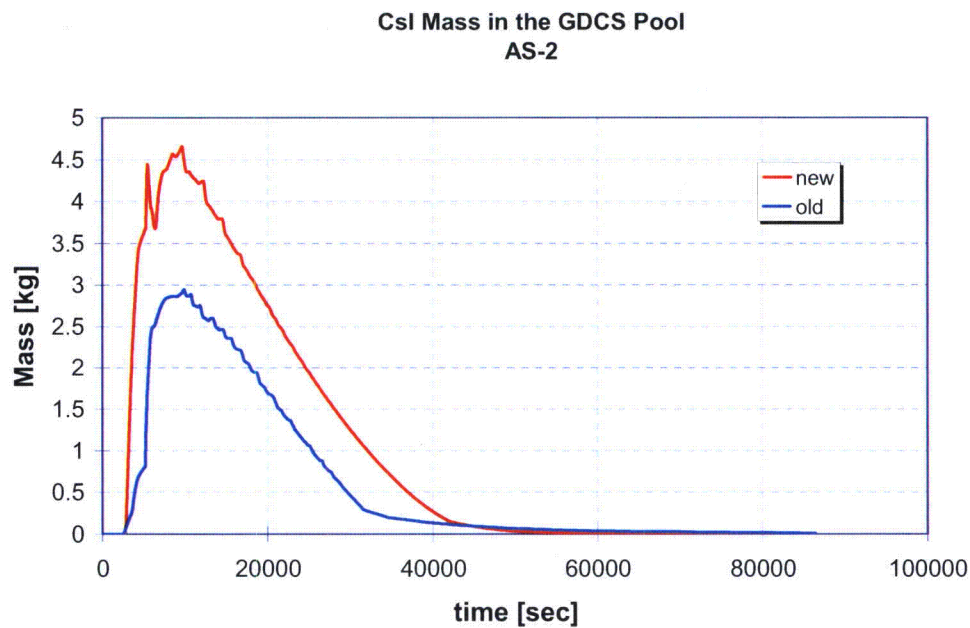


Figure G-19. Total CsI mass in the RPV pool. AS-2.



**Figure G-20.** Total CsI mass in the Wetwell pool. AS-2.



**Figure G-21.** Total CsI mass in the GDCS pool. AS-2.

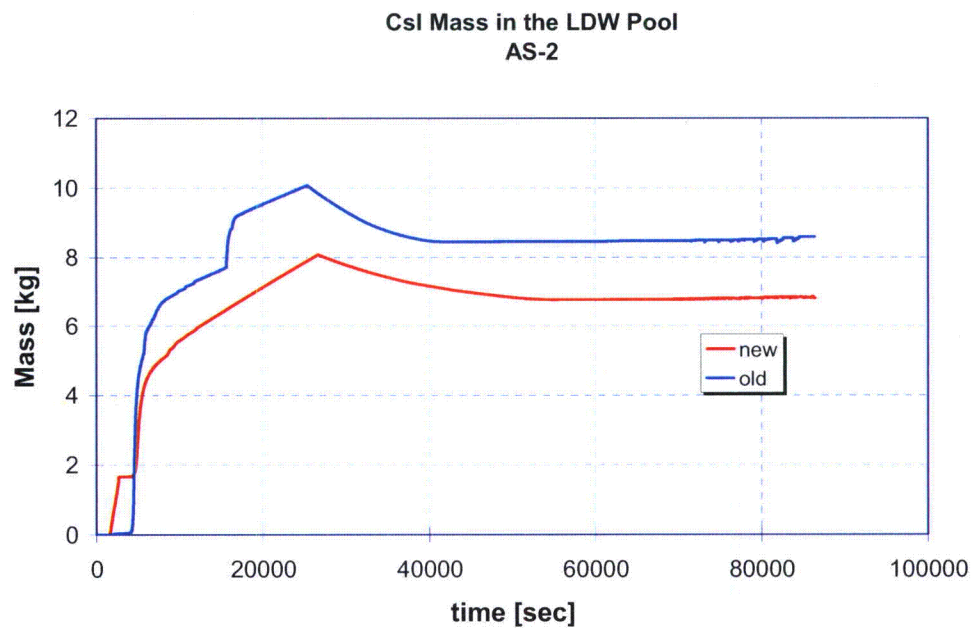


**Figure G-22.** Total CsI mass in the Lower Drywell pool. AS-2.

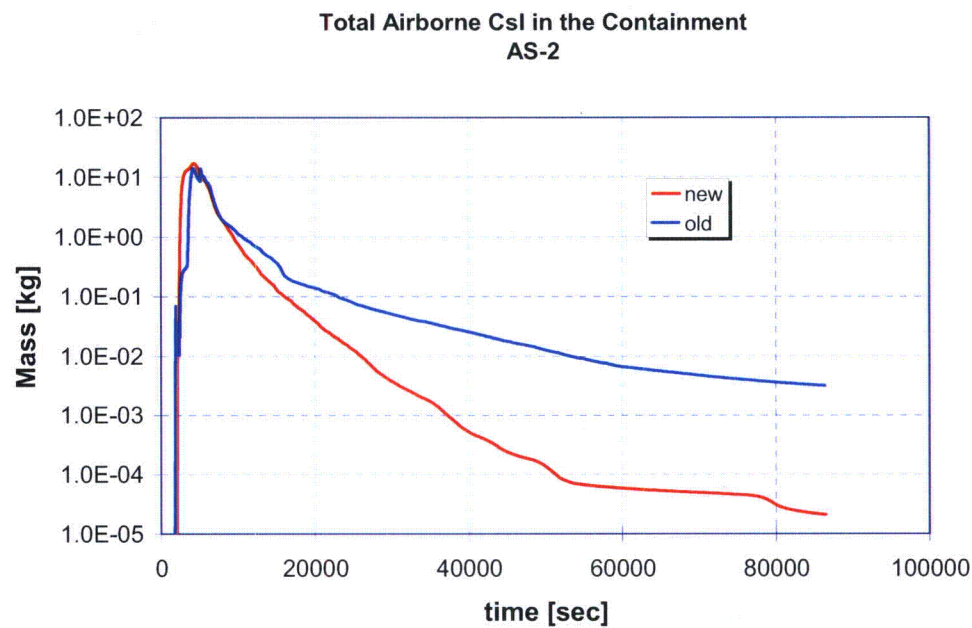


**Figure G-23.** Total airborne CsI mass in the containment. AS-2.

### Airborne CsI in the Drywell Volumes AS-2

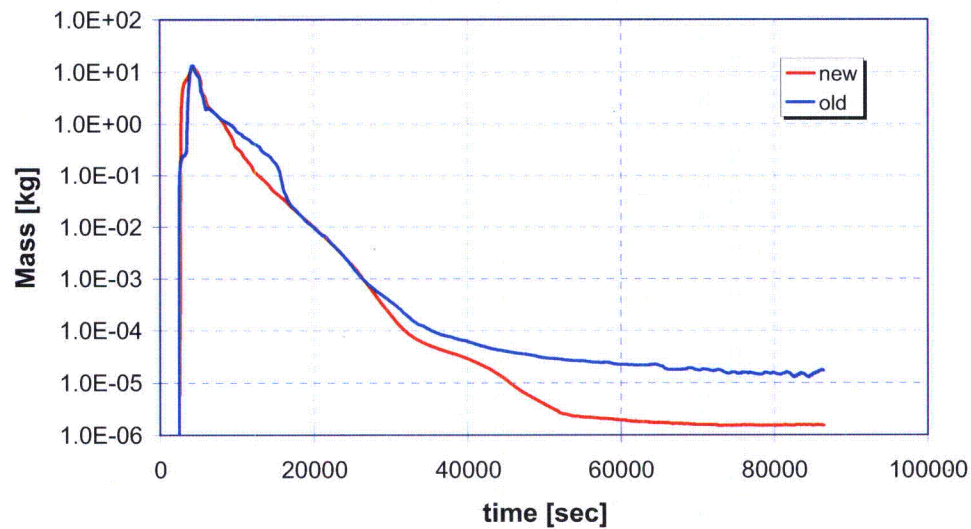


Figure G-24. Total airborne CsI mass in the Drywell control volumes. AS-2.

### Airborne CsI in the Wetwell AS-2

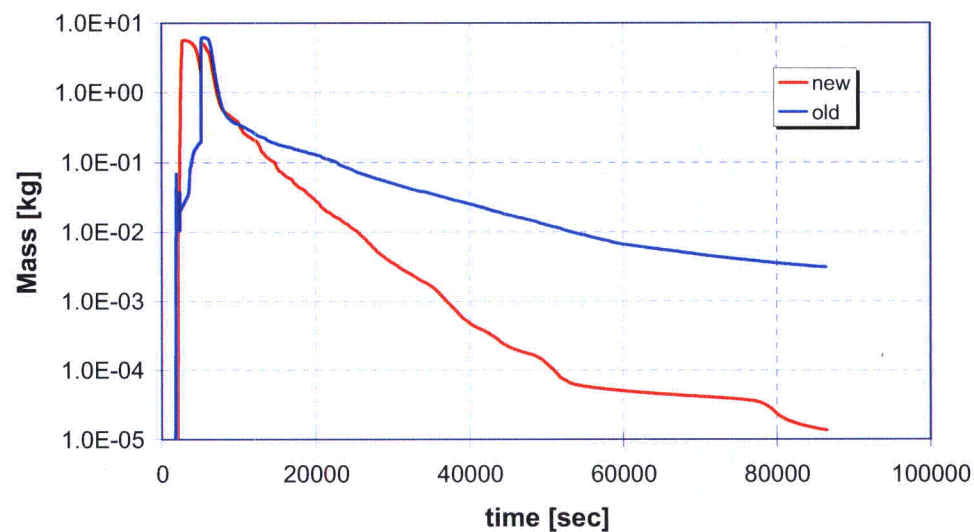
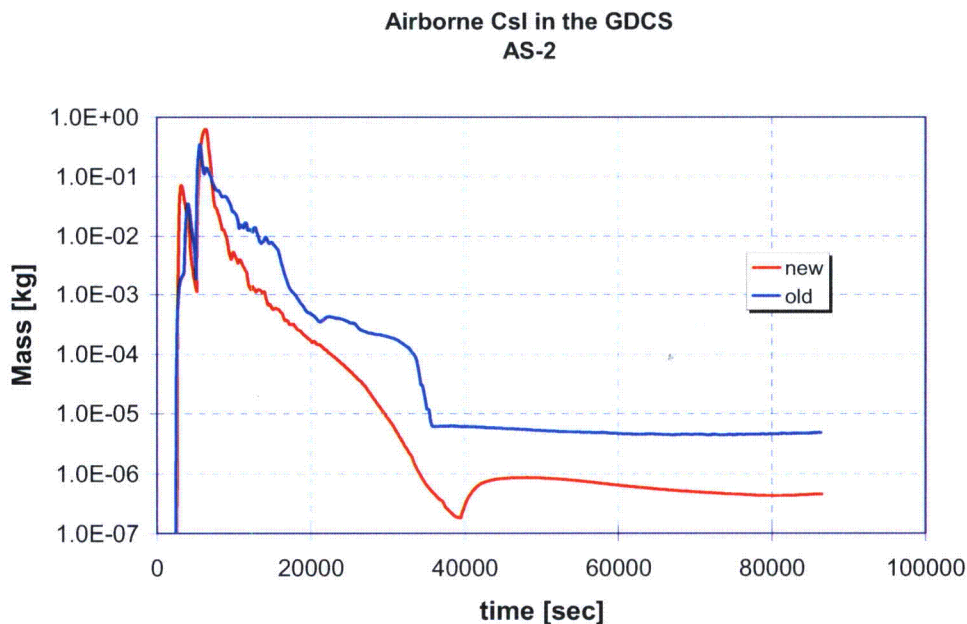
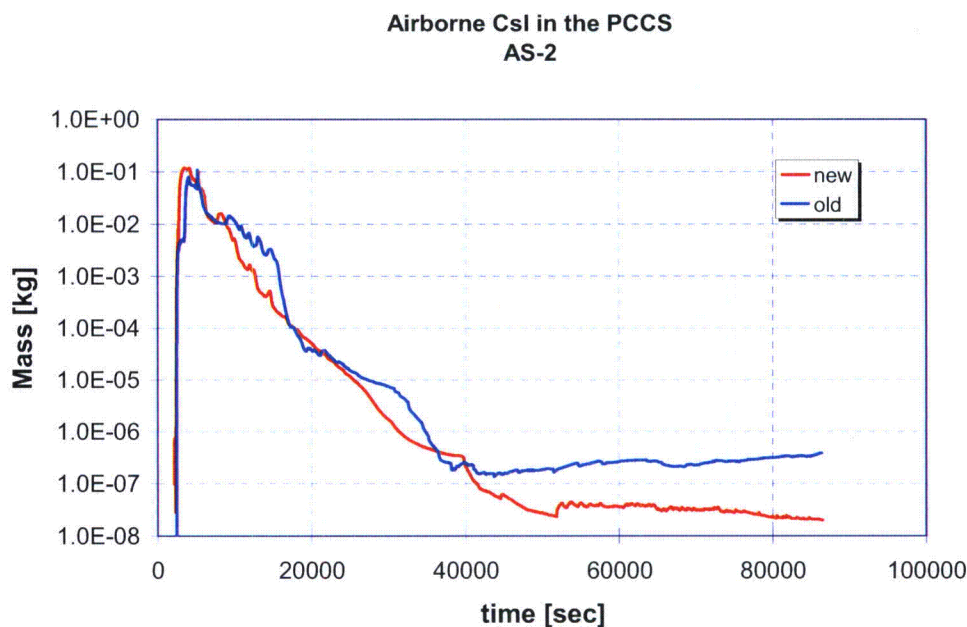


Figure G-25. Total airborne CsI mass in the Wetwell. AS-2.



**Figure G-26.** Airborne CsI ass in the GDCS. AS-2.



**Figure G-27.** Airborne CsI mass in the PCCS. AS-2.

### CsI Release from Upper Drywell Through Nominal Leakage Path AS-2

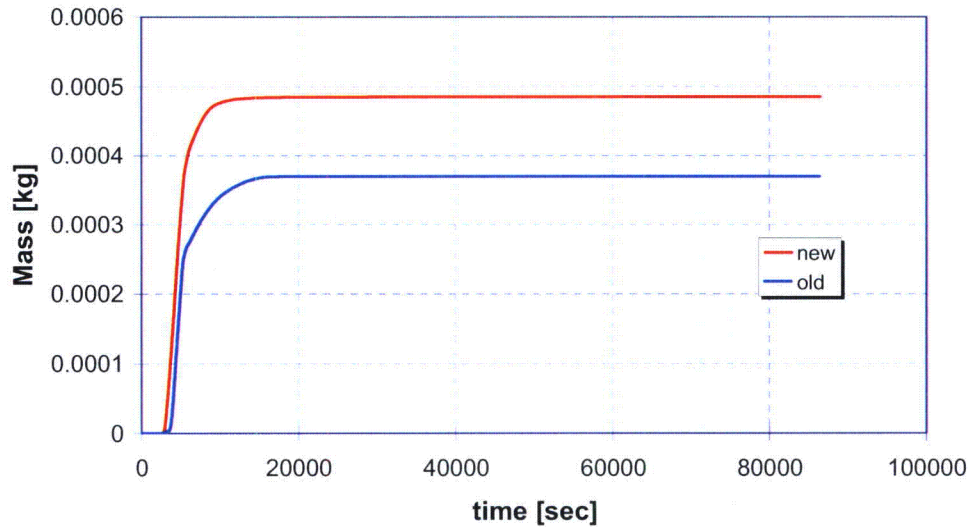


**Figure G-28.** Cumulative CsI release from the Upper Drywell via nominal leakage path. AS-2.

### Average Decontamination Factor of CsI in PCCS AS-2

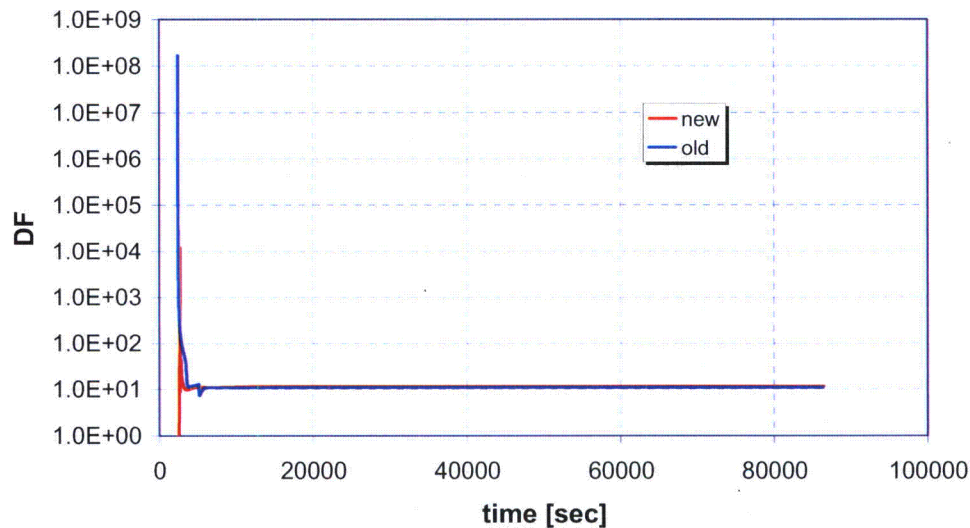


**Figure G-29.** Average decontamination factor of CsI in the PCCS. Calculated as CsI flow in to the PCCS divided by the sum of CsI flow through the PCCS Drain Lines and Vent Lines. AS-2.



### CsI Decontamination Factor Over Timestep in PCCS AS-2

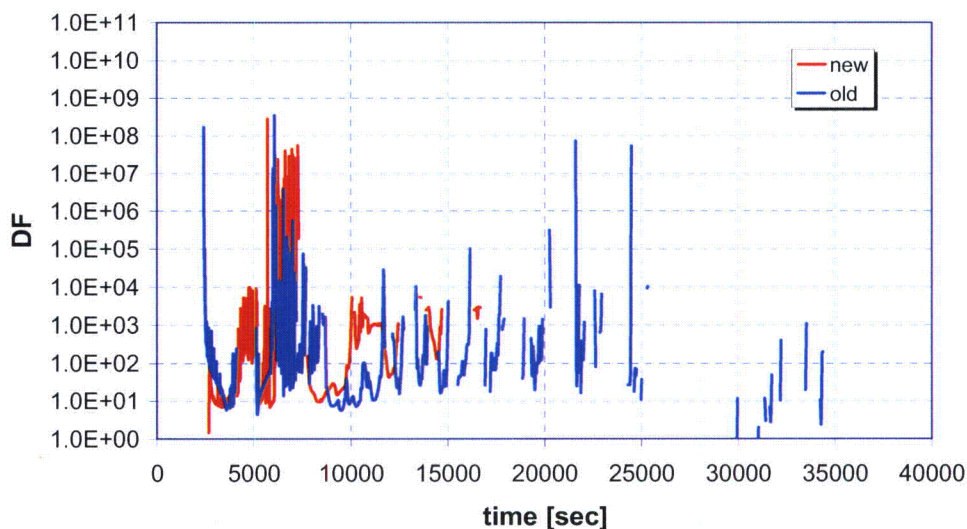


**Figure G-30.** Decontamination factor of CsI in the PCCS calculated over a MELCOR plot file time step as the incoming CsI mass over a time step divided by the outgoing CsI mass (Drain Lines+Vent Line) over a time step. AS-2.

### Average Containment Decontamination Factor AS-2

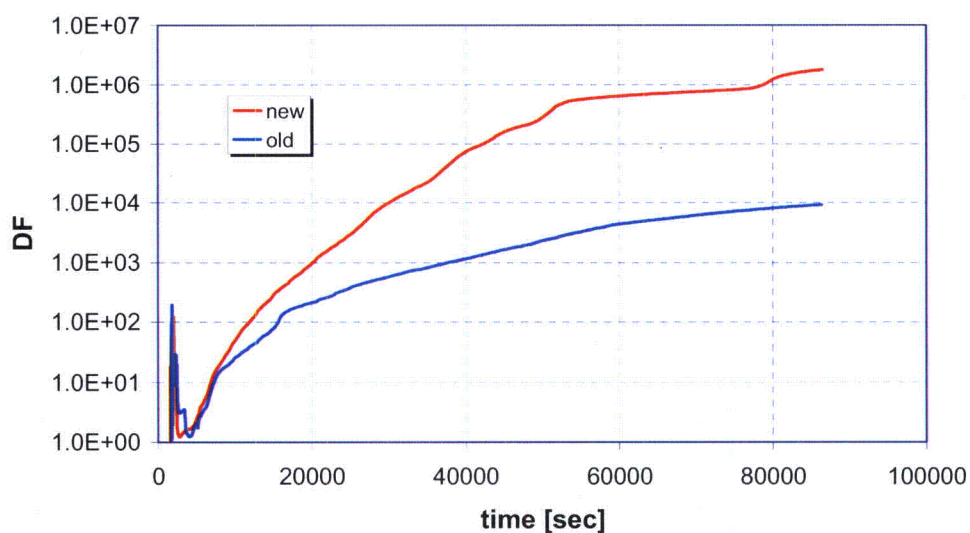


**Figure G-31.** Average CsI decontamination factor in the containment calculated as total CsI release from RPV to containment divided by total airborne mass of CsI in the containment. AS-2.

## 27 APPENDIX H: Comparison of results : AS-3 without MSIV leak of FR Part 2 and FR Part 3

In all following plots the curve indicated as "new" is a result calculated with the updated MELCOR input (MSL, MSDL and Main Condenser and SRVs, SRV/ADS and DPV models, the IC vent line always closed) and with code version 1.8.6YH. "old" is FR Part 2 result.

The comparison of the results of AS-3 showed that:

1. The average decontamination factor of CsI in the containment is the same or higher in the "new" runs than in the "old" runs. Thus the results of FR Part 2 are conservative in respect to the updated analyses.
2. The average decontamination factor of CsI in the PCCS is the same or higher in the "new" runs than in the "old" runs. Thus the results of FR Part 2 are conservative in respect to the updated analyses.
3. The total airborne CsI mass in the containment is lower in the "new" runs than in the "old" runs. The peak airborne CsI mass is reached earlier in the "new" runs than in the "old" results. The results of FR Part 2 are conservative in respect to the updated analyses.
4. The masses of CsOH in the containment water pools are lower in the "new" runs than in the "old" runs. The CsOH mass in the Wetwell pool is 34 % lower in the "new" runs than in the old runs. Based on the sensitivity studies even 10 % of the "old" CsOH mass does not make Wetwell pool acidic. Respectively, the CsOH mass in the LDW pool in the "new" results is 45 % lower in the "old" results. The ChemSheet sensitivity runs for CsOH mass suggest that the effect of "new" run results being non-conservative is that LDW pool becomes acidic earlier but by less than 5 % from the results calculated with the FR Part 2 CsOH data. The "new" CsOH mass in the GDSC pool is 36 % of the "old" result. Based on ChemSheet sensitivity calculations (50 % case) this would mean that the "new" results would turn the GDSC pool acidic earlier but less than 18.2 % earlier than in estimates calculated using the CsOH mass in results reported in FR Part 2.
5. The cumulative CsI leakage through nominal leakage path is lower in the "new" results than in the "old" results. Thus, the results based on FR Part 2 calculations are conservative in respect to the FR Part 3 results.
6. Containment pressure is lower in the "new" runs than in the "old" old runs. Thus, the "old" results reported in FR Part 2 are conservative in respect to the "new" FR Part 3 results.

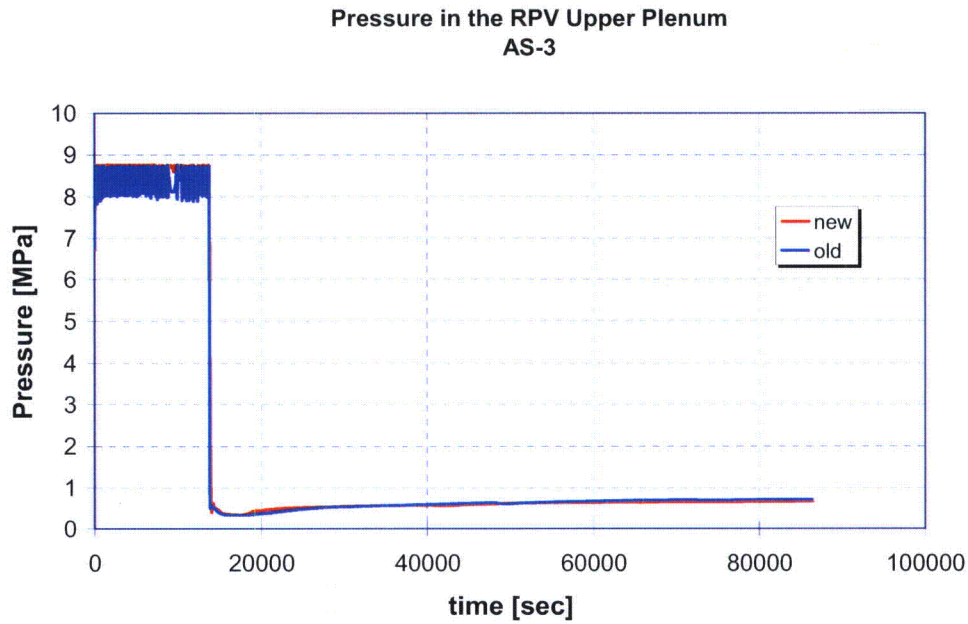


**Figure H-1.** *Pressure in the RPV. AS-3.*

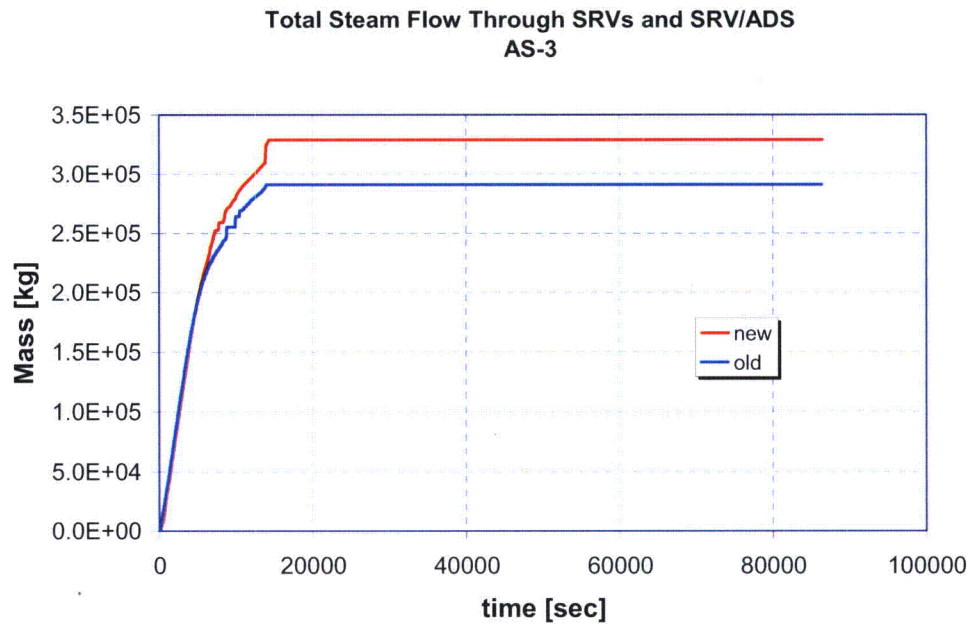


**Figure H-2.** *Total cumulative steam flow through SRVs and SRV/ADS valves. AS-3.*

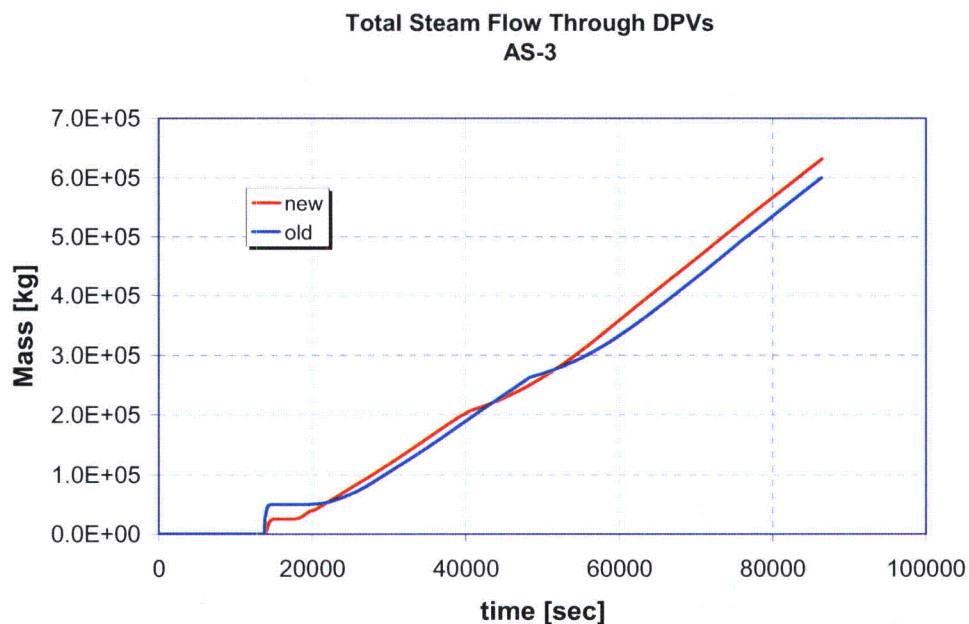


**Figure H-3.** Total cumulative steam flow through DPVs. AS-3.

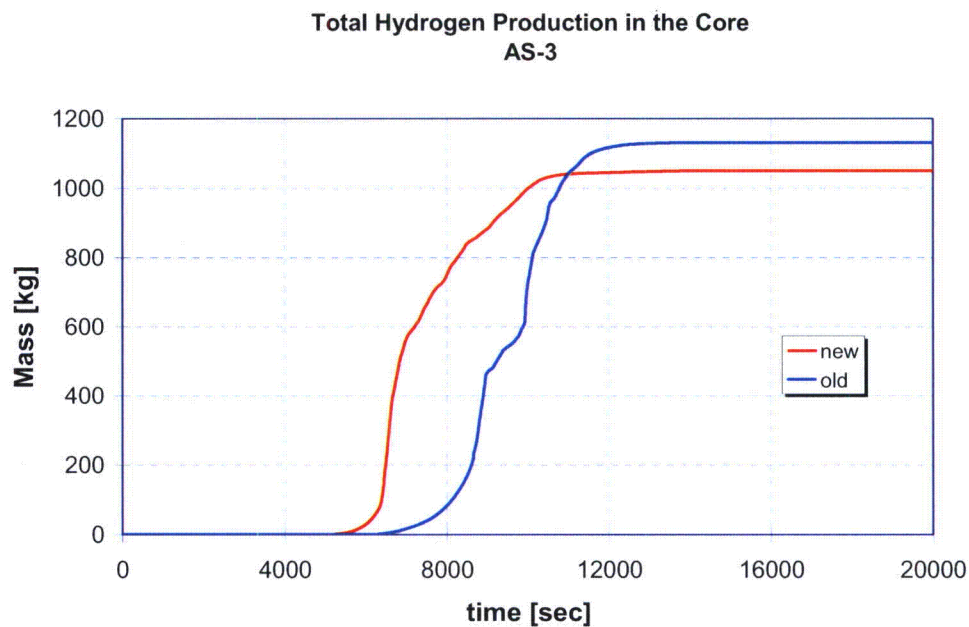


**Figure H-4.** Total hydrogen production in the core. AS-3.

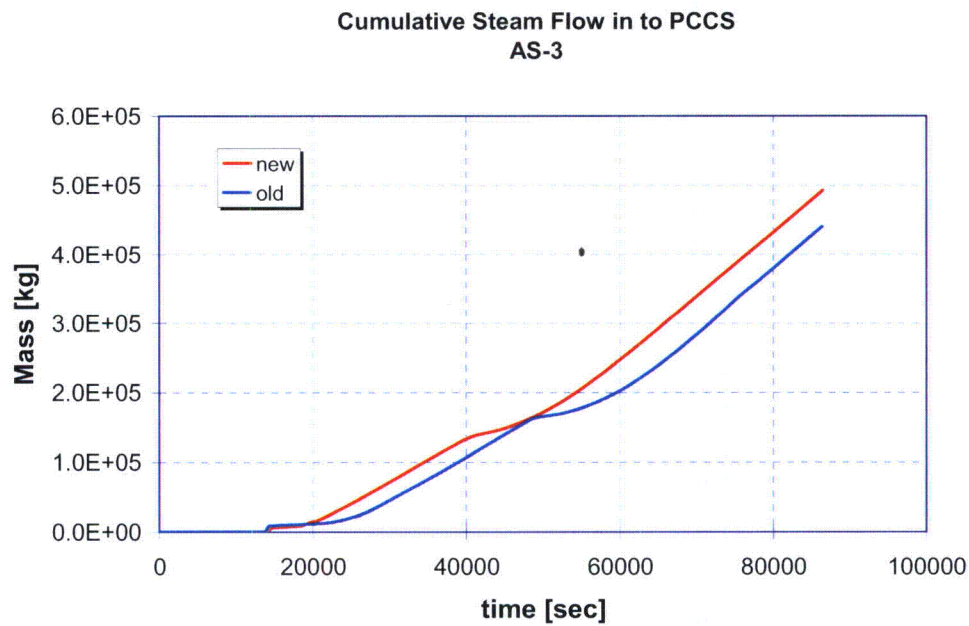


**Figure H-5.** Cumulative steam in-flow to the PCCS. AS-3.

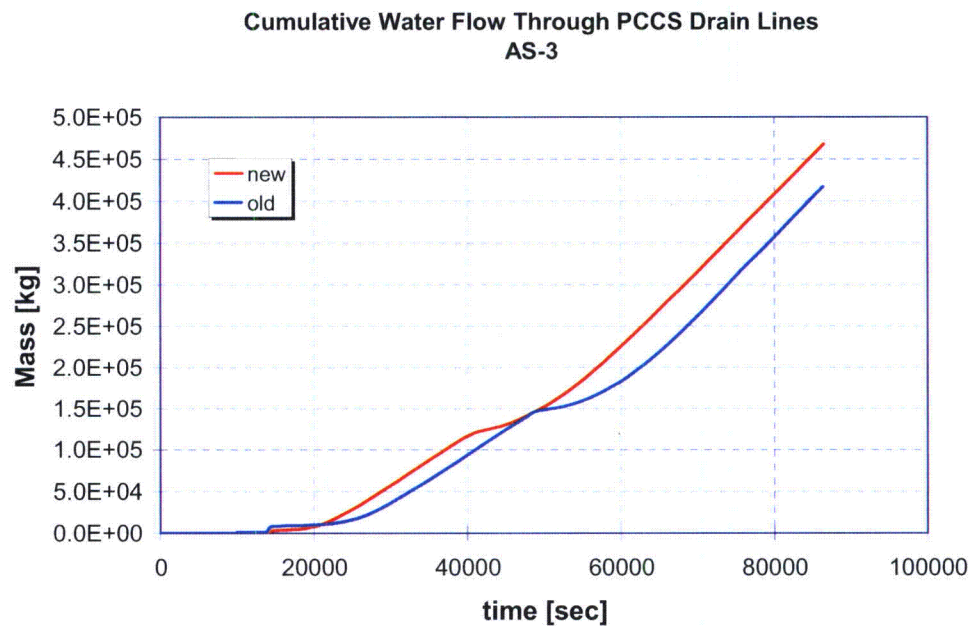


**Figure H-6.** Cumulative water flow through the PCCS Drain Lines. AS-3.

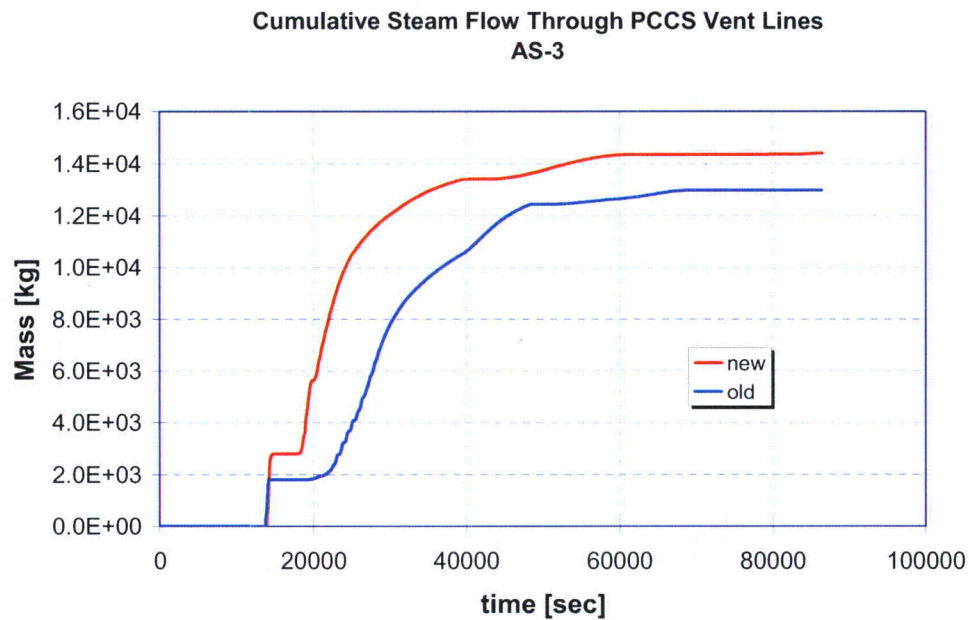


**Figure H-7.** Cumulative steam flow through the PCCS Vent Lines. AS-3.

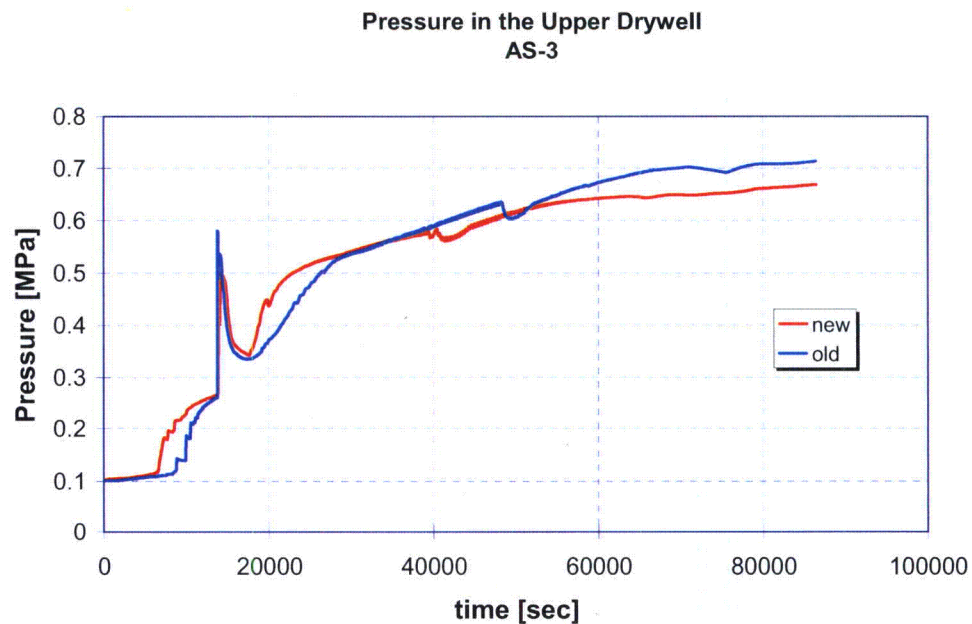


**Figure H-8.** Pressure in the Upper Drywell. AS-3.



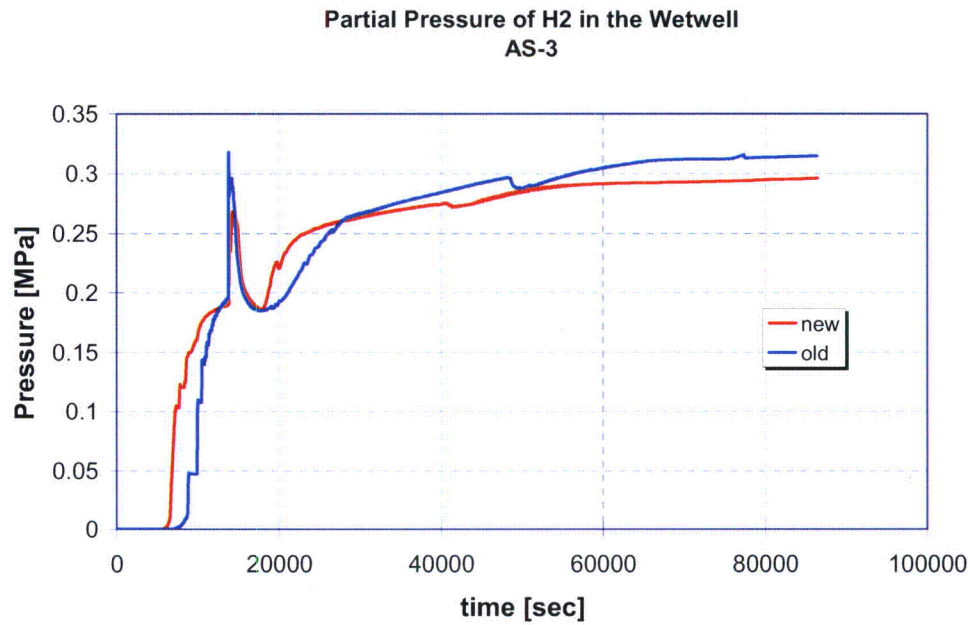


**Figure H-9.** *Partial pressure of hydrogen in the Wetwell. AS-3.*

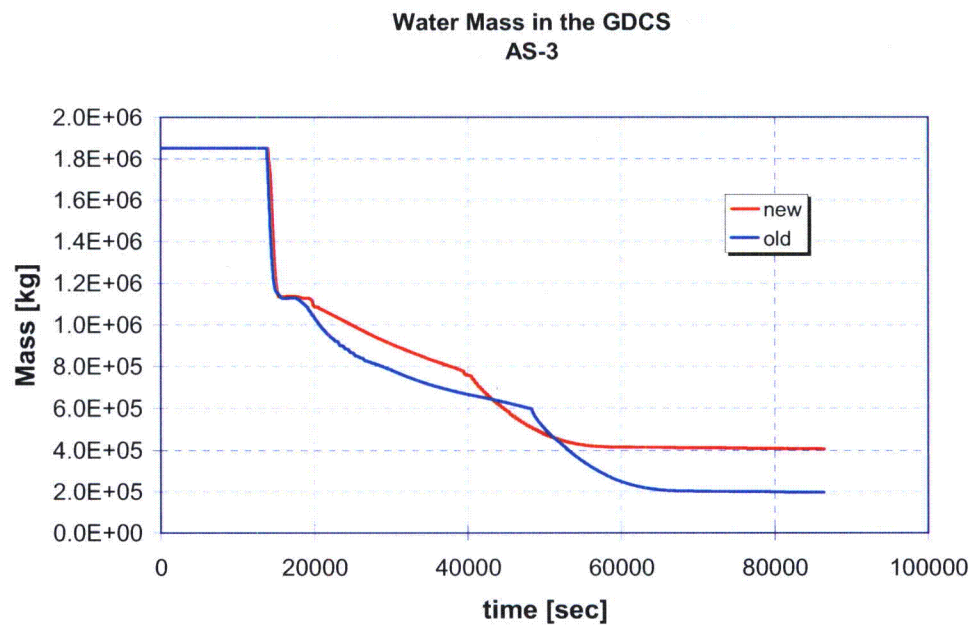


**Figure H-10.** *Water mass in the GDSCS pool. AS-3.*

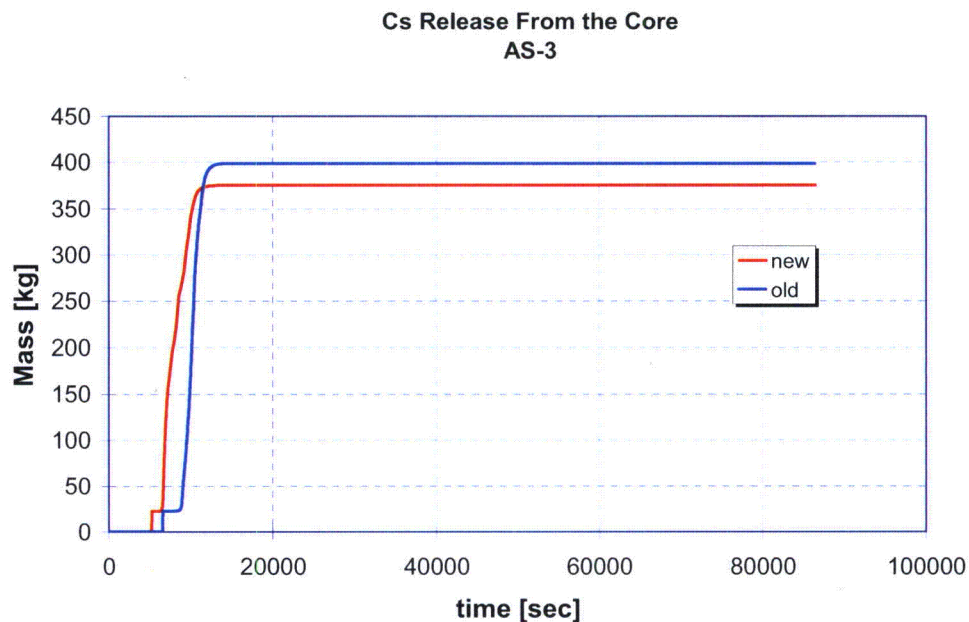


**Figure H-11.** Total Cesium release from the core. AS-3.

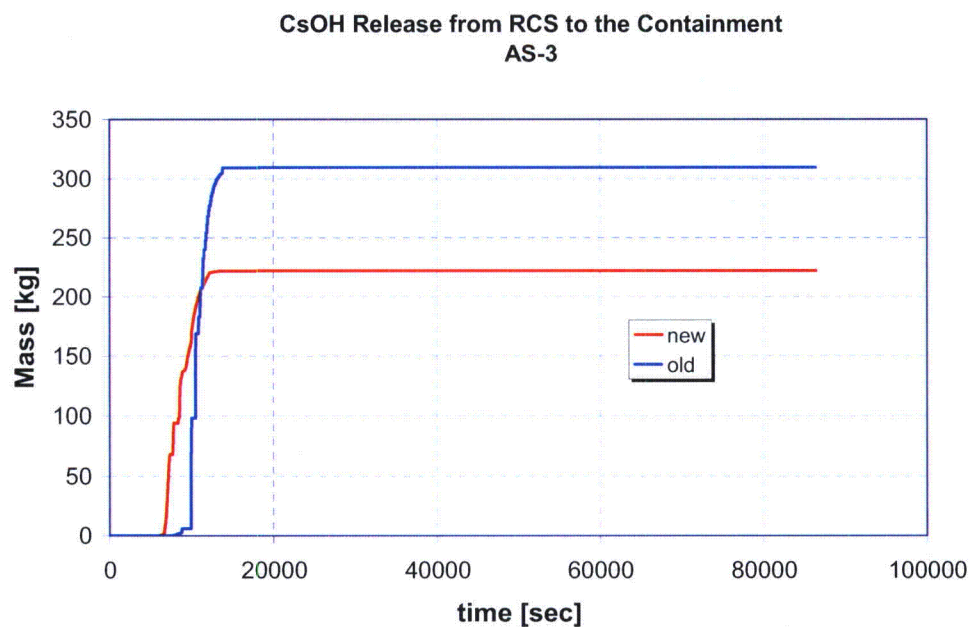


**Figure H-12.** Total CsOH release from the RPV to the containment. AS-3.

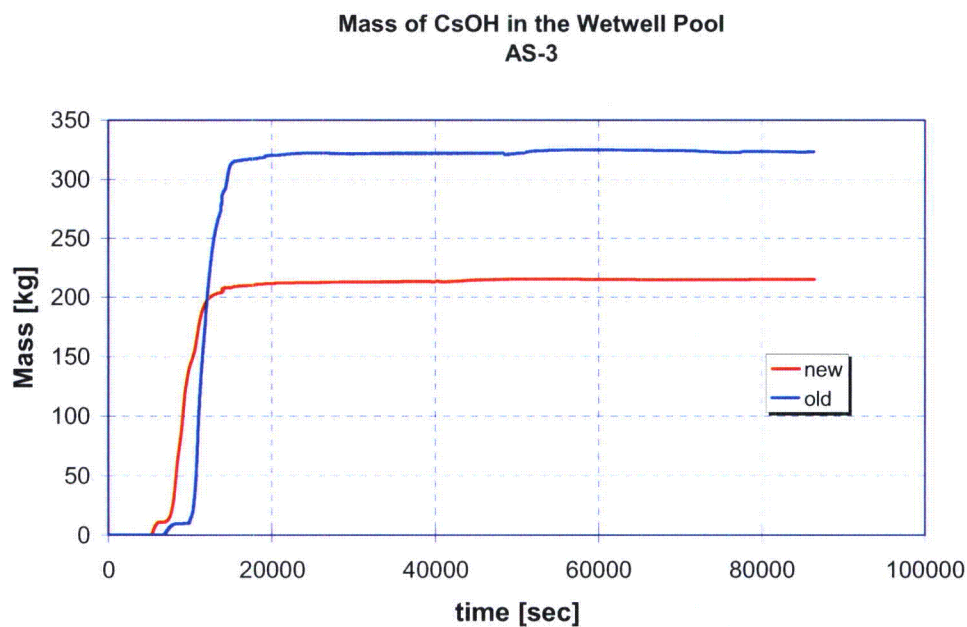


**Figure H-13.** Total mass of CsOH in the Wetwell pool. AS-3.

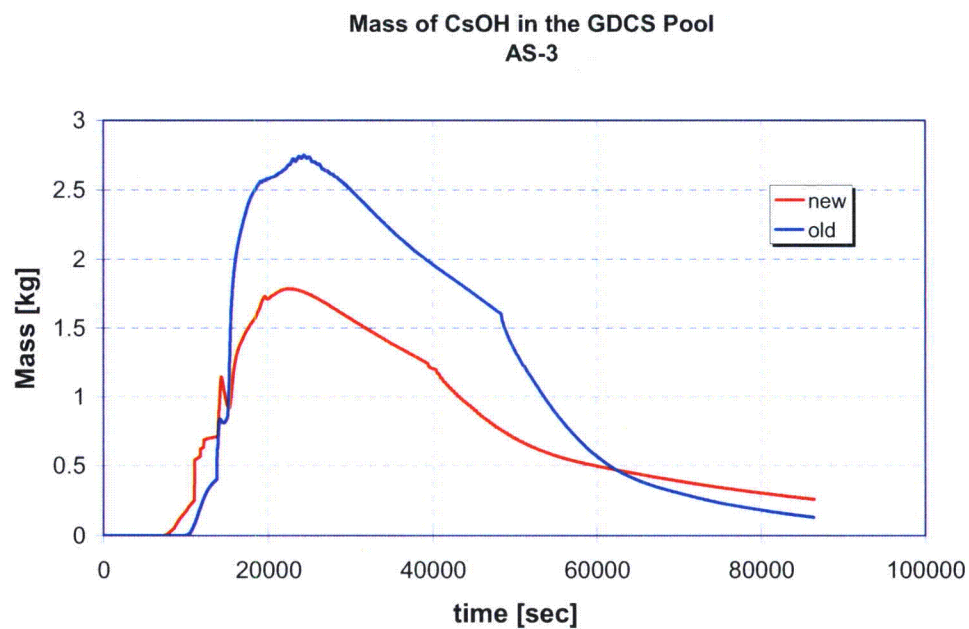


**Figure H-14.** Total mass of CsOH in the GDSCS pool. AS-3.

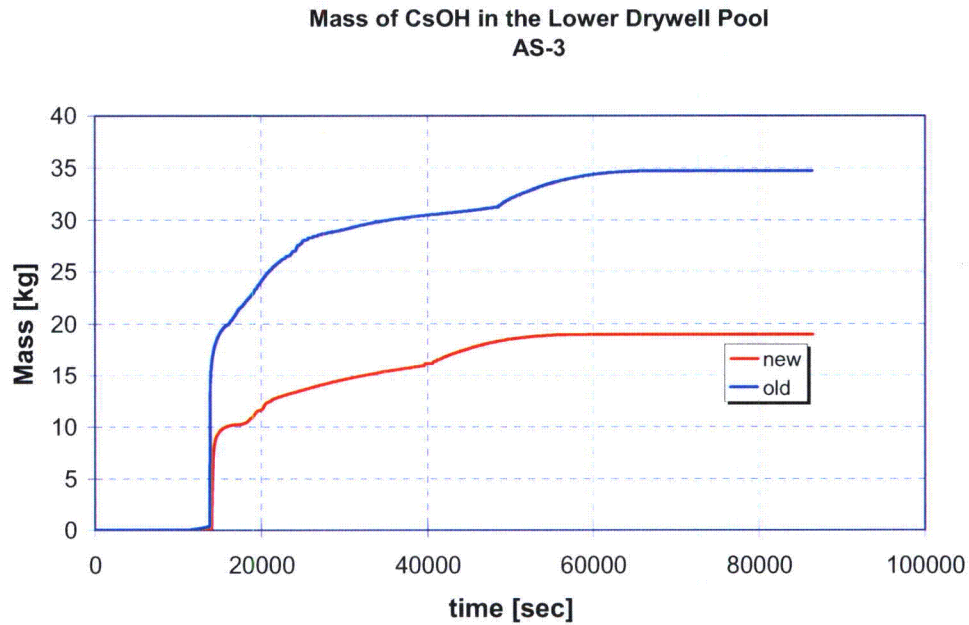


**Figure H-15.** *CsOH mass in the Lower Drywell pool. AS-3.*

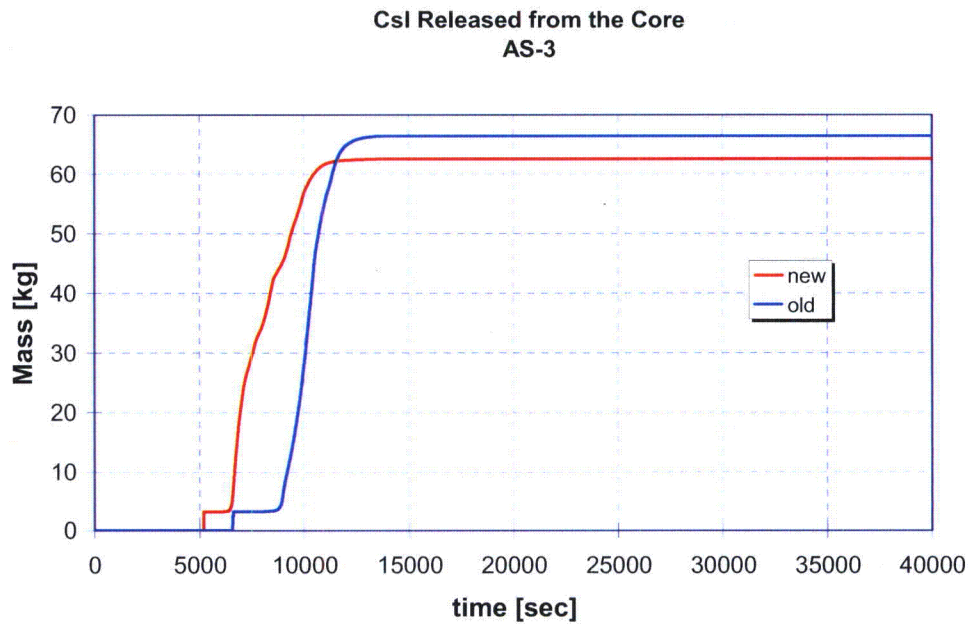


**Figure H-16.** *Total mass of CsI released from the core. AS-3.*

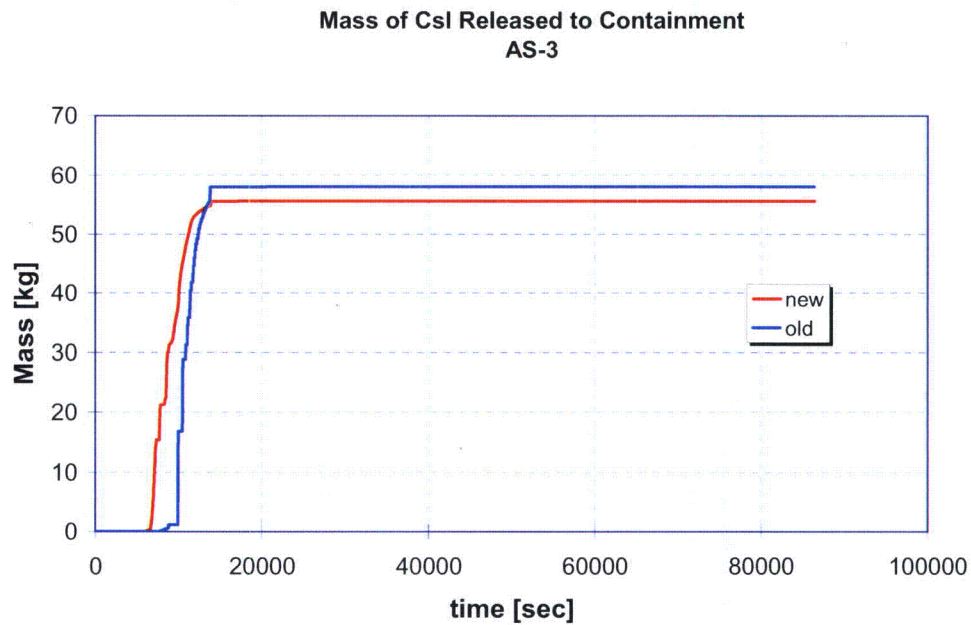


**Figure H-17.** Total mass of CsI released from the RPV to the containment. AS-3.

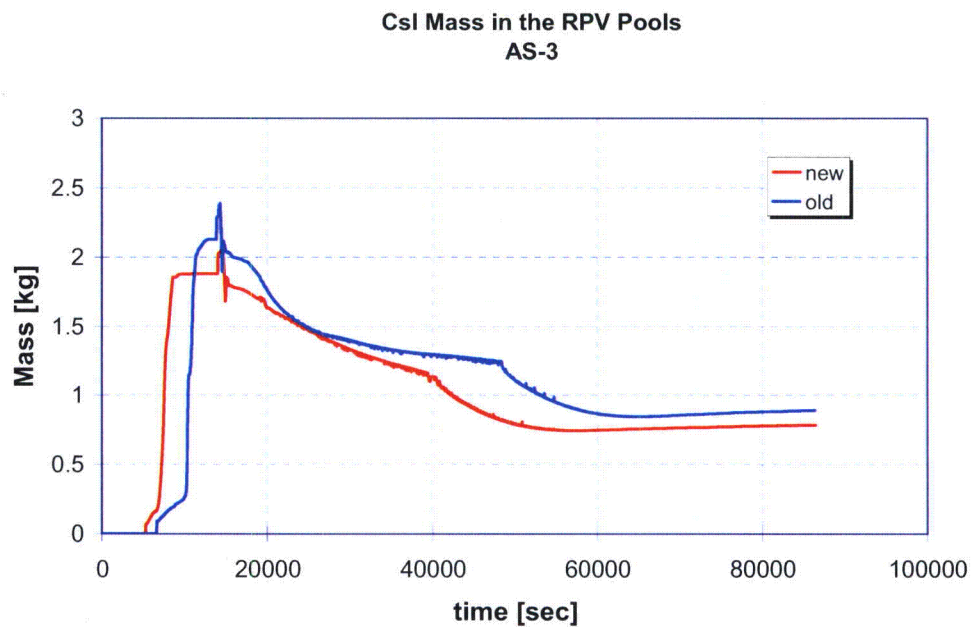


**Figure H-19.** Total CsI mass in the RPV water. AS-3.

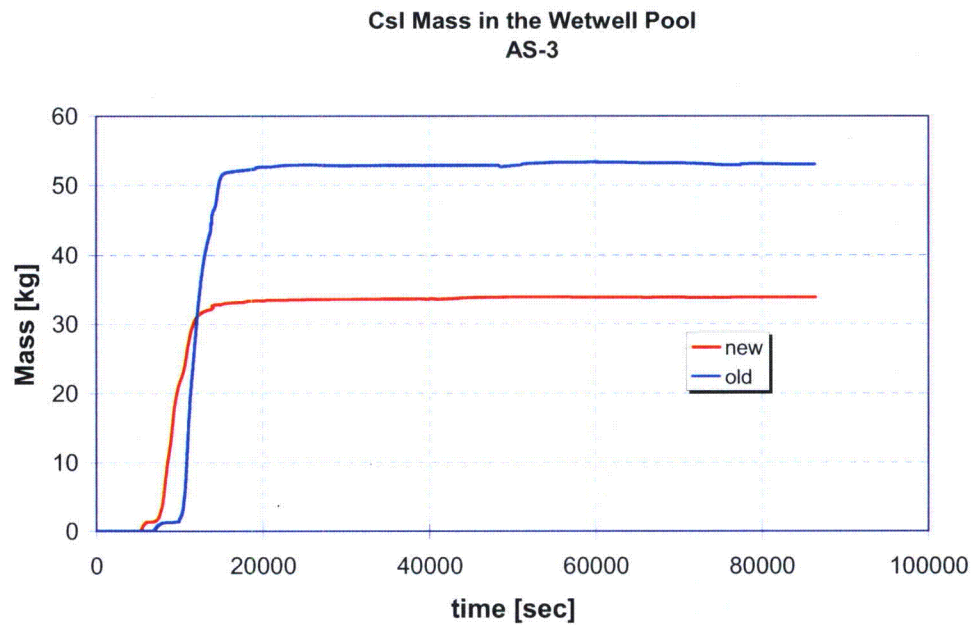


**Figure H-20.** Total CsI mass in the Wetwell pool. AS-3.

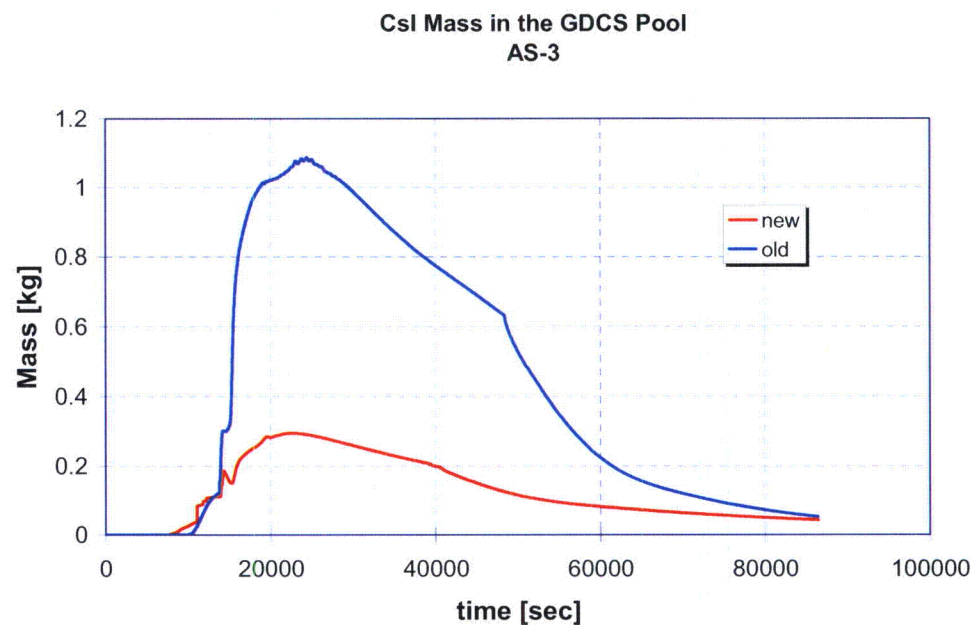


**Figure H-21.** Total CsI mass in the GDCS pool. AS-3.



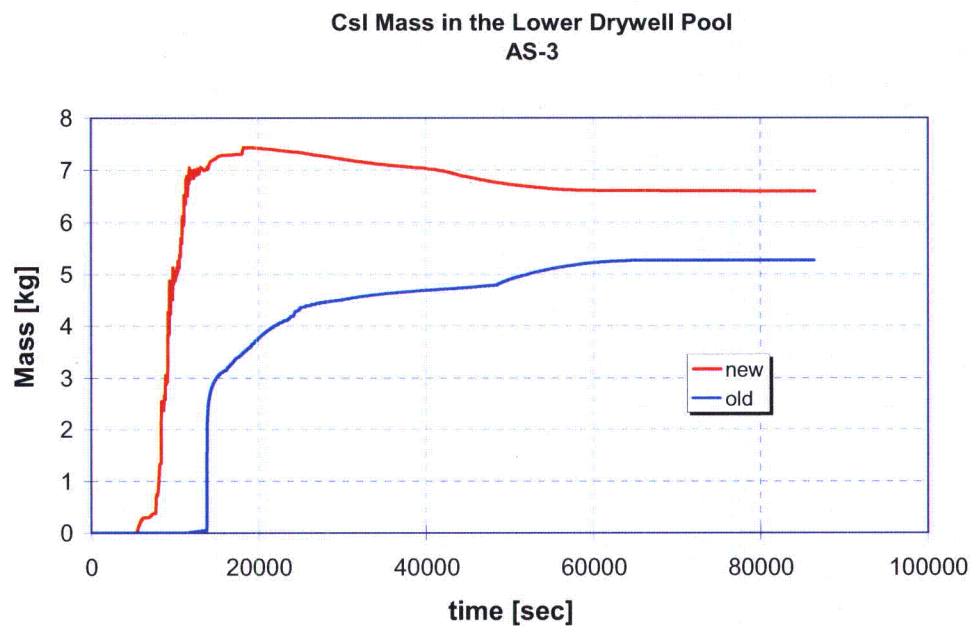


**Figure H-22.** Total CsI mass in the Lower Drywell pool. AS-3.

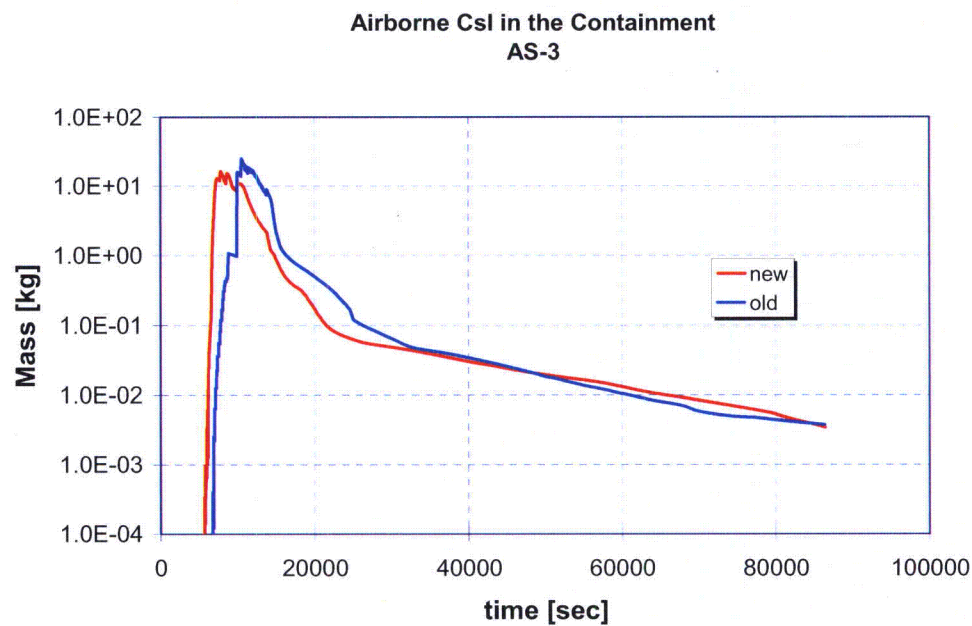


**Figure H-23.** Total airborne CsI mass in the containment. AS-3.

### CsI Release from the Containment by Nominal Leak AS-3

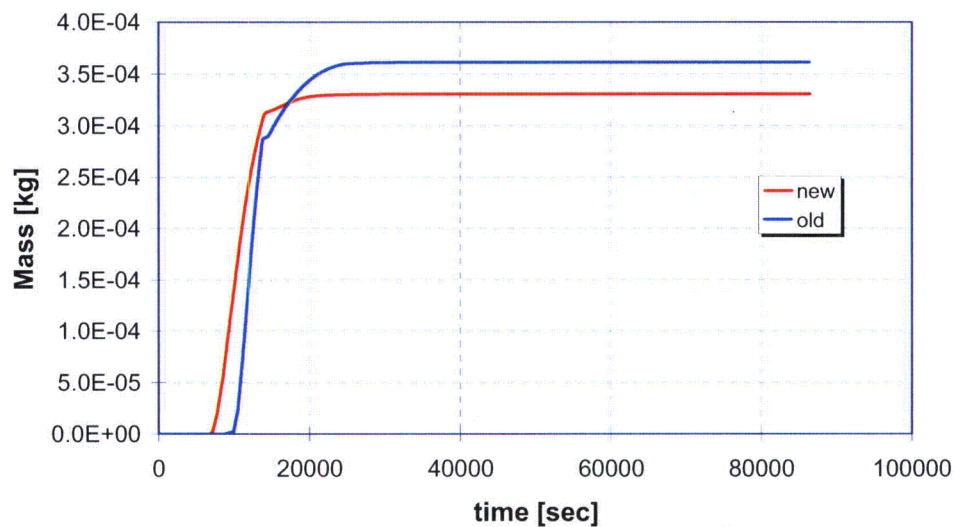


**Figure H-24.** Cumulative release of CsI from the Upper Drywell via nominal leakage path. AS-3.

### CsI Average Decontamination Factor in the PCCS AS-3

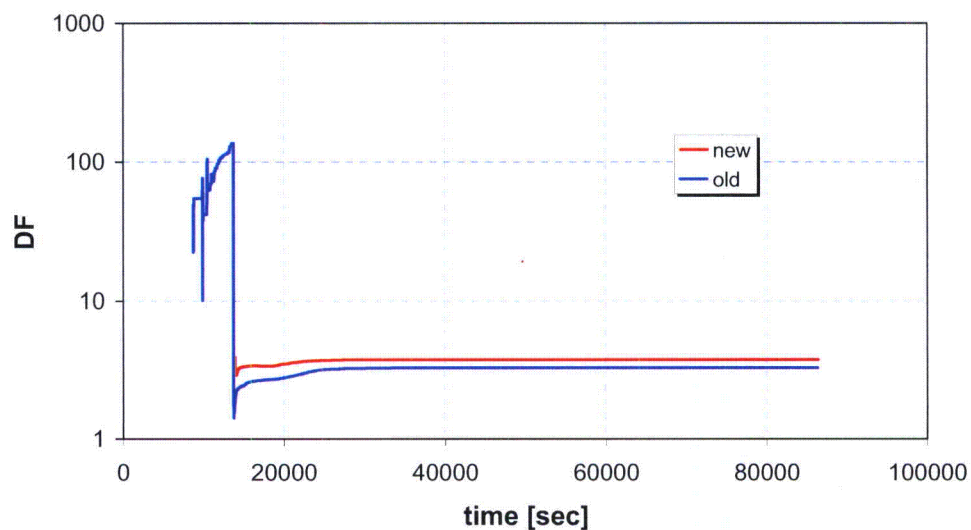


**Figure H-25.** Average decontamination factor of CsI in the PCCS. Calculated as CsI flow in to the PCCS divided by the sum of CsI flow through the PCCS Drain Lines and Vent Lines. AS-3.

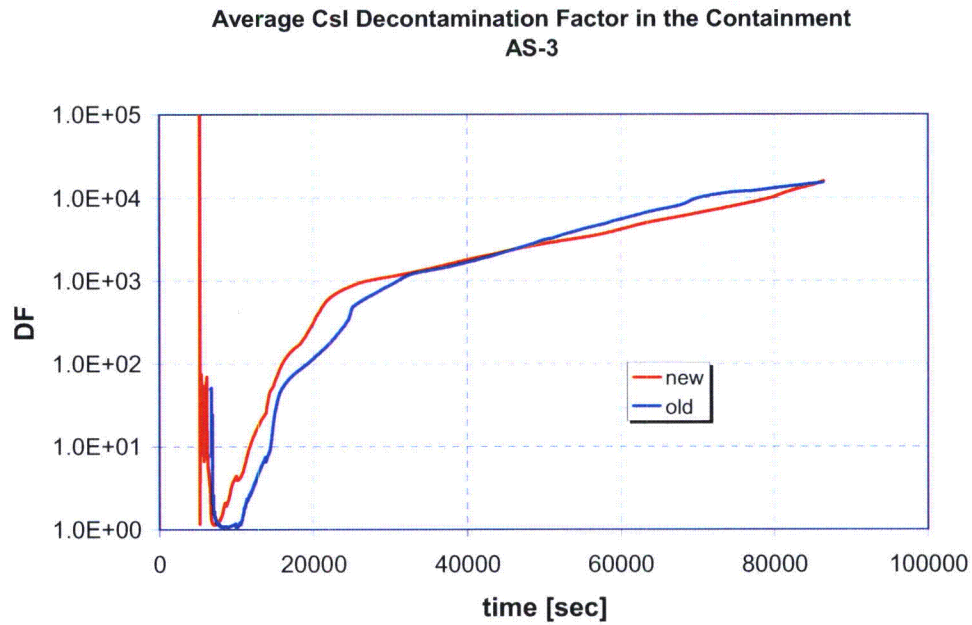


**Figure H-26.** Average CsI decontamination factor in the containment calculated as total CsI release from RPV to containment divided by total airborne mass of CsI in the containment. AS-3.

**Enclosure 3**

**MFN 07-466, Supplement 1**

**Affidavit for GE-Hitachi Nuclear Energy Americas LLC  
Proprietary Information for the NRC**

**Executed by Larry J Tucker, March 31, 2008**

# GE-Hitachi Nuclear Energy Americas LLC

## AFFIDAVIT

I, **Larry J. Tucker**, state as follows:

- (1) I am Manager, New Units Engineering, GE-Hitachi Nuclear Energy Americas LLC ("GEH"), have been delegated the function of reviewing the information described in paragraph (2) which is sought to be withheld, and have been authorized to apply for its withholding.
- (2) The information sought to be withheld is contained in Enclosure 1 of MFN 07-466, Supplement 1, Mr. James C. Kinsey to U.S. Nuclear Regulatory Commission, *MFN 07-466, Supplement 1 – Transmittal of Estimation and Modeling of Effective Fission Product Decontamination Factor for ESBWR Containment – Part 3, VTT-R-06771-07, Revision 2*, dated March 31, 2008. The information in Enclosure 1, which is entitled *MFN 07-466, Supplement 1 – Transmittal of Estimation and Modeling of Effective Fission Product Decontamination Factor for ESBWR Containment – Part 3, VTT-R-06771-07, Revision 2*, contains GEH Proprietary Information. Each page is stamped "GEH Proprietary Information." Paragraph (3) of this affidavit provides the basis for the proprietary determination.
- (3) In making this application for withholding of proprietary information of which it is the owner or licensee, GEH relies upon the exemption from disclosure set forth in the Freedom of Information Act ("FOIA"), 5 USC Sec. 552(b)(4), and the Trade Secrets Act, 18 USC Sec. 1905, and NRC regulations 10 CFR 9.17(a)(4), and 2.390(a)(4) for "trade secrets" (Exemption 4). The material for which exemption from disclosure is here sought also qualify under the narrower definition of "trade secret", within the meanings assigned to those terms for purposes of FOIA Exemption 4 in, respectively, Critical Mass Energy Project v. Nuclear Regulatory Commission, 975F2d871 (DC Cir. 1992), and Public Citizen Health Research Group v. FDA, 704F2d1280 (DC Cir. 1983).
- (4) Some examples of categories of information which fit into the definition of proprietary information are:
  - a. Information that discloses a process, method, or apparatus, including supporting data and analyses, where prevention of its use by GEH's competitors without license from GEH constitutes a competitive economic advantage over other companies;
  - b. Information which, if used by a competitor, would reduce his expenditure of resources or improve his competitive position in the design, manufacture, shipment, installation, assurance of quality, or licensing of a similar product;

- c. Information which reveals aspects of past, present, or future GEH customer-funded development plans and programs, resulting in potential products to GEH;
- d. Information which discloses patentable subject matter for which it may be desirable to obtain patent protection.

The information sought to be withheld is considered to be proprietary for the reasons set forth in paragraphs (4)a. and (4)b. above.

- (5) To address 10 CFR 2.390(b)(4), the information sought to be withheld is being submitted to NRC in confidence. The information is of a sort customarily held in confidence by GEH, and is in fact so held. The information sought to be withheld has, to the best of my knowledge and belief, consistently been held in confidence by GEH, no public disclosure has been made, and it is not available in public sources. All disclosures to third parties, including any required transmittals to NRC, have been made, or must be made, pursuant to regulatory provisions or proprietary agreements which provide for maintenance of the information in confidence. Its initial designation as proprietary information, and the subsequent steps taken to prevent its unauthorized disclosure, are as set forth in paragraphs (6) and (7) following.
- (6) Initial approval of proprietary treatment of a document is made by the manager of the originating component, the person most likely to be acquainted with the value and sensitivity of the information in relation to industry knowledge, or subject to the terms under which it was licensed to GEH. Access to such documents within GEH is limited on a "need to know" basis.
- (7) The procedure for approval of external release of such a document typically requires review by the staff manager, project manager, principal scientist, or other equivalent authority for technical content, competitive effect, and determination of the accuracy of the proprietary designation. Disclosures outside GEH are limited to regulatory bodies, customers, and potential customers, and their agents, suppliers, and licensees, and others with a legitimate need for the information, and then only in accordance with appropriate regulatory provisions or proprietary agreements.
- (8) The information identified in paragraph (2), above, is classified as proprietary because it identifies detailed GEH ESBWR calculations related to the pH sensitivity in the containment pools and iodine deposition in the main steam lines and interconnected piping. Development of these calculations for the pH sensitivity in the containment pools and iodine deposition in the main steam lines and interconnected piping was achieved at a significant cost to GEH, on the order of a hundred thousand dollars and would result in a significant economic and competitive advantage to a competitor, and constitutes a major GEH asset.
- (9) Public disclosure of the information sought to be withheld is likely to cause substantial harm to GEH's competitive position and foreclose or reduce the availability of profit-making opportunities. The information is part of GEH's



comprehensive BWR safety and technology base, and its commercial value extends beyond the original development cost. The value of the technology base goes beyond the extensive physical database and analytical methodology and includes development of the expertise to determine and apply the appropriate evaluation process. In addition, the technology base includes the value derived from providing analyses done with NRC-approved methods.

The research, development, engineering, analytical and NRC review costs comprise a substantial investment of time and money by GEH.

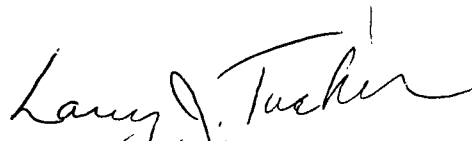
The precise value of the expertise to devise an evaluation process and apply the correct analytical methodology is difficult to quantify, but it clearly is substantial.

GEH's competitive advantage will be lost if its competitors are able to use the results of the GEH experience to normalize or verify their own process or if they are able to claim an equivalent understanding by demonstrating that they can arrive at the same or similar conclusions.

The value of this information to GEH would be lost if the information were disclosed to the public. Making such information available to competitors without their having been required to undertake a similar expenditure of resources would unfairly provide competitors with a windfall, and deprive GEH of the opportunity to exercise its competitive advantage to seek an adequate return on its large investment in developing and obtaining these very valuable analytical tools.

I declare under penalty of perjury that the foregoing affidavit and the matters stated therein are true and correct to the best of my knowledge, information, and belief.

Executed on this 31<sup>st</sup> day of March, 2008.

A handwritten signature in black ink, reading "Larry J. Tucker". The signature is fluid and cursive, with the first name "Larry" and last name "Tucker" clearly distinguishable.

Larry J. Tucker  
GE-Hitachi Nuclear Energy Americas LLC